

Functional Block Copolymers via Anionic Polymerization for Electroactive Membranes

Alison R. Schultz

Thesis submitted to the faculty of the
Virginia Polytechnic Institute and State University in partial fulfillment
of the requirements for the degree of

Masters of Science
in
Chemistry

Timothy E. Long (Chair)
Robert Moore
James E. McGrath
April 26, 2013
Blacksburg, Virginia

Keywords: water purification, random copolymer, ionic liquids, anionic
polymerization, NexarTM, thermomechanical property

Functional Block Copolymers via Anionic Polymerization for Electroactive Membranes

Alison R. Schultz

Abstract

Ion-containing block copolymers blend ionic liquid properties with well-defined polymer architectures. This provides conductive materials with robust mechanical stability, efficient processability, and tunable macromolecular design. Conventional free radical polymerization and anion exchange achieved copolymers containing *n*-butyl acrylate and phosphonium ionic liquids. These compositions incorporated vinylbenzyl triphenyl phosphonium and vinylbenzyl tricyclohexyl phosphonium cations bearing chloride (Cl), or bis(trifluoromethane sulfonyl)imide (Tf₂N) counteranions. Differential scanning calorimetry and dynamic mechanical analysis provided corresponding thermomechanical properties. Factors including cyclic substituents, counteranion type, as well as ionic concentration significantly influenced phosphonium cation association.

1, 1'-(1, 4-Butanediyl)bis(imidazole) neutralized NexarTM sulfonated pentablock copolymers and produced novel electrostatically crosslinked membranes. Variable temperature FTIR and ¹H NMR spectroscopy confirmed neutralization. Atomic force microscopy and small angle X-ray scattering studied polymer morphology and revealed electrostatic crosslinking characteristics. Tensile analysis, dynamic mechanical analysis, thermogravimetric analysis, and vapor sorption thermogravimetric analysis investigated polymer properties. The neutralized polymer demonstrated enhanced thermal stability, decreased water adsorption, and well-defined microphase separation. These findings highlight NexarTM sulfonated pentablock copolymers as reactive platforms for novel, bis-imidazolium crosslinked materials.

4-Vinylbenzyl piperidine is a novel styrenic compound that observably autopolymerizes. *In situ* FTIR spectroscopy monitored styrene and 4-vinylbenzyl piperidine thermal polymerizations. A pseudo-first-order kinetic treatment of the thermal polymerization data provided observed rate constants for both monomers. An Arrhenius analysis derived thermal activation energy values. 4-Vinylbenzyl piperidine exhibited activation energy 80 KJ/mol than styrene. The monomer differs from styrene in its piperidinyl structure. Consequently, *in situ* FTIR spectroscopy also monitored styrene thermal polymerization with variable N-benzyl piperidine concentrations. Under these circumstances, styrene revealed activation energy 60 KJ/mol less than its respective bulk value. The similarities in chemical structure between styrene and 4-vinylbenzyl piperidine suggested thermally initiated polymerization occurred by the Mayo mechanism. The unique substituent is proposed to offer additional cationic effects for enhancing polymerization rates.

Living anionic polymerization of 4-vinylbenzyl piperidine achieved novel piperidinyl-containing polymers. Homopolymer and copolymer architectures of this design offer structural integrity, and emphasize base stability. Sequential anionic polymerization afforded a 10K g/mol poly(tert-butyl styrene-co-4-vinylbenzyl piperidine) diblock and a 50K poly(tert-butyl styrene-co-isoprene-co-4-vinylbenzyl piperidine) triblock. Alkylation studies involving a phosphonium bromide salt demonstrated the future avenues for piperidinium based polymer designs. These investigations introduce piperidinyl macromolecules as paradigms for a new class of ammonium based ionic materials.

ACKNOWLEDGEMENTS

I would like to thank my advisor, Prof. Timothy Long, for his guidance, encouragement, and support during my three years of graduate school. I am grateful for his advisement in helping me achieve my scientific goals and grow as a polymer chemist. I would also like to extend my gratitude to my committee members for their participation and support: Prof. James McGrath and Prof. Robert Moore.

I would like to acknowledge Dr. Renlong Gao for his mentorship during my first two years of graduate school. He taught me the importance of working aggressively toward achieving my goals in research. Special thanks also to Dr. Mana Tamami for her friendship and guidance throughout the last three years. I will always cherish the moments we shared together in Blacksburg. I would like to thank all my senior group members, previous and present, for their encouragement, discussions, and support: Shijing Cheng, Mike Allen, Sean Hemp, Nancy Zhang, Tianyu Wu, Matthew Green, Steve June, David Inglefield, Daniel Buckwalter. I am also thankful to our post-docs, previous and present, for their advisement: Erin Murphy, Adam Smith, and Asem Abdulahad.

I would like to thank my collaborators in our research: Dr. Frederick Beyer in the Army Research Laboratory, and Dr. Carl Willis in Kraton Polymers. I would like to thank our funding source from the U.S. Army Research Laboratory and the U.S. Army Research Office under contract/grant number W911NF-07-1-0452 Ionic Liquids in Electro-Active Devices Multidisciplinary University Research Initiative (ILEAD MURI).

Finally, I am forever grateful to my family for their continued love and support in my life endeavors. I am thankful for both my older sisters, Samantha and Danielle. Their love and friendship continues to motivate me in pursuing my goals. I would like to thank Danielle for being a strong role model throughout my graduate career in chemistry. She is a true mentor and scientist. I am deeply thankful to my parents, Leon and Joan Schultz. Words cannot quantify how much I love them. Their love and support throughout my life has strengthened me to pursue all my life goals.

Table of Contents

| | |
|--|-----------|
| Chapter 1. Charged Block Copolymers for Water Purification..... | 1 |
| 1.1 Abstract | 1 |
| 1.2 An Introduction to Reverse Osmosis | 2 |
| 1.2.1 Cellulose Acetate Membranes..... | 2 |
| 1.2.2 Polyamide Thin Film Composite Membranes | 4 |
| 1.2.3 Sulfonated Poly(arylene ether sulfone) Membranes | 6 |
| 1.3 Charged Block Copolymers for Ion Selective Reverse Osmosis Membranes | 8 |
| 1.3.1 An Overview of Nexar™ Sulfonated Pentablock Copolymers..... | 8 |
| 1.4 Produced Water Treatment with Reverse Osmosis Membranes | 13 |
| 1.5 Desalination Strategy Involving Ion Concentration Polarization | 14 |
| 1.6 Conclusions | 15 |
| 1.7 References | 16 |
| Chapter 2. Thermomechanical and Morphological Properties of Random Copolymers Containing Phosphonium Ionic Liquids | 18 |
| 2.1 Abstract | 18 |
| 2.2 Introduction | 19 |
| 2.3 Experimental | 20 |
| 2.3.1 Materials..... | 20 |
| 2.3.3 Analytical Methods | 21 |
| 2.3.4 Synthesis of Phosphonium Salt Monomers..... | 21 |
| 2.3.5 Synthesis of Phosphonium-Containing Random Copolymers | 22 |
| 2.3.6 Anion-Exchange Reaction of Phosphonium-Containing Random Copolymers | 23 |
| 2.4 Results and Discussion..... | 24 |
| 2.5 Conclusions | 31 |
| 2.6 Acknowledgements | 31 |
| 2.7 References | 32 |
| Chapter 3. Structure-Morphology-Property Characterization of Sulfonated Styrenic Pentablock Copolymer Neutralized with a Bis(imidazolyl)alkane..... | 34 |
| 3.1 Abstract | 34 |
| 3.2 Introduction | 35 |
| 3.3 Experimental | 37 |
| 3.3.1 Materials..... | 37 |
| 3.3.2 Analytical Methods | 37 |
| 3.3.3 Synthesis of 1,1'-(1,4-butanediyl)bis(imidazole)..... | 38 |
| 3.3.4 Preparation of KP-SO ₃ [BisIm] ⁺ Membrane | 39 |
| 3.4 Results and Discussion..... | 39 |
| 3.5 Conclusions | 46 |
| 3.6 Acknowledgements | 46 |
| 3.7 References | 47 |
| Chapter 4. Investigating the Thermal Polymerization of 4-Vinylbenzyl piperidine | 49 |
| 4.1 Abstract | 49 |
| 4.2 Introduction | 50 |
| 4.3 Experimental | 52 |
| 4.3.1 Materials..... | 52 |
| 4.3.2 Analytical Methods | 52 |

| | |
|---|-----------|
| 4.3.3 Synthesis of 4-Vinylbenzyl piperidine | 52 |
| 4.3.4 <i>In Situ</i> FTIR Monitoring and Thermal Polymerization of Styrene and 4-Vinylbenzyl piperidine..... | 53 |
| 4.3.5 Thermal Polymerization of Styrene with N-benzyl piperidine | 53 |
| 4.4 Results and Discussion..... | 54 |
| 4.5 Conclusions | 59 |
| 4.6 Acknowledgements | 59 |
| 4.7 References | 60 |
| Chapter 5. Anionic Polymerization of 4-Vinylbenzyl piperidine: Developing a New Class of Ammonium Based Ionic Polymers | 62 |
| 5.1 Abstract | 62 |
| 5.2 Introduction | 63 |
| 5.3 Experimental | 64 |
| 5.3.1 Materials..... | 64 |
| 5.3.2 Analytical Methods | 64 |
| 5.3.3 Synthesis of 4-Vinylbenzyl piperidine | 65 |
| 5.3.4 Poly(vinylbenzyl piperidine) Synthesis | 65 |
| 5.3.5 <i>In Situ</i> FTIR Monitoring and Anionic Polymerization of 4-Vinylbenzyl piperidine..... | 66 |
| 5.3.6 Poly(<i>tert</i> -butyl styrene-co-vinylbenzyl piperidine) Synthesis | 66 |
| 5.3.7 Poly(<i>tert</i> -butyl styrene-co-isoprene-co-vinylbenzyl piperidine) Synthesis | 66 |
| 5.3.8 Alkylation Reaction on Piperidinyl Containing Polymers | 67 |
| 5.4 Results and Discussion..... | 67 |
| 5.5 Conclusions | 72 |
| 5.6 Acknowledgements | 72 |
| 5.7 References | 73 |
| Chapter 6. Future Directions | 75 |
| 6.1 Controlled Polymerization of 4-(Diphenylphosphino) styrene..... | 75 |
| 6.2 Effects of Alkyl Spacer Distance in Bis-imidazolium Neutralized Sulfonated Styrenic Pentablock Copolymers | 76 |
| 6.3 Synthesis of Piperidinyl Based ABC Copolymers..... | 77 |

List of Figures

| | |
|---|----|
| Figure 1.1. General scheme for thin film composite membrane architecture..... | 4 |
| Figure 1.2. Chemical structure for polyaryl ether sulfone, Udel®. | 6 |
| Figure 1.3. General reaction scheme for synthesizing sulfonated polysulfone from Udel® and a) chlorosulfonic acid and b) SO ₃ /triethylphosphate complex. | 7 |
| Figure 1.4. Chemical structure of random, disulfonated poly(arylene ether sulfone) for BPS-X. | 7 |
| Figure 1.5. Chemical Structure of Nexar® sulfonated pentablock copolymer..... | 8 |
| Figure 1.6. Transmission electron micrographs for dilute pentablock copolymer solutions: (a) 50 mol% sulfonation and (b) 26 mol% sulfonation. Dark region indicates stained micelles (0.5 wt tBS and SS blocks are RuO ₄ stained). | 10 |
| Figure 1.7. Graphical representation of sodium chloride permeability vs. donor cell salt concentration for block copolymers and Nafion® 111. | 11 |
| Figure 1.8. Schematic diagram of an ICP desalination process, based on electrokinetic desalination under the influence of an external pressure field | 14 |
| Figure 2.1. ¹ H NMR spectra of Poly(<i>n</i> BA-co-TPhPCI) with 18 mol% of TPhPCI..... | 23 |
| Figure 2.2. Dynamic mechanical temperature sweep for poly(<i>n</i> BA-co-TPhPCI) | 26 |
| Figure 2.3. Dynamic mechanical temperature sweep for poly(<i>n</i> BA-co-TCPCI)..... | 27 |
| Figure 2.4. Dynamic mechanical temperature sweep for poly(<i>n</i> BA-co-TPhPCI) and poly(<i>n</i> BA- co-TCPCI) with 18 mol % of TPhPCI and TCPCI. | 28 |
| Figure 2.5. Dynamic mechanical temperature sweep for poly(<i>n</i> BA-co-TPhPCI) and poly(<i>n</i> BA- co-TCPCI) with 24 mol% of TPhPCI and 23 mol% of TCPCI | 28 |
| Figure 2.6. Dynamic mechanical temperature sweep for poly(<i>n</i> BA-co-TCPCI) with 23 mol% of TCPCI after anion-exchange reaction..... | 30 |
| Figure 2.7. Dynamic mechanical temperature sweep for poly(<i>n</i> BA-co-TPhPCI) with 24 mol% of TPhPCI after anion-exchange reaction. | 30 |
| Figure 3.1. Variable temperature FTIR spectra for Nexar™ sulfonic acid membrane | 40 |
| Figure 3.2. Variable temperature FTIR spectra for Nexar™ bis-imidazolium neutralized sulfonated styrenic pentablock copolymer membrane | 40 |
| Figure 3.3. Surface morphology of (a) Nexar™ polymer, KP-SO ₃ H (b) Nexar™ polymer, KP- SO ₃ [BisIm] ⁺ | 41 |
| Figure 3.4. SAXS for Nexar™ non-neutralized and bis-imidazolium neutralized sulfonated styrenic pentablock copolymer membranes | 42 |
| Figure 3.5. Degree of hydration of sulfonic groups λ (= moles of water/ moles of sulfonation) | 43 |
| Figure 3.6. Tensile stress–strain curves for Nexar™ non-neutralized and bis-imidazolium neutralized sulfonated styrenic pentablock copolymer membranes | 44 |
| Figure 3.7. Dynamic mechanical temperature sweep for Nexar™ bis-imidazolium neutralized sulfonated styrenic copolymer membrane | 45 |
| Figure 4.1. Pseudo-first-order kinetic plot for styrene thermal polymerization. | 55 |

| | |
|--|----|
| Figure 4.2. Pseudo-first-order kinetic plot for 4-vinylbenzyl piperidine thermal polymerization. | 55 |
| Figure 4.3. Arrhenius plot for styrene thermal polymerization 80 °C, 100 °C, and 130 °C..... | 56 |
| Figure 4.4. Arrhenius plot for the thermal polymerization of 4-vinylbenzyl piperidine at 80 °C, 100 °C, and 130 °C..... | 56 |
| Figure 4.5. Pseudo-first-order kinetic plot for styrene thermal polymerization with N-benzyl piperidine..... | 58 |
| Figure 4.6. Arrhenius plot for the thermal polymerization of N-benzyl piperidine at 80 °C, 100 °C, and 130 °C..... | 58 |
| Figure 5.1. Pseudo-first order kinetic plot for 4-vinylbenzyl piperidine | 68 |
| Figure 5.2. ¹ H-NMR characterization of poly(VBP). 400 MHz, CDCl ₃ , 22 °C | 68 |
| Figure 5.3. THF SEC trace for poly(VBP). THF SEC, 1 mL/min, 40 °C, absolute molecular weight | 69 |

List of Tables

| | |
|---|----|
| Table 1.1. Relative block compositions for copolymers A and B..... | 10 |
| Table 1.2. Ion exchange capacities (IECs) and the sulfonation fractions for the middle block styrene repeat units in block copolymers A and B. | 11 |
| Table 2.1. Relative molecular weight characterization of Poly(<i>n</i> BA-co-TPhPCI)s | 24 |
| Table 2.2. Relative molecular weight characterization of Poly(<i>n</i> BA-co-TCPCI)s | 25 |
| Table 2.3. Thermal characterization of phosphonium- containing homopolymers | 29 |
| Table 3.1. Tensile stress–strain results for Nexar™ non-neutralized and bis-imidazolium neutralized sulfonated styrenic pentablock copolymer membranes | 44 |
| Table 3.2. Thermal degradation temperatures for Nexar™ non-neutralized and bis-imidazolium neutralized sulfonated styrenic pentablock copolymer membranes | 44 |
| Table 5.1. Number-average molecular weights and narrow molecular weight distributions of piperidinyl composites..... | 70 |
| Table 5.2. Thermomechanical properties for polyVBP and poly(VBP-TPhPBr) ⁺ | 72 |

List of Schemes

| | |
|--|----|
| Scheme 1.1. General reaction scheme for cellulose acetate synthesis. | 2 |
| Scheme 1.2. General reaction scheme for synthesizing polyamide-based composites | 4 |
| Scheme 2.1. General reaction scheme for copolymerizing <i>n</i> BA with vinylbenzyl triphenyl phosphonium chloride and vinylbenzyl tricyclohexyl phosphonium chloride..... | 24 |
| Scheme 2.2. Anion exchange of phosphonium-containing random copolymers | 29 |
| Scheme 3.1. General reaction scheme for neutralizing Nexar TM sulfonated pentablock copolymer with 1,1'-(1,4-butanediyl)bis(imidazole) | 36 |
| Scheme 4.1. Mayo thermal-initiation mechanism for styrene..... | 50 |
| Scheme 4.2. Mayo thermal-initiation mechanism for 4-vinylbenzyl piperidine..... | 52 |
| Scheme 4.3. Proposed Mayo thermal polymerization mechanism of 4-vinylbenzyl piperidine with competing cationic polymerization mechanism | 57 |
| Scheme 5.1. General reaction scheme for the anionic polymerization of 4-vinylbenzyl piperidine | 67 |
| Scheme 5.2. Anionic polymerization of poly(<i>tert</i> -butylstyrene-co-vinylbenzyl piperidine) from sequential monomer addition..... | 69 |
| Scheme 5.3. Anionic polymerization of poly(<i>tert</i> -butylstyrene-co-isoprene-co-vinylbenzyl piperidineBS-I-VBP) from sequential monomer addition..... | 70 |
| Scheme 5.4. Alkylating Poly(VBP) with bromoalkanes to develop a new class of piperidinium containing polymers | 71 |

Chapter 1. Charged Block Copolymers for Water Purification

1.1 Abstract

Desalination membranes composed of charged block copolymers show potential as an efficient and low cost method for converting saline water into fresh water. Advancements in reverse osmosis technology rendered development for these polymeric materials, which today exhibit a promising future in desalination methods involving ion concentration polarization. This review discusses the progression toward charged block copolymer production and proposes their potential electroactive membrane application in treating salinated water. Common water purification membranes include cellulose acetate (CA) based membranes, polyamide thin film composite (TFC) structures, sulfonated polysulfones, sulfonated pentablock copolymers, and nafion. Desalination membranes must tolerate heat, chlorination, and bacteria. Sulfonated styrenic block copolymers are growing as leading ion selective reverse osmosis membranes. Their design imparts selective charge placement along a well-defined polymer backbone.

Keywords: desalination, reverse osmosis, cellulose acetate, polyamide, sulfonated polysulfone, block copolymer, nafion

1.2 An Introduction to Reverse Osmosis:

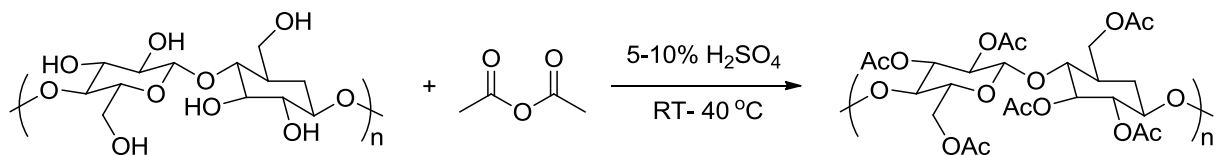
Water desalination technology became a top research priority during the late 1940s and throughout the Kennedy administration. In the early 1950s, Yuster proposed the Gibb's adsorption equation as a theoretical foundation for salt water conversion¹:

$$U = -\frac{1}{2RT} \left(\frac{\partial \sigma}{\partial \ln a} \right)_{TA}$$

In this equation, U expresses the adsorption of solute in moles per sq. cm of surface, R is the gas constant, T is absolute temperature, σ is the surface tension of solution, a is the solute activity, and A is the surface area of the solution.¹

Dr. Yuster applied this mathematical formula to determine that brines will have a 3-4 Å thick layer of relatively pure water when in contact with air or other hydrophobic surfaces. Based on this information, he suggested the possibility of collecting fresh water from a brine solution through a continuous skimming procedure. It was this idea that ultimately developed into reverse osmosis membrane technology.¹

1.2.1 Cellulose Acetate Membranes:



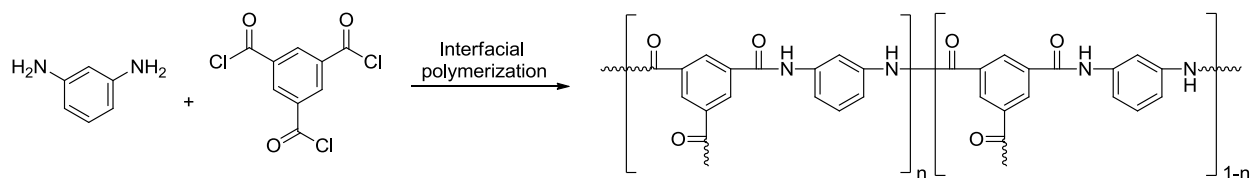
Scheme 1. General reaction scheme for cellulose acetate synthesis.⁴

The first reverse osmosis demonstration was conducted in 1959. At this time, two of Yuster's students, Loeb and Sourirajan, revealed the demineralization properties of cellulose acetate (CA) based membranes.² The researchers showed that such membranes were capable of rejecting 99.5% NaCl content from feed solutions containing ca. 52,500 mg/L. The membranes passed fresh water at reasonable flow rates of ca. 5-11 gallons per square foot per day at realistic pressures of ca. 1500-2000 psig.¹⁻³

While conducting this research, Loeb and Sourirajan concluded that the degree of acetylation heavily influenced desalination (Scheme 1).⁴ Membranes with high acetylation exhibited high salt rejection and low flux rates, while membranes with low acetylation showed low salt rejection and high flux rates.^{1,2} Furthermore, the researchers concluded that CA membranes were incompatible with high temperatures. When desalinating boiling feed solutions, they observed that membranes began to shrink.^{1,2} Other researchers verified these results and determined that ideal feed solution temperatures fell in the range of room temperature to 35 °C.⁵⁻⁸ Overall, Loeb and Sourirajan's success served as a major cornerstone in reverse osmosis membrane technology. The outcome of their research led to the development of the world's first commercial reverse osmosis plant in 1965.¹

Although commercially available for water desalination, CA membranes possess some flaws. The main disadvantage of these membranes is their susceptibility to undergo hydrolysis. As Loeb and Sourirajan concluded, boiling feed solutions will cause CA membranes to shrink. This is the effect of hydrolysis, which will occur when membranes are exposed to high temperatures and extreme pH conditions. Due to this hydrolysis reaction, CA membranes are only compatible with feed solution temperatures ranging from room temperature to 35 °C and pH ranges of 4 to 6.⁴⁻⁸

1.2.2 Polyamide Thin Film Composite Membranes:



Scheme 2. General reaction scheme for synthesizing polyamide-based composites.⁹

In pursuit of expanding reverse osmosis technology from CA membranes, a new class of polymeric material evolved from thin film composite (TFC) structures (Scheme 2).^{9,10} TFCs are composed of a thin polymer layer (barrier layer) formed over an asymmetric support (Figure 1). Polysulfones typically comprise these supports, which attributes their porous properties. Supports are cast on a backing material, usually made from polyester fibers, and are ca. 50 μm in thickness. The barrier layer is most commonly a crosslinked aromatic polyamide film with a thickness range from 20 to over 500 nm (Figure 1).⁹⁻¹²

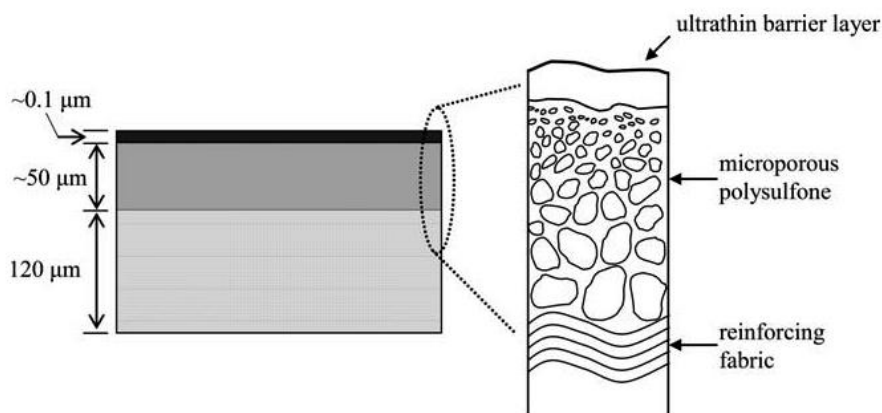


Figure 1. General scheme for thin film composite membrane architecture.⁹

For several years research companies produced various interfacial membranes based on diverse polyamines for commercial production.^{11,13-16} Among these products, the NF-30 ranks as a leading commercially available membrane.^{10,17} Cadotte and FilmTech first introduced this TFC membrane in 1978. Its production stems from the interfacial polymerization between monomeric

aromatic amines with aromatic acyl halides (Figure 1).^{10,17} Acyl halides with functionalities greater than 2.0 serve as a major feature in this synthetic strategy.¹⁷ In particular, Cadotte observed best results when using trimesoyl chloride.¹⁷ Overall, the synthetic method led to an advanced membrane that displayed both high salt rejection and high flux characteristics under seawater conditions. Using feed solutions tuned for standard seawater conditions, NF-30 showed better than 99% salt rejection at a flux rate of ca. 17 gallons per foot per day under a pressure of 800 psig.¹⁷

The NF-30 membrane was a major advancement in reverse osmosis technology. In comparison to cellulose acetate membranes, the NF-30 desalinates feed solutions with a higher salt rejection level, at higher flux rates, and at temperatures exceeding 35 °C. Another advantage to the NF-30 was its chemical resistance to acids and bases.^{10,17} Consequently, the NF-30 has served among the leading commercially available desalination membranes for the past thirty years.

The main disadvantage with the NF-30 membrane is its intolerance to halogen-based disinfectants such as hypochlorous acid and hypochlorite ion.^{10,12,17,18} In order to avoid aromatic chlorination, the NF-30 membrane can only be used in pH conditions greater than 5.^{10,17} Consequently, research continued to expand off Cadotte's work in order to produce a membrane more compatible with water chlorination treatments.

1.2.3 Sulfonated Poly(arylene ether sulfone) Membranes

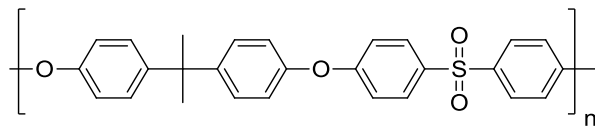


Figure 2. Chemical structure for polyaryl ether sulfone, Udel®.¹⁸

Research ultimately progressed toward polysulfone based membranes in order to develop materials that could tolerate chlorination. Polyaryl ether sulfone, also known as Udel®, is among such common commercially available membranes (Figure 2).¹⁹ Unlike aromatic polyamides, polysulfones incorporate aromatic rings and chemically strong bonds between carbon, sulfur, and oxygen. Also, these polymers do not contain chlorine sensitive amide linkages. The main challenge with these membranes, however, is that they are hydrophobic. As a result, nonporous conventional polysulfones are limited in desalination because of its poor water permeation and flux rates.^{19,20}

For several years many researchers pursued post sulfonation reactions in order to reduce hydrophobicity. Among these investigations, Quentin is notably accredited for treating Udel® polysulfone with chlorosulfonic acid (Figure 3a).^{19,21} Noshay and Robeson are also recognized for their alternative method involving a 2:1 complex containing sulfur trioxide and triethylphosphate (Figure 3b).^{19,22,23} The development of these reactions helped lead to developing polysulfone membranes suitable for desalination. However, such methods are difficult to control the degree of sulfonation and may lead to undesirable side reactions such as polymer cleavage and branching.¹⁹

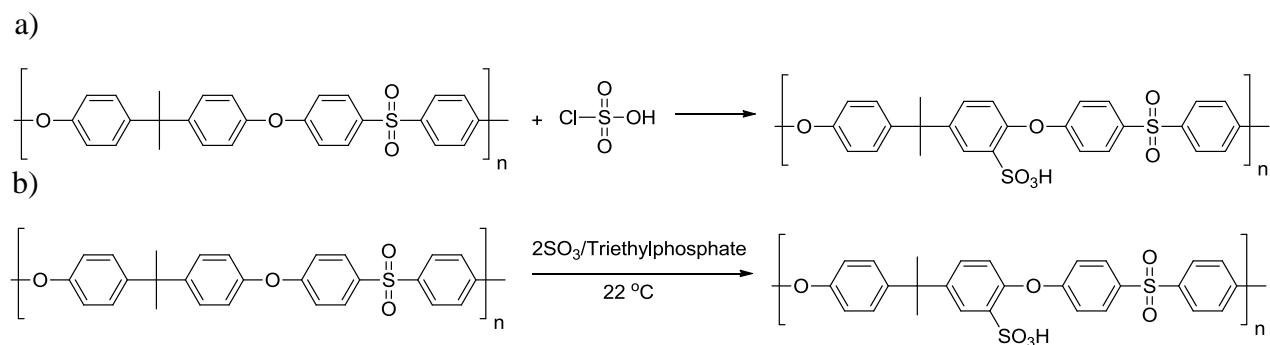


Figure 3. General reaction scheme for synthesizing sulfonated polysulfone from Udel® and a) chlorosulfonic acid and b) 2SO₃/triethylphosphate complex.¹⁸

McGrath *et. al.* modified polysulfone with hydrophilic comonomers to circumvent this issue. The advantage of this method is the production of membranes that exhibit selective ion transport while maintaining high tolerance to aqueous chlorine. McGrath *et. al.* produced a collection of directly copolymerized sulfonated poly(arylene ether sulfones) using this method.^{20,24-29} The BPS-X series is included in this collection (Figure 4).²⁹

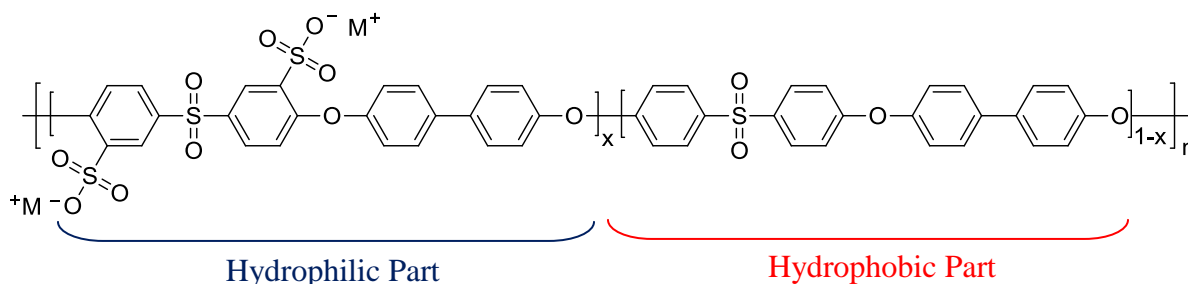


Figure 4. Chemical structure of random, disulfonated poly(arylene ether sulfone) for BPS-X.²⁸

According to these researchers, disulfonation levels can be varied in BPS copolymers. Their findings indicated that BPS membranes withstand chlorine exposure while achieving good but not excellent salt rejection. The researchers reported 98.2% salt rejection using a BPS membrane with 20 mol% sulfonation.^{20,29} This result was obtained with a feed solution containing 2,000 ppm NaCl and 500 ppm NaOCl and a pressure of 400 psig.^{20,29} Increasing sulfonation levels led to an increase in water permeability, and led to a decrease in salt rejection.^{20,29}

Overall, the work conducted with sulfonated (polyarylene ether sulfones) helped reverse osmosis technology progress from polyamide thin film composite membranes and conventional polysulfone membranes. They showed strong resistance to chlorine while achieving moderate salt rejection levels. However, the main drawback for these random copolymer systems is their limitation in sulfonation. McGrath *et. al.* determined that these linear systems become water soluble at high sulfonation levels.^{20,29}

1.3 Charged Block Copolymers for Future Ion Selective Reverse Osmosis Membranes:

1.3.1 An Overview of Nexar[®] Sulfonated Pentablock Copolymers

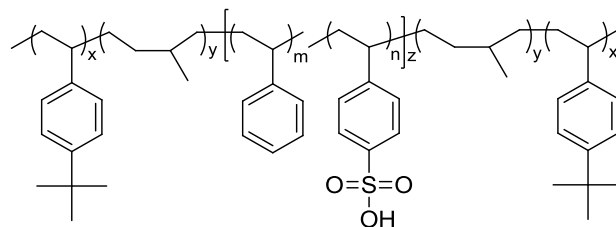


Figure 5. Chemical Structure of Nexar[®] sulfonated pentablock copolymer, (tBS-HI-SS-HI-tBS).³⁰

A current approach toward developing ion selective reverse osmosis membranes involves sulfonated styrenic block copolymers. Such architectures transport ions and absorb high water content while retaining mechanical and physical properties such as tensile strength, elongation, flexibility, etc.³⁰ Consequently, these polymeric materials exhibit ideal desalination characteristics. In 2007, Willis and researchers at Kraton Performance Polymers, Inc. (Houston, TX) developed Nexar[®] sulfonated pentablock copolymers (Figure 5).^{31,32} These materials serve as commercial prototypes for charged block copolymer based desalination membranes. Nexar[®] pentablock copolymers incorporate outer hydrophobic tert-butyl styrene end blocks (tBS),

hydrogenated isoprene inner blocks (HI), and a middle styrenic block that selectively undergoes sulfonation via a post-polymerization sulfonation process (SS).³¹

According to Kraton's product brochure, Nexar[®] polymers withstand chlorination, reveal high ionic conductivity, and offer contamination removal specificity.³³ These attributes are suitable for water purification technologies involving reverse osmosis.³³ They are also compatible for alternative methods including: electrodialysis, electrodialysis reversal, and reversed electrodialysis.³³ Nexar[®] polymers also offer a flexible platform for modification. This characteristic enables control over hydrophilic/hydrophobic properties.³¹ Sulfonation tunes the polymers' hydrophilic nature, which occurs selectively along the inner block to provide ionic channels for water and ion transportation.³¹ Varying *tert*-butyl styrene outer blocks tunes the polymers' hydrophobic property, which limits water permeation.³¹ Consequently, modification controls Nexar[®] membranes' swelling and mechanical properties when hydrated.

In 2010, Winey *et. al.* conducted small-angle X-ray scattering (SAXS) and transmission electron microscopy (TEM) analysis to investigate the solution morphology of these pentablock copolymers.³⁴ This analysis provided insight into Nexar[®] polymers' architecture in cyclohexane and heptane solutions and revealed the morphological influence of sulfonation levels. According to SAXS results, interpreted with the Kinning-Thomas model³⁵, Nexar[®] polymers revealed spherical micellar morphology.³⁴ This resulted for all sulfonated levels. Under the nonpolar solvent conditions, an outer shell (corona) of solvated HI-tBS and an inner core of insoluble SS characterized the formed micelles.³⁴ As the level of sulfonation increased, Winey *et. al.* noticed an overall decrease in micelle density, an increase in the micelle core radius, and an increase in the distance between cores.³⁴ The researchers supported these results with TEM images (Figure 6).³⁴

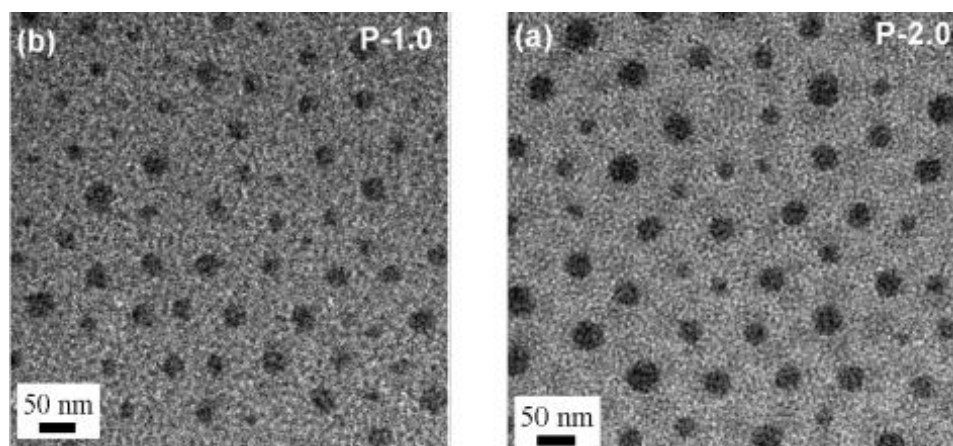


Figure 6. Transmission electron micrographs for dilute pentablock copolymer solutions: (a) 50 mol% sulfonation and (b) 26 mol% sulfonation. Dark region indicates stained micelles (0.5 wt tBS and SS blocks are RuO₄ stained).³³

This analysis successfully presented insight into Nexar[®] polymers' solution morphology. It serves as a guide to understanding correlations between solution morphology, solution viscosity, and membrane morphology. Currently, Winey *et. al.* are conducting membrane morphology studies. These findings will be published in the near future.³⁴

Freeman *et. al.* conducted a series of experiments to evaluate water and salt transport properties for a family of Nexar[®] polymers.³¹ This investigation involved two base copolymers (A and B) with structural properties highlighted in Table I & II.³¹

Table I. Relative block compositions for copolymers A and B.³⁰

| Block Copolymer | Relative Block Composition (by mass) | | |
|-----------------|--------------------------------------|-----------------------|---------|
| | <i>Tert</i> -butyl styrene | Hydrogenated isoprene | Styrene |
| A | 0.62 | 0.64 | 1.00 |
| B | 1.04 | 0.72 | 1.00 |

Table II. Ion exchange capacities (IECs) and the sulfonation fractions for the middle block styrene repeat units in block copolymers A and B.³⁰

| Block copolymer A | | Block copolymer B | |
|-------------------|----------------------|-------------------|----------------------|
| IEC [meq/g] | Sulfonation fraction | IEC [meq/g] | Sulfonation fraction |
| 1.46 | 0.30 | 0.4 | 0.10 |
| 1.6 | 0.33 | 0.7 | 0.18 |
| 2.0 | 0.41 | 1.0 | 0.26 |
| | | 1.5 | 0.39 |
| | | 2.0 | 0.52 |

As seen from Table I, hydrophobic *tert*-butyl styrene content varies copolymer A from B. Table II indicates the degree of sulfonation for both copolymers. Taking these structural properties into account, Freeman *et. al.* employed water permeability, salt permeability, and surface charge (zeta potential) experiments to characterize the copolymers.³¹

Water uptake analysis revealed a directly proportional relationship between water permeability and sulfonation levels. It also showed that water uptake reduced when *tert*-butyl styrene content increased.³¹ Salt permeability analysis produced similar results, showing a directly proportional relationship between sodium chloride uptake and sulfonation fraction. Likewise, increasing hydrophobic content along the copolymer reduced salt uptake. In addition to these

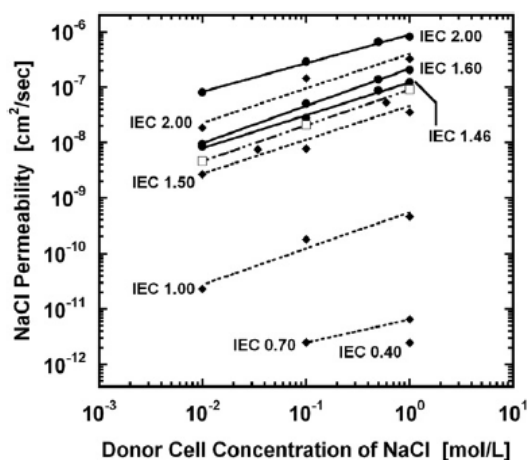


Figure 7. Graphical representation of sodium chloride permeability vs. donor cell salt concentration for block copolymers A (●) and B (◆) and Nafion® 111 (□). IEC values in units of meq/g.³⁰

factors, Freeman *et. al.* also noticed comparable behavior between salt uptake and the donor cell sodium concentration levels. This suggested that these membranes operate under Donnan exclusion effects. Overall, these trends seemed to compare and even exceed salt permeability measurements For Nafion[®] 111. These results are highlighted in Figure 7.³¹

In addition to these experiments, Freeman *et. al.* also evaluated the surface charge properties for both block copolymers. The researchers applied the Fairbrother Mastin approximation to calculate zeta potentials for the pentablock copolymers with varying sulfonation.³⁶ Before running the test, the researchers soaked each membrane in a 10mM NaCl solution to convert all sulfonated styrene middle blocks along the pentablock copolymer backbones into sodium sulfonate. Once this was accomplished, the NaOH or HCl solutions adjusted the pH environments from 10 to 3 in increments of 0.3. The researchers measured streaming potentials while changing this variable. The data collected in this experiment revealed that zeta potentials became more neutral as sulfonation levels increased. Alternatively, these values became more negative for an unsulfonated membrane. These results indicate that an uncharged hydrophobic membrane is more susceptible to undergo surface sorption with anionic species. As sulfonation increases, membranes will preferentially attract cationic species. This interaction inhibits surface sorption.³¹

Freeman and researchers' work highlights the unique properties of Nexar[®] pentablock copolymer membranes. Among these properties is resistance to pH fluctuation, indicating durability in the presence of chlorine and anionic species. Another advantage of these systems is their unique architectural structure that allows selective tuning to adjust degree of charge and hydrophobicity. Such control will offer manufacturing companies the luxury of manipulating these membranes to meet the requirements of varying water purification demands.

1.4 Produced Water Treatment with Reverse Osmosis Membranes:

One of the main challenges in treating produced water with commercially available reverse osmosis membranes is that such films have a strong tendency to foul in the presence of hydrocarbon based solutions.³⁷⁻⁴⁸ Fouling occurs when the hydrocarbon particulates or other contaminants deposit on a membranes surface, making it more difficult to desalinate a feed solution at effective flux rates.^{44,45} In order to adjust current reverse osmosis membranes, such as polyamide thin film composites, some research has shown the effectiveness of modifying the membranes with smooth hydrophilic membrane coatings.³⁷⁻⁴⁸ Typical coatings consist of PEG-based hydrogels, which are well known for their hydrophilicity, biocompatibility, and their applicability in modification syntheses.^{44,45}

The main disadvantage to incorporating hydrogel based coatings, is that it includes an additional step for manufacturing companies that requires extra materials and costs.⁴⁹ A proposed alternative to this method involves utilizing charged block copolymers in a desalination process based on ion concentration polarization (ICP), a phenomenon that happens when an ion current is passed through ion-selective membranes.⁵⁰⁻⁵⁶

1.5 Desalination Strategy Involving Ion Concentration Polarization:

Sung Jae Kim *et. al.* exploited the ion selectivity characteristics of a Nafion[®] membrane and developed a direct seawater desalination process using this phenomenon.⁴⁶ A diagram of this experiment is seen in Figure 8.⁴⁶

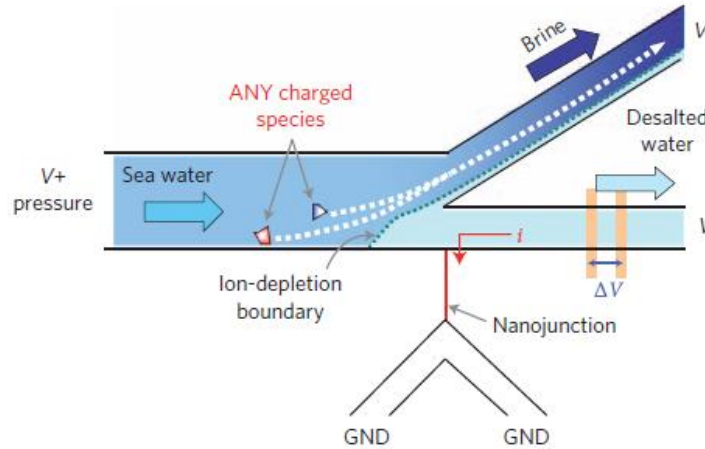


Figure 8. Schematic diagram of an ICP desalination process, based on electrokinetic desalination under the influence of an external pressure field.⁴⁵

In this system, ICP triggers the cation exchange membrane and directs concentrations of cations and anions in solution toward the cathodic side of the junction and away from the anodic side. In effect, brine flows away from the membrane as fresh water permeates to a collection channel. Additional charged contaminants follow as brine diverts into a “salted” stream. The purification method also removed particles including bacteria, viruses, red blood cells, and white blood cells. This indicated that the membrane conductivity interactions diverted contaminants from fouling the surface. Overall, the researchers determined that ICP desalination systems could remove up to 99% of salt from feed solutions containing 500 mM NaCl. This process occurred with zero fouling and at power consumption less than 3.5 Whl⁻¹.⁴⁶

Freeman *et al.* showed that Nexar[®] pentablock copolymers exhibit similar salt permeability characteristics as Nafion[®].³¹ This may suggest that both materials are comparable

perm-selective ion transport membranes. As result, Nexar[®] membranes possibly hold a promising future in ICP desalination technology. One advantage to exploiting Nexar[®] films in such systems is their flexibility in modification. Sulfonated styrenic middle block units can undergo chemical transformation to produce a library of charged pentablock copolymers. Such an advantage could selectively produce ICP water purification membranes suitable for a variety of contaminated waters, ranging from seawater to produced wastewater from hydraulic fracturing.

1.6 Conclusions:

This chapter briefly described commonly studied desalination membranes. A current approach toward developing ion selective reverse osmosis membranes involves sulfonated styrenic polymers. Sulfonated polysulfones first highlighted the chlorine resistant, robust nature of sulfonated water purification membranes. Technology is advancing toward sulfonated block copolymer membranes. Such architectures transport ions and absorb high water content while retaining mechanical and physical properties such as tensile strength, elongation, flexibility, etc. Consequently, charged block copolymers show potential as an efficient and low cost method for converting saline water into fresh water.

1.7 References:

- (1) Loeb, S. In *Synthetic Membranes* **1981**, 153, 1.
- (2) Loeb, S.; Sourirajan, S. In *Saline Water Conversion* **1963**, 38, 117.
- (3) Sagle AC, F. B. In *The Future of Desalination in Texas*; Arroyo, J. A., Ed.; Texas Water Development Board: Austin, TX, 2004; Vol. II, p 137.
- (4) Malm, C. J.; Tanghe, L. J.; Laird, B. C. *Industrial & Engineering Chemistry* **1946**, 38, 77.
- (5) Kesting, R. E. *Journal of Applied Polymer Science* **1965**, 9, 663.
- (6) Kesting, R. E.; Barsh, M. K.; Vincent, A. L. *J. Appl. Polym. Sci.* **1965**, 9, 1873.
- (7) Kesting, R. E.; Subcasky, W. J.; Paton, J. D. *Journal of Colloid and Interface Science* **1968**, 28, 156.
- (8) Košutić, K.; Kunst, B. *Journal of Applied Polymer Science* **2001**, 81, 1768.
- (9) Hogan, P. A.; Sudjito; Fane, A. G.; Morrison, G. L. *Desalination* **1991**, 81, 81.
- (10) Geise, G. M.; Lee, H.-S.; Miller, D. J.; Freeman, B. D.; McGrath, J. E.; Paul, D. R. *Journal of Polymer Science Part B: Polymer Physics* **2010**, 48, 1685.
- (11) Cadotte, J. E.; Petersen, R. J.; Larson, R. E.; Erickson, E. E. *Desalination* **1980**, 32, 25.
- (12) Cadotte John, E. In *Materials Science of Synthetic Membranes*; American Chemical Society: 1985; Vol. 269, p 273.
- (13) Cadotte, J.; Forester, R.; Kim, M.; Petersen, R.; Stocker, T. *Desalination* **1988**, 70, 77.
- (14) Kurihara, M.; Himeshima, Y. *Polym. J.* **1991**, 23, 513.
- (15) Kurihara, M.; Uemura, T.; Nakagawa, Y.; Tonomura, T. *Desalination* **1985**, 54, 75.
- (16) Riley, R. L.; Fox, R. L.; Lyons, C. R.; Milstead, C. E.; Seroy, M. W.; Tagami, M. *Desalination* **1976**, 19, 113.
- (17) Robert J, P. *Journal of membrane science* **1993**, 83, 81.
- (18) Avlonitis, S.; Hanbury, W. T.; Hodgkiess, T. *Desalination* **1992**, 85, 321.
- (19) Johnson, B. C.; Yilgor, I.; Tran, C.; Iqbal, M.; Wightman, J. P.; Lloyd, D. R.; McGrath, J. E. *J. Polym. Sci., Polym. Chem. Ed.* **1984**, 22, 721.
- (20) Park, H. B.; Freeman, B. D.; Zhang, Z.-B.; Sankir, M.; McGrath, J. E. *Angewandte Chemie International Edition* **2008**, 47, 6019.
- (21) Quentin, J. P.; Rhone-Poulenc S. A. . 1979, p 23 pp.
- (22) Robeson, L. M.; Matzner, M.; Union Carbide Corp., USA . 1982, p 57 pp.
- (23) Noshay, A.; Robeson, L. M. *J. Appl. Polym. Sci.* **1976**, 20, 1885.
- (24) Harrison, W. L.; Hickner, M. A.; Kim, Y. S.; McGrath, J. E. *Fuel Cells* **2005**, 5, 201.
- (25) Hickner, M. A.; Ghassemi, H.; Kim, Y. S.; Einsla, B. R.; McGrath, J. E. *Chem. Rev.* **2004**, 104, 4587.
- (26) Sumner, M. J.; Harrison, W. L.; Weyers, R. M.; Kim, Y. S.; McGrath, J. E.; Riffle, J. S.; Brink, A.; Brink, M. H. *J. Membr. Sci.* **2004**, 239, 199.
- (27) Wang, S. McGrath, J. E. In *Synthetic Methods In Step-Growth Polymers*; Rogers, M. E. L., Timothy E., Ed.; Wiley: New York, 2003, p 327.
- (28) Xie, W.; Cook, J.; Park, H. B.; Freeman, B. D.; Lee, C. H.; McGrath, J. E. *Polymer* **2011**, 52, 2032.

- (29) Xie, W.; Park, H.-B.; Cook, J.; Lee, C. H.; Byun, G.; Freeman, B. D.; McGrath, J. E. *Water Sci. Technol.* **2010**, *61*, 619.
- (30) Winkler, D. L. E.; Shell Oil Co. . 1971, p 3 pp.
- (31) Geise, G. M.; Freeman, B. D.; Paul, D. R. *Polymer* **2010**, *51*, 5815.
- (32) Willis, C. L.; Handlin, D. L., Jr.; Trenor, S. R.; Mather, B. D.; Kraton Polymers Research B.V., Neth. . 2007, p 98pp.
- (33) Kraton Polymers LLC. *Nexar Polymers: Delivering New Solutions Today*. Kraton Polymers LLC; Houston **2010**. <http://www.nexarpolymers.com>
- (34) Choi, J.-H.; Kota, A.; Winey, K. I. *Industrial & Engineering Chemistry Research* **2010**, *49*, 12093.
- (35) Kinning, D. J.; Thomas, E. L. *Macromolecules* **1984**, *17*, 1712.
- (36) Elimelech, M.; Chen, W. H.; Waypa, J. J. *Desalination* **1994**, *95*, 269.
- (37) Freeman, B. D., Pinnau, I. *Advanced Materials for Membrane Separations*; American Chemical Society: Washington, DC, 2004; Vol. 876.
- (38) Belfort, G. *Desalination* **1980**, *34*, 159.
- (39) Belfort, G.; Alexandrowicz, G.; Marx, B. *Desalination* **1976**, *19*, 127.
- (40) Cohen, R. D.; Probstein, R. F. *Journal of Colloid and Interface Science* **1986**, *114*, 194.
- (41) Elimelech, M.; Xiaohua, Z.; Childress, A. E.; Seungkwan, H. *Journal of membrane science* **1997**, *127*, 101.
- (42) Greenlee, L. F.; Lawler, D. F.; Freeman, B. D.; Marrot, B.; Moulin, P. *Water Research* **2009**, *43*, 2317.
- (43) Potts, D. E.; Ahlert, R. C.; Wang, S. S. *Desalination* **1981**, *36*, 235.
- (44) Sagle, A. C. *Polymer* **2009**, *50*, 756.
- (45) Sagle, A. C.; Van, W. E. M.; Ju, H.; McCloskey, B. D.; Freeman, B. D.; Sharma, M. M. *J. Membr. Sci.* **2009**, *340*, 92.
- (46) Zhang, Q.; Zhang, S.; Dai, L.; Chen, X. *Journal of membrane science* **2010**, *349*, 217.
- (47) Ju, H.; McCloskey, B. D.; Sagle, A. C.; Wu, Y.-H.; Kusuma, V. A.; Freeman, B. D. *J. Membr. Sci.* **2008**, *307*, 260.
- (48) Hatakeyama, E. S.; Ju, H.; Gabriel, C. J.; Lohr, J. L.; Bara, J. E.; Noble, R. D.; Freeman, B. D.; Gin, D. L. *J. Membr. Sci.* **2009**, *330*, 104.
- (49) Sung Jae, K.; Sung Hee, K.; Kwan Hyung, K.; Jongyoon, H. *Nature Nanotechnology* **2010**, *5*, 297.
- (50) Block, M.; Kitchener, J. A. *J. Electrochem. Soc.* **1966**, *113*, 947.
- (51) Choi, J.-H.; Lee, H.-J.; Moon, S.-H. *Journal of Colloid and Interface Science* **2001**, *238*, 188.
- (52) Forgacs, C.; Ishibashi, N.; Leibovitz, J.; Sinkovic, J.; Spiegler, K. S. *Desalination* **1972**, *10*, 181.
- (53) Kim, S. J.; Song, Y.-A.; Han, J. *Chem. Soc. Rev.* **2010**, *39*, 912.
- (54) Pu, Q.; Yun, J.; Temkin, H.; Liu, S. *Nano Letters* **2004**, *4*, 1099.
- (55) Rubinstein, I.; Shtilman, L. *J. Chem. Soc., Faraday Trans. 2* **1979**, *75*, 231.
- (56) Rubinstein, I.; Zaltzman, B. *Phys. Rev. E: Stat. Phys., Plasmas, Fluids, Relat. Interdiscip. Top.* **2000**, *62*, 2238.

Chapter 2. Thermomechanical and Morphological Properties of Random Copolymers Containing Phosphonium Ionic Liquids

2.1 Abstract

Conventional free radical polymerization and anion exchange achieved copolymers of *n*-butyl acrylate and phosphonium ionic liquids. Copolymers containing vinylbenzyl triphenyl phosphonium and vinylbenzyl tricyclohexyl phosphonium cations bearing chloride (Cl), or bis(trifluoromethane sulfonyl)imide (Tf₂N) counteranions were specifically investigated to elucidate the effects of cyclic substituents and counteranions on structure-property relationships. Differential scanning calorimetry (DSC) and dynamic mechanical analysis (DMA) provided the thermomechanical properties of these phosphonium cation-containing random copolymers. Factors including cyclic substituents, counteranion type, as well as ionic concentration significantly influenced phosphonium cation association.

KEYWORDS: anion exchange, counteranion, copolymerization, glass transition, ionic liquids, phosphonium, radical polymerization

2.2 Introduction

Polymeric ionic liquids (PILs) are unique macromolecules that incorporate cationic or anionic pendant sites along a polymer backbone. PILs offer beneficial ionic liquid properties such as ionic conductivity, thermal and chemical stability, and anion exchange capability.¹⁻³ These features blend with enhanced performing polymers to provide novel conductive membranes with robust mechanical stability, efficient processability, and tunable macromolecular design.^{1,4-9} PILs offer promising applications in areas such as water purification^{10,11}, CO₂ absorption^{12,13}, gene delivery^{14,15}, biosensors¹⁶, fuel cells^{17,18}, and actuators.¹⁹⁻²¹

PIL synthesis involves either polymerizing ionic liquid monomers or functionalizing existing polymers. Most studies highlight polymers containing ammonium and imidazolium cations with counteranions such as halides, tetrafluoroborate (BF₄), hexafluorophosphate (PF₆), and bis(trifluoromethanesulfonyl)imide ((CF₃SO₂)₂N).^{1,2,9,22-27} These charged polymers exhibit alkylation efficiency, thermal stability, and base stability.^{1,9,16} Current research is shifting toward phosphonium containing PILs. These compositions demonstrate enhanced performance characteristics over traditional ammonium and imidazolium analogues. Phosphonium derivatives offer increased thermal stabilities^{28,29}, biocompatibility^{14,15}, antimicrobial activity^{10,30}, and ionic aggregation.³¹

Post-polymerization modification and free radical polymerization strategies achieve phosphonium PILs. Synthetic studies report styrenic-, acrylate-, and methacrylate- based phosphonium monomers. Long *et. al.* studied random copolymers involving *n*-butyl acrylate (*n*BA) and phosphonium salts containing either octyl (OPCl) or butyl (BPCl) chains.³ This research emphasized counteranion and alkyl chain length effects on thermal and mechanical

properties. Long *et. al.* later employed nitroxide-mediated polymerization to synthesize ABA copolymers.³² These compositions emulated the original *n*BA-co-trialkyl phosphonium PIL design, but enforced phase separation for enhanced thermomechanical properties. Other synthetic studies disclose atom transfer (ATRP)³³, and reversible addition-fragmentation transfer (RAFT)^{14,34,35} polymerization methods for achieving well-defined phosphonium PILs.

In this study, *n*BA is copolymerized with vinylbenzyl phosphonium cyclic monomers using conventional free radical polymerization. Copolymers involving vinylbenzyl triphenyl phosphonium and vinylbenzyl tricyclohexyl phosphonium cations bearing chloride (Cl), or bis(trifluoromethane sulfonyl)imide (Tf₂N) counteranions are specifically investigated to elucidate the effects of cyclic substituents and counteranions on structure-property relationships. Developing an understanding and a sense of control over these relationships will help further expand the versatile and highly useful nature of phosphonium-containing polymers.

2.3 Experimental

2.3.1 Materials

Triphenylphosphine (99+%), tricyclohexylphosphine (99+%), 4-vinylbenzyl chloride (90%), 2,6-di-*tert*-butyl-4-methylphenol (99%), sodium tetrafluoroborate (NaBF₄) (98%), and lithium bis(trifluoromethane sulfonyl)imide (LiTf₂N) (99%) were purchased from Aldrich and used without further purification. *n*-Butyl acrylate (99%) was purchased from Aldrich and was vacuum distilled from calcium hydride. α,α' -Azobis(isobutyronitrile) (AIBN; from Fluka) was recrystallized from methanol. Hexanes (Fisher Scientific, HPLC grade), tetrahydrofuran (THF; Fisher Scientific, HPLC grade), and N,N-dimethylformamide (DMF; Fisher Scientific, HPLC grade, anhydrous) were used as received. Triphenyl-4-vinylbenzyl phosphonium chloride

(TPhPCI) and tricyclohexyl-4-vinylbenzyl phosphonium chloride (TCPCI) were synthesized according to the previous literature.^{3,36}

2.3.2 Analytical Methods

¹H NMR and ³¹P NMR spectra were collected in CDCl₃ on a Varian INOVA spectrometer operating at 400 MHz, 23 °C. Fast atom bombardment mass spectrometry was conducted in positive ion mode on a JEOL HX110 dual focusing mass spectrometer. Size exclusion chromatography (SEC) was used to determine the molecular weights of phosphonium-containing random copolymers at 50 °C in DMF with 0.05 M lithium bromide (LiBr) at 1 mL/min. DMF SEC was performed on a Waters SEC equipped with two Waters Styragel HR5E (DMF) columns, a Waters 717plus autosampler, and a Waters 2414 differential refractive index detector. Reported molecular weights are relative to polystyrene standards.

Thermogravimetric analysis (TGA) was performed on a TA Instruments Q500TM TGA from ambient to 600 °C at 10 °C/min. Thermal degradation temperatures (Tds) were determined at 5% weight loss. Differential scanning calorimetry (DSC) was performed under a nitrogen flush of 50 mL/min at a heating rate of 10 °C/min on a TA instruments Q1000TM DSC. Dynamic mechanical analysis (DMA) was conducted on a TA Instruments Q800 Dynamic Mechanical Analyzer in tension mode at a frequency of 1 Hz, an oscillatory amplitude of 15 μm, and a static force of 0.01 N. The temperature ramp was 3 °C/min. The glass transition temperature (Tg) was determined at the onset temperature.

2.3.3 Synthesis of Phosphonium Salt Monomers.

All monomers were synthesized following similar procedures in the previous literature.^{3,37} The synthesis of triphenyl-(4-vinylbenzyl)phosphonium chloride follows as an example. Triphenylphosphine (7.16 g, 27.3 mmol) and 2,6-di-*tert*-butyl-4-methylphenol (0.1g,

0.453 mmol) were added to a flame-dried 100 mL round bottomed flask, containing a magnetic stir bar and reflux condenser. Dry acetonitrile (60 mL) was added and the solution was purged under N₂ for 15 min. 4-Vinylbenzyl chloride (4.62 mL, 32.8 mmol) was added to the flask dropwise. The yellow solution was heated to 82 °C for 24 h, and the monomer was precipitated into 1 L of a diethyl ether. The solid was vacuum filtered and washed with hexanes. The resulting white crystals were dried at reduced pressure (0.5 mmHg) to obtain a final yield of 10.5 g (93% yield). ¹H NMR (400 MHz, CDCl₃, 25 °C, δ): 5.20 (1H, d, vinyl proton), 5.60 (1H, d, vinyl proton), 5.53 (2H, d, -CH₂-P), 6.60 (1H, dd, vinyl proton), 6.9-7.3 (4H, m, aromatic protons), 7.5-8.0 (15H, m, aromatic protons). ³¹P NMR: 22.92. Mass Spectrometry: Theoretical, m/z 379.1616; Experimental, m/z 379.1629.

2.3.4 Synthesis of Phosphonium-Containing Random Copolymers.

Poly(*n*BA-co-TPhPCl) and poly(*n*BA-co-TCPCl) random copolymers were synthesized using conventional free radical polymerization with AIBN as the initiator in DMF solution. A typical synthesis was performed as follows: TPhPCl (0.705 g, 1.70 mmol) was weighed into a 25 mL, round-bottomed flask containing a magnetic stirbar. The flask was sealed with a rubber septum and purged with N₂ for 20 min. Anhydrous DMF (8 mL, 20 wt % of solid) was subsequently added to the flask to dissolve the phosphonium-containing monomer. Purified *n*-butyl acrylate (1.18 mL, 8.2 mmol) was syringed into the reaction flask. Lastly, AIBN (8.2 mg, 0.5 mol %) was dissolved in 5 mL of anhydrous DMF and flushed with dry nitrogen for 10 min and was then syringed into the reaction mixture. The reaction flask was placed in an oil bath at 65 °C for 24 h with constant stirring. After polymerization, DMF was removed on vacuum distillation. The product was dialyzed against methanol for 3 days. The final products were dried at 50 °C under reduced pressure (0.5 mmHg) for 24 h. ¹H-NMR confirmed mole fraction of

phosphonium units in the copolymer series. Integrating total aromatic protons to methylene protons achieved mole fraction values (Figure 1). The product contained 18 mol% TPhPCl and 82 mol % *n*BA.

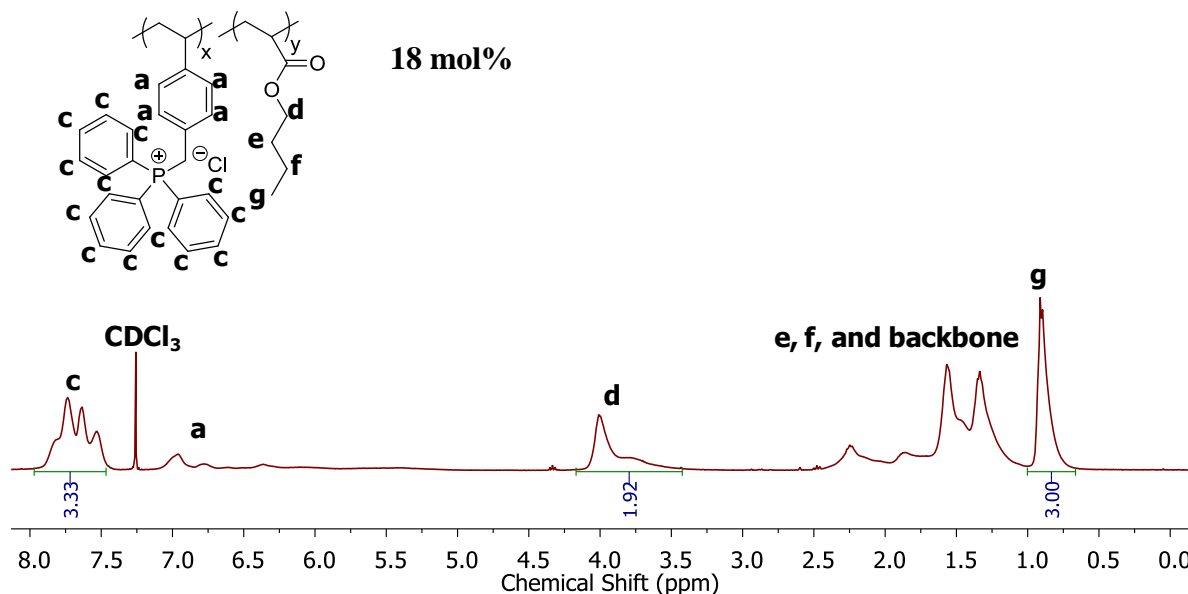
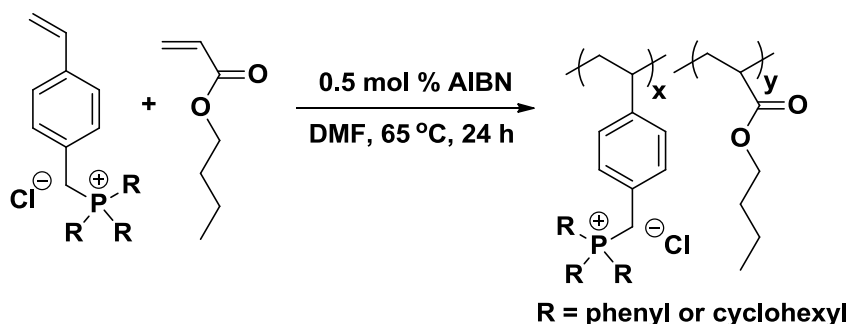


Figure 1. ^1H NMR spectra of Poly(*n*BA-co-TPhPCl) with 18 mol% of TPhPCl.

2.3.5 Anion-Exchange Reaction of Phosphonium-Containing Random Copolymers.

The following protocol describes a typical anion exchange of chloride with Tf_2N in phosphonium-containing polymers. 6.00 g (excess) of LiTf_2N was dissolved in 200 mL of dichloromethane, and 1 g of phosphonium-containing polymer was dissolved in 10 mL of dichloromethane. The dissolved polymer was added dropwise to the LiTf_2N solution and was allowed to mix overnight at room temperature. The final solution was filtered and washed with 100 mL deionized water three times. The organic phases were collected and titrated with silver nitrate. Silver chloride precipitate was not observed, indicating complete chloride anion exchange. Dichloromethane was roto-evaporated, and the product was dried under reduced pressure at 30 °C for 48 h.

2.4 Results and Discussion



Scheme 1. General reaction scheme for copolymerizing *n*BA with vinylbenzyl triphenyl phosphonium chloride and vinylbenzyl tricyclohexyl phosphonium chloride.

Phosphonium chloride monomers substituted with either triphenyl (TPhPCl) or tricyclohexyl (TCPCl) groups were readily synthesized in a single step alkylation reaction. Scheme 1 depicts the conventional free radical polymerization strategy for synthesizing poly(TPhPCl), poly(TCPCl), poly(*n*BA-co-TPhPCl), and poly(*n*BA-co-TCPCl) random copolymers. ¹H-NMR confirmed all polymers and determined the mole fraction of phosphonium units in the copolymer series. Final copolymers had similar compositions to the feed, indicating successful copolymerization. SEC was employed to determine relative molecular weights for all polymers. Dynamic light scattering ensured 0.05 M LiBr in DMF as a proper SEC solvent with minimal aggregation. Tables I and II summarize mole fraction values and relative molecular weights.

Table I. Relative Molecular Weight Characterization of Poly(*n*BA-co-TPhPCl)s

| PhPCl in Feed (mol %) | PhPCl in Polymer (mol %) | PhPCl in Polymer (wt %) | M _n by SEC (g/mol x 10 ⁻³) | M _w /M _n |
|-----------------------|--------------------------|-------------------------|---|--------------------------------|
| 4 | 4 | 10 | 36.3 | 2.17 |
| 8 | 10 | 22 | 42.5 | 2.13 |
| 17 | 18 | 40 | 46.1 | 2.28 |
| 24 | 24 | 55 | 67.1 | 2.46 |
| 50 | 55 | 80 | 68.6 | 2.33 |
| 100 | 100 | 100 | 82.8 | 2.21 |

Table II. Relative Molecular Weight Characterization of Poly(*n*BA-co-TCPCl)s

| CPCl in Feed (mol %) | CPCl in Polymer (mol %) | CPCl in Polymer (wt %) | M _n by SEC (g/mol x 10 ⁻³) | M _w /M _n |
|----------------------|-------------------------|------------------------|---|--------------------------------|
| 4 | 5 | 10 | 34.8 | 1.85 |
| 8 | 12 | 22 | 51.0 | 1.90 |
| 17 | 18 | 41 | 56.2 | 2.03 |
| 24 | 23 | 52 | 52.6 | 1.80 |
| 50 | 46 | 76 | 45.3 | 2.09 |
| 100 | 100 | 100 | 93.8 | 2.26 |

Both phosphonium containing random copolymer series revealed comparable molecular weights and charged mole fractions. DMA provided thermomechanical insight by plotting tensile storage modulus (G') and tan delta versus temperature (Figures 2 and 3). Poly(*n*BA-co-TPhPCl) formed free standing films for both the 18 mol% and 24 mol% samples. Both polymers revealed a gradual storage moduli loss from -80 °C and revealed microphase separation in the tan delta plot. Two distinct tan delta peaks were observed. The first peak occurred at -40 °C, corresponding to the glass transition behavior in the *n*BA matrix phase. The second distinct peak was associated with the glass transition behavior in the ionic clusters, which shifted to higher temperatures with increasing charge content. 18 mol% TPhPCl revealed a modulus loss at 115 °C, indicating ionic disassociation and polymer flow. 24 mol% TPhPCl revealed an increase storage modulus and a broadened rubbery plateau. The additional charge association shifted the flow temperature to 155 °C. These results indicated that the increased ionic content enhanced the storage modulus due to ionic aggregation. These findings agreed with previous mechanical relaxation studies regarding metal-salt neutralized ionomers.³⁸⁻⁴⁰ Cheng *et. al.* also observed the same phenomenon when increasing charge content in random copolymers containing OPCl and BPCl.³¹

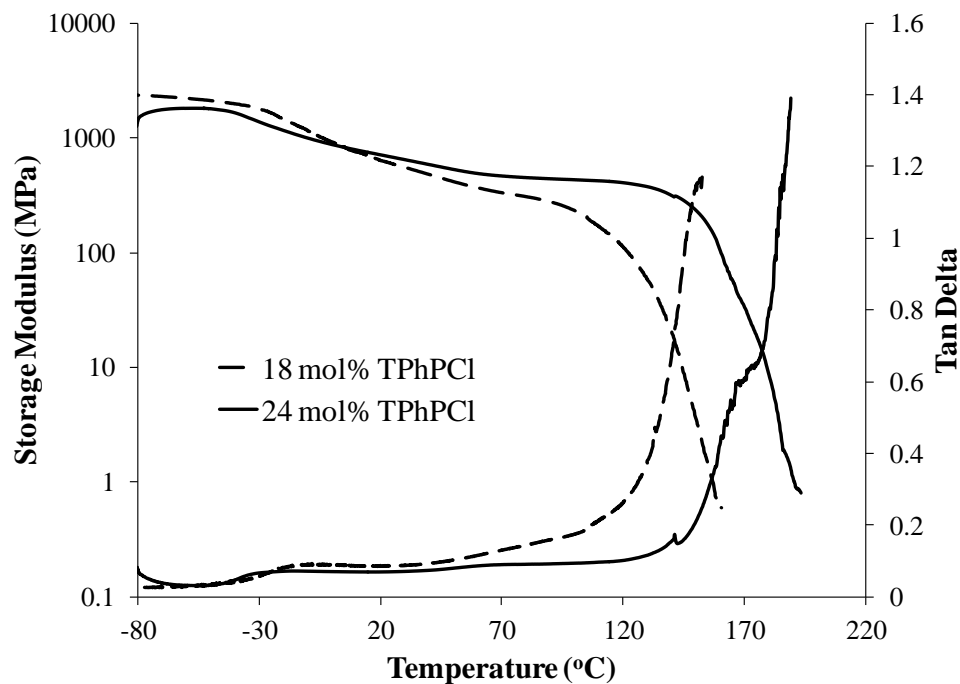


Figure 2. Dynamic mechanical temperature sweep for poly(*n*BA-co-TPhPCI) with 18 and 24 mol% of TPhPCI.

18 mol% and 23 mol% TCPCI based polymers also formed free standing films and revealed microphase separation. The first transition at -40 °C remained consistent with the *n*BA matrix. Increasing charge content from 18 mol% to 23 mol% resulted in increased storage modulus and a broadened rubbery plateau. Charge disassociation and onset polymer flow temperatures shifted from 84 °C to 106 °C. These results further suggested that increased ionic association directly corresponded to enhanced thermomechanical properties.

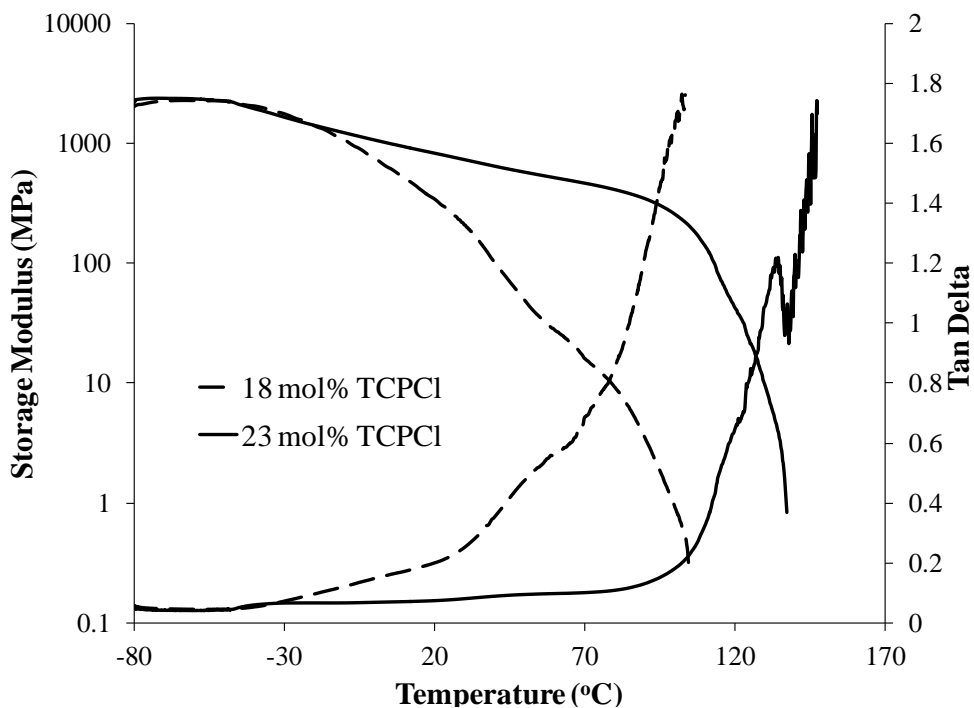


Figure 3. Dynamic mechanical temperature sweep for poly(*n*BA-co-TCPCl) with 18 and 23 mol% of TCPCl.

In comparison to the TCPCl based copolymers, poly(*n*BA-co-TPhPCl)s revealed enhanced thermomechanical properties (Figures 4 and 5). Thermomechanical data for both compositions at constant ionic charge and relative molecular weights emphasized these differences. The TPhPCl membranes exhibited pronounced rubbery plateaus, increased storage modulus, and increased onset flow temperatures. TCPCl analogues similarly revealed these behaviors, but were less prominent at lower temperatures. These patterns correlated to the aryl substituents on phosphonium cations, which promote phosphonium electrostatic interactions in relatively nonpolar polymer matrices. Cheng *et. al.* observed similar results for OPCl and BPCl copolymers, noting that the shorter and more polar butyl chains in BPCl systems assisted phosphonium aggregation.³¹ Moore *et. al.* also reported a decrease in relaxation temperature in increasing alkyl substituent lengths in phosphonium-containing NafionTM membranes.⁴¹

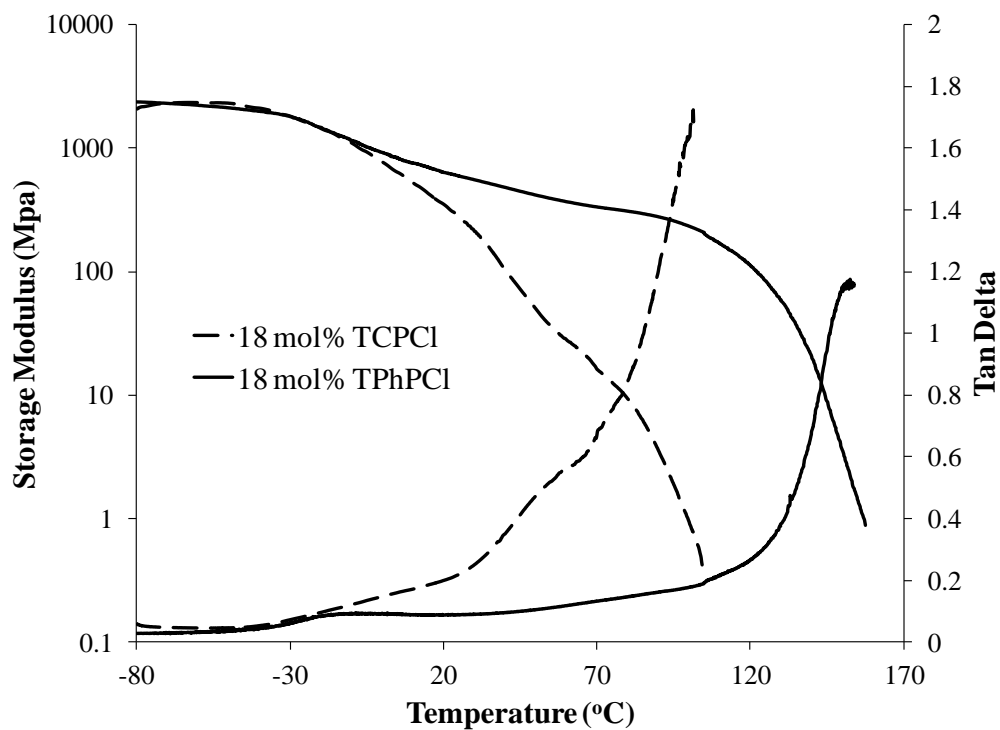


Figure 4. Dynamic mechanical temperature sweep for poly(*n*BA-co-TPhPCI) and poly(*n*BA-co-TCPCI) with 18 mol % of TPhPCI and TCPCI.

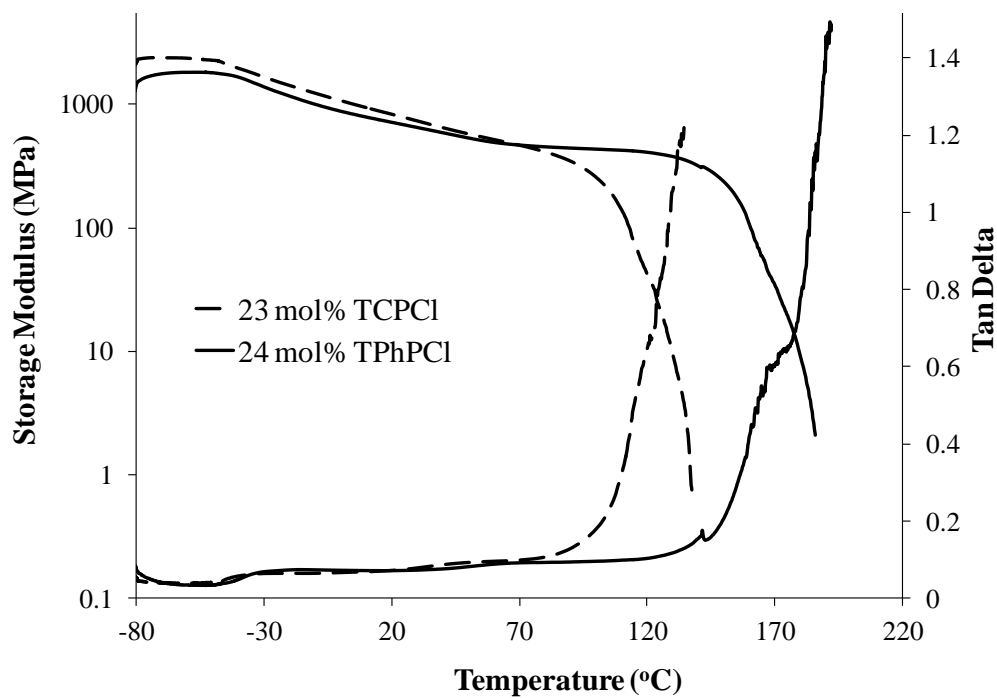
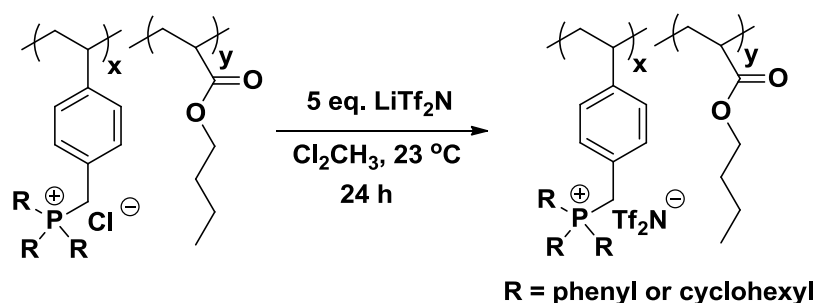


Figure 5. Dynamic mechanical temperature sweep for poly(*n*BA-co-TPhPCI) and poly(*n*BA-co-TCPCI) with 24 mol% of TPhPCI and 23 mol% of TCPCI



Scheme 2. Anion exchange of phosphonium-containing random copolymers.

Anion exchange along phosphonium containing polymer backbones with LiTf_2N achieved PIL structural variation, while maintaining architectural integrity. Scheme 2 depicts the LiTf_2N exchange reactions with poly(TPhPCl), poly(TCPCl), poly(*n*BA-co-TPhPCl), and poly(*n*BA-co-TCPCl) random copolymers. Exchanging chloride with the hydrophobic Tf_2N anion significantly altered thermomechanical properties. Table III summarizes the effects of homopolymer anion exchange on glass transition temperatures (T_g). TPhPCl and TCPCl homopolymers exhibited T_g values of 265 °C and 245 °C, respectively. The high temperatures were attributed to additional steric bulk and rigidity from the cyclic substituents. Replacing chloride with Tf_2N drastically lowered the T_g values by approximately 100 °C. Delocalized Tf_2N counteranions hindered ionic association and promoted macromolecular mobility.

Table III. Thermal Characterization of Phosphonium-Containing Homopolymers

| Name | R | X | Homopolymer T_g (°C) |
|-----------------------|------------|-------------------|---------------------------|
| TPhPCl | Phenyl | Cl | 266 |
| TPhPTf ₂ N | Phenyl | Tf ₂ N | 110 |
| TCPCl | Cyclohexyl | Cl | 245 |
| TCPTf ₂ N | Cyclohexyl | Tf ₂ N | 125 |

Figure 6 and 7 highlights LiTf_2N exchange effects on DMA curves for phosphonium containing random copolymers. Hindered ionic association also promoted macromolecular mobility within the copolymer systems. DMA curves reflected this hindrance in storage modulus loss and decreased flow temperatures. Nevertheless, Tf_2N exchange did not alter the

glass transition behavior for the *n*BA matrix. This highlighted phosphonium containing random copolymers for their continuous microphase separation.

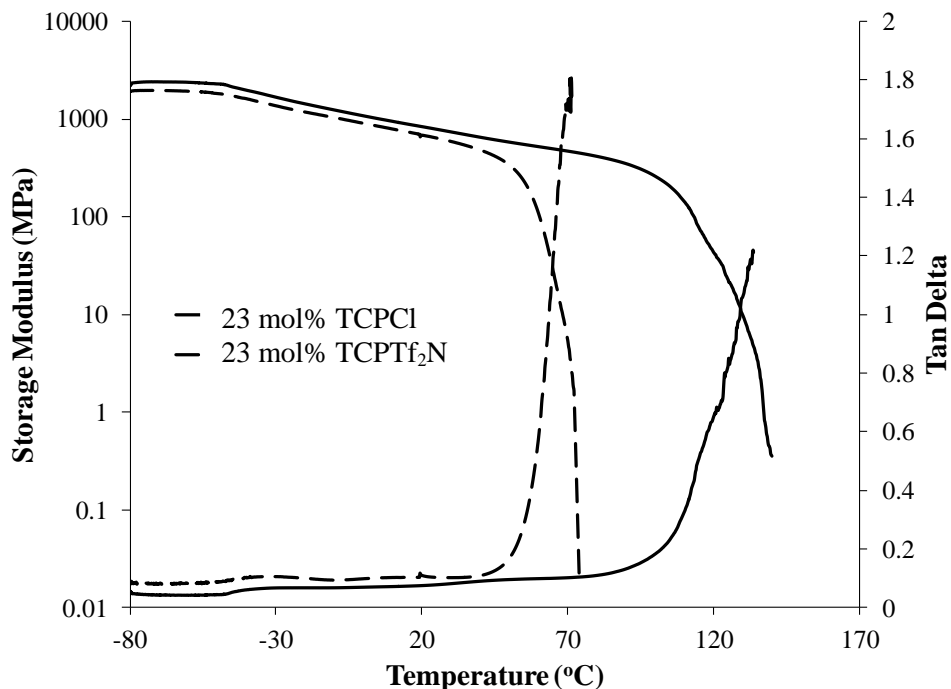


Figure 6. Dynamic mechanical temperature sweep for poly(*n*BA-co-TCPCl) with 23 mol% of TCPCl after anion-exchange reaction.

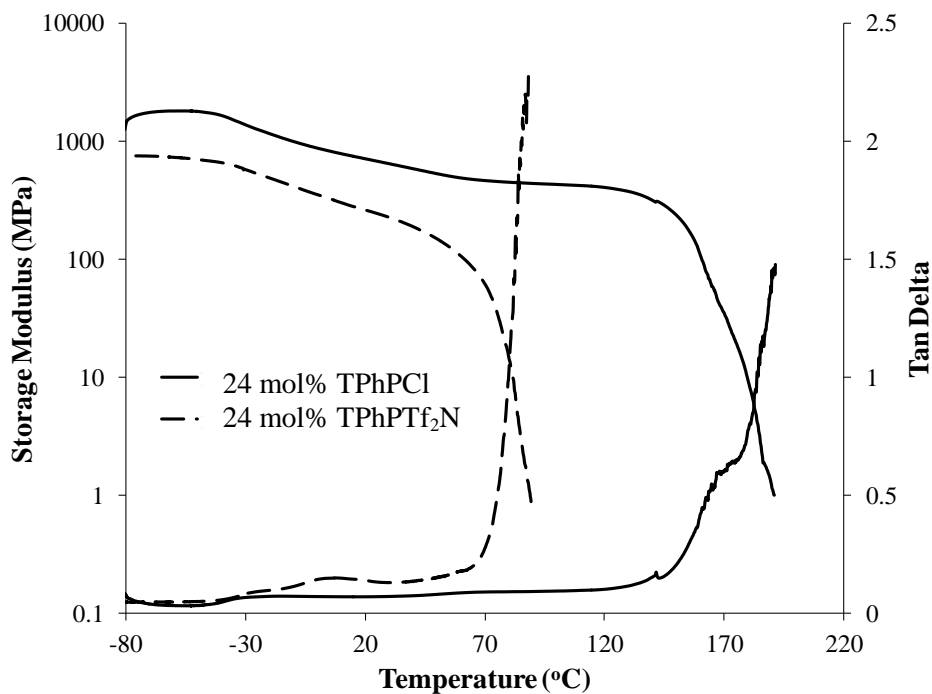


Figure 7. Dynamic mechanical temperature sweep for poly(*n*BA-co-TPhPCl) with 24 mol% TPhPCl after anion-exchange reaction.

2.5 Conclusions

In this study, we synthesized a series of styrenic phosphonium ionic liquids possessing various cyclic substituents and investigated the influence of chemical structure on the thermomechanical behaviors of phosphonium-containing random copolymers with *n*BA. DMA analysis of phosphonium ionomers containing tricyclohexyl substituents revealed lower plateau moduli than triphenyl analogues with constant ionic concentration. Anion exchange with LiTf₂N resulted in plasticized polymer matrices and provided liquid-like, viscous behavior.

2.6 Acknowledgements

This material is based on work supported by the U.S. Army Research Laboratory and the U.S. Army Research Office under contract/grant number W911NF-07-1-0452 Ionic Liquids in Electro-Active Devices Multidisciplinary University Research Initiative (ILEAD MURI).

2.7 References

- (1) Green, M. D.; Long, T. E. *Polym. Rev.* **2009**, *49*, 291.
- (2) Allen, M. H.; Hemp, S. T.; Zhang, M.; Zhang, M.; Smith, A. E.; Moore, R. B.; Long, T. E. *Polym. Chem.* **2013**, *4*, 2333.
- (3) Cheng, S.; Zhang, M.; Wu, T.; Hemp, S. T.; Mather, B. D.; Moore, R. B.; Long, T. E. *Journal of Polymer Science Part A: Polymer Chemistry* **2012**, *50*, 166.
- (4) Couture, G.; Alaaeddine, A.; Boschet, F.; Ameduri, B. *Progress in Polymer Science* **2011**, *36*, 1521.
- (5) Tang, J.; Tang, H.; Sun, W.; Radosz, M.; Shen, Y. *Polymer* **2005**, *46*, 12460.
- (6) Marcilla, R.; Sanchez-Paniagua, M.; Lopez-Ruiz, B.; Lopez-Cabarcos, E.; Ochoteco, E.; Grande, H.; Mecerreyes, D. *Journal of Polymer Science Part A: Polymer Chemistry* **2006**, *44*, 3958.
- (7) Marcilla, R.; Alcaide, F.; Sardon, H.; Pomposo, J. A.; Pozo-Gonzalo, C.; Mecerreyes, D. *Electrochemistry Communications* **2006**, *8*, 482.
- (8) Ueki, T.; Watanabe, M. *Macromolecules* **2008**, *41*, 3739.
- (9) Lu, J.; Yan, F.; Texter, J. *Prog. Polym. Sci.* **2009**, *34*, 431.
- (10) Hatakeyama, E. S.; Ju, H.; Gabriel, C. J.; Lohr, J. L.; Bara, J. E.; Noble, R. D.; Freeman, B. D.; Gin, D. L. *J. Membr. Sci.* **2009**, *330*, 104.
- (11) Wang, K.; Zeng, Y.; He, L.; Yao, J.; Suresh, A. K.; Bellare, J.; Sridhar, T.; Wang, H. *Desalination* **2012**, *292*, 119.
- (12) Zhang, Y.; Zhang, S.; Lu, X.; Zhou, Q.; Fan, W.; Zhang, X. P. *Chem. Eur. J.* **2009**, *15*, 3003.
- (13) Shannon, M. S.; Hindman, M. S.; Danielsen, S. P. O.; Tedstone, J. M.; Gilmore, R. D.; Bara, J. E. *Sci. China: Chem.* **2012**, *55*, 1638.
- (14) Hemp, S. T.; Smith, A. E.; Bryson, J. M.; Allen, M. H.; Long, T. E. *Biomacromolecules* **2012**, *13*, 2439.
- (15) Monge, S.; Canniccioni, B.; Graillot, A.; Robin, J.-J. *Biomacromolecules* **2011**, *12*, 1973.
- (16) Anderson, E. B.; Long, T. E. *Polymer* **2010**, *51*, 2447.
- (17) Ghassemi, H.; Riley, D. J.; Curtis, M.; Bonaplata, E.; McGrath, J. E. *Appl. Organomet. Chem.* **1998**, *12*, 781.
- (18) Gu, S.; Cai, R.; Yan, Y. *Chem. Commun.* **2011**, *47*, 2856.
- (19) Green, M. D.; Choi, J.-H.; Winey, K. I.; Long, T. E. *Macromolecules* **2012**, *45*, 4749.
- (20) Gao, R.; Wang, D.; Heflin, J. R.; Long, T. E. *J. Mater. Chem.* **2012**, *22*, 13473.
- (21) Wu, T.; Wang, D.; Zhang, M.; Heflin, J. R.; Moore, R. B.; Long, T. E. *ACS Appl. Mater. Interfaces* **2012**, *4*, 6552.
- (22) Allen, M. H.; Green, M. D.; Getaneh, H. K.; Miller, K. M.; Long, T. E. *Biomacromolecules* **2011**, *12*, 2243.
- (23) Allen, M. H., Jr.; Wang, S.; Hemp, S. T.; Chen, Y.; Madsen, L. A.; Winey, K. I.; Long, T. E. *Macromolecules (Washington, DC, U. S.)*, Ahead of Print.
- (24) Chen, H.; Elabd, Y. A. *Macromolecules* **2009**, *42*, 3368.
- (25) Tang, H.; Tang, J.; Ding, S.; Radosz, M.; Shen, Y. *J. Polym. Sci., Part A: Polym. Chem.* **2005**, *43*, 1432.
- (26) Green, M. D.; Allen, M. H., Jr.; Dennis, J. M.; Salas-de, I. C. D.; Gao, R.; Winey, K. I.; Long, T. E. *Eur. Polym. J.* **2011**, *47*, 486.

- (27) Schneider, Y.; Modestino, M. A.; McCulloch, B. L.; Hoarfrost, M. L.; Hess, R. W.; Segalman, R. A. *Macromolecules* **2013**, *46*, 1543.
- (28) Ren, H.; Sun, J.; Wu, B.; Zhou, Q. *Polym. Degrad. Stab.* **2007**, *92*, 956.
- (29) Rana, U. A.; Vijayaraghavan, R.; Walther, M.; Sun, J.; Torriero, A. A. J.; Forsyth, M.; MacFarlane, D. R. *Chem Commun* **2011**, *47*, 11612.
- (30) Sagle, A. C.; Van, W. E. M.; Ju, H.; McCloskey, B. D.; Freeman, B. D.; Sharma, M. M. *J. Membr. Sci.* **2009**, *340*, 92.
- (31) Cheng, S.; Zhang, M.; Wu, T.; Hemp, S. T.; Mather, B. D.; Moore, R. B.; Long, T. E. *J. Polym. Sci., Part A: Polym. Chem.* **2012**, *50*, 166.
- (32) Cheng, S.-J.; Beyer, F. L.; Mather, B. D.; Moore, R. B.; Long, T. E. *Macromolecules* **2011**, *44*, 6509.
- (33) Borguet, Y. P.; Tsarevsky, N. V. *Polym. Chem.* **2012**, *3*, 2487.
- (34) Wang, R.; Lowe, A. B. *J. Polym. Sci., Part A: Polym. Chem.* **2007**, *45*, 2468.
- (35) Stokes, K. K.; Orlicki, J. A.; Beyer, F. L. *Polym. Chem.* **2011**, *2*, 80.
- (36) Kanazawa, A.; Ikeda, T.; Endo, T. *J. Polym. Sci., Part A: Polym. Chem.* **1993**, *31*, 1441.
- (37) Hatakeyama, E. S.; Ju, H.; Gabriel, C. J.; Lohr, J. L.; Bara, J. E.; Noble, R. D.; Freeman, B. D.; Gin, D. L. *Journal of membrane science* **2009**, *330*, 104.
- (38) Tachino, H.; Hara, H.; Hirasawa, E.; Kutsumizu, S.; Tadano, K.; Yano, S. *Macromolecules* **1993**, *26*, 752.
- (39) Capek, I. *Adv. Colloid Interface Sci.* **2005**, *118*, 73.
- (40) MacKnight, W. J.; Kajiyama, T.; McKenna, L. *Polym. Eng. Sci.* **1968**, *8*, 267.
- (41) Page, K. A.; Cable, K. M.; Moore, R. B. *Macromolecules* **2005**, *38*, 6472.

Chapter 3: Structure-Morphology-Property Characterization of Sulfonated Styrenic Pentablock Copolymer Neutralized with a Bis(imidazolyl)alkane

3. 1 Abstract

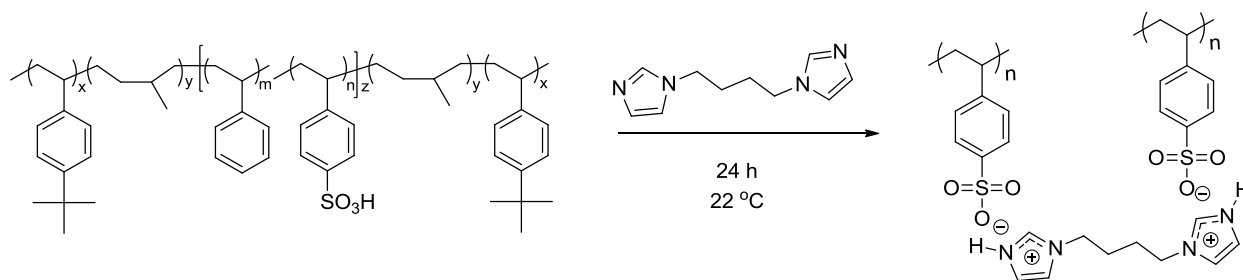
1, 1'-(1, 4-Butanediyl)bis(imidazole) neutralized NexarTM sulfonated pentablock copolymers and produced novel electrostatically crosslinked membranes. The subsequent influences on NexarTM morphology and membrane properties were studied. Variable temperature FTIR and ¹H NMR spectroscopy confirmed neutralization. Atomic force microscopy (AFM) and small angle X-ray scattering (SAXS) studied polymer morphology and revealed electrostatic crosslinking characteristics. Tensile analysis, dynamic mechanical analysis (DMA), thermogravimetric analysis (TGA), and vapor sorption thermogravimetric analysis (TGASA) investigated the polymer network properties. The neutralized polymer demonstrated enhanced thermal stability, decreased water adsorption, and well-defined microphase separation. These findings highlight NexarTM sulfonated pentablock copolymers as reactive platforms for novel, bis-imidazolium crosslinked materials.

Keywords: polymer network, NexarTM, SAXS, thermomechanical, ionic liquid

3.2 Introduction

Sulfonated polymers strike continued interest for their commercial applications in areas such as water purification¹⁻³, proton exchange membranes,⁴⁻¹¹ and actuators.¹²⁻¹⁴ Polymers containing sulfonic acid repeat units provide opportunities for chemical modification and optimization. Neutralization is commonly employed to substitute sulfonic acid protons with charged species.^{13,15} These reactions occur quantitatively and achieve a variety of novel materials with differing properties. Numerous researchers demonstrated this efficient modification process with a range of both metallic ions and organic ionic liquids (ILs).¹⁶⁻²³ Antonietti *et al.* neutralized poly(styrenesulfonate) with alkyltrimethylammoniums and produced highly mesomorphous materials.²⁴ Long *et al.* reported novel N-alkyl imadazolium neutralized sulfonated pentablock copolymers and their application in enhanced actuation.¹³ Geise *et al.* disclosed an aluminum crosslinked sulfonated pentablock copolymer and its desalination properties.^{15,25}

Neutralization is emerging as an efficient modification process for achieving crosslinked polymeric networks and supramolecular assemblies.²⁶ These architectures offer unique properties applicable for self-healing^{26,27}, water purification¹⁵, and gas separation²⁸⁻³⁰ materials. Numerous studies in this area highlight neutralization with multivalent alkali metals. These ionic species achieve crosslinked networks, but often fail to impart flexibility within the assembled structures. Dicationic ILs are alternative cross-linking agents that impart variable alkyl spacers for charge separation.^{27,31,32} These spacers alleviate charge repulsion within networked systems while enhancing free volume.³³



Scheme 1. General reacton scheme for neutralizing NexarTM sulfonated pentablock copolymer with 1,1'-(1,4-butanediyl)bis(imidazole) KP-SO₃[BisIm]⁺ (IEC 2.0)

Herein, we describe a facile approach to prepare a bis-imidazolium neutralized pentablock copolymer from NexarTM. Polymers of this structure are commercially available from Kraton Polymers LLC. Sequential living anionic polymerization and selective post sulfonation affords well-defined pentablock NexarTM polymers. These architectures incorporate a sulfonated polystyrene central block with an ion exchange capacity (IEC) of 2.0. IEC refers to the milliequivalents of sulfonic acid per gram of polymer (mequiv. per g). Neutralization achieves a novel bis-imidazolium crosslinked sulfonated pentablock ABCBA copolymer. This architectural design highlights a hydrophilic, bis-imidazolium polystyrene sulfonated central (C) block that imparts electrostatic crosslinks for enhanced mechanical strength, hydrogenated polyisoprene (B) block soft segments that provides membrane flexibility, and a hydrophobic poly(*tert*-butyl styrene) (A) block hard segments that impart additional mechanical strength.

In this study, we discuss the effects of bis-imidazolium neutralization on NexarTM morphology and membrane properties. Winey *et. al.* previously utilized transmission electron microscopy (TEM) and small angle X-ray scattering (SAXs) to elucidate the solution morphology of sulfonic acid containing NexarTM polymers in cyclohexane.³⁴ NexarTM revealed a spherical micellar configuration. Sulfonated polystyrene central blocks formed a dense core of micelles, reinforced by H-bonding interactions along the sulfonic acid units. Our novel bis-imidazolium neutralized NexarTM polymer imparts a cationic cross-linking agent in place of the

sulfonic acid proton. As expected, this modification influenced micellar configuration and membrane performance. Variable temperature fourier transform infrared (FTIR) spectroscopy, atomic force microscopy (AFM) and SAXs probed the network system's modification and morphology. Tensile analysis, dynamic mechanical analysis (DMA), thermogravimetric analysis (TGA), and vapor sorption thermogravimetric analysis (TGASA) investigated the polymer network's membrane performance. These findings highlight NexarTM sulfonated pentablock copolymers as reactive platforms for novel, bis-imidazolium crosslinked materials.

3.3 Experimental

3.3.1 Materials

Imidazole (99%), and 1,4-dibromobutane (99%) were purchased from Aldrich and used as received. A sulfonated pentablock copolymer was synthesized and provided by Kraton Polymers LLC. The neutral block copolymer poly(tert-butyl styrene-b-styrene-b-hydrogenated isoprene-b-tert-butyl styrene) was synthesized through the sequential living anionic polymerization of tert-butyl styrene, isoprene, styrene, isoprene, and tertbutylstyrene, and a subsequent hydrogenation of the isoprene blocks. The corresponding sulfonated pentablock copolymers were obtained through a selective sulfonation of the styrene middle block.

3.3.2 Analytical Methods

Atomic force microscopy (AFM) was conducted on a Veeco MultiMode AFM using a tapping mode under ambient conditions. Variable temperature fourier transform infrared spectroscopy (FTIR) employed a Varian 670 IR using a PIKE GladiATR attachment and a temperature ramp of 5°C/32 scans over the range 40-195 °C. Vapor sorption thermogravimetric analysis (TGASA) was conducted with a TA Instruments Q5000 in the isotherm mode for 120

minutes at 30 °C followed by a 5% relative humidity ramp for 19 cycles. Dynamic mechanical analysis (DMA) measurements were performed on a TA Instruments Q800 dynamic mechanical analyzer in the film tension mode at a frequency of 1 Hz and a temperature ramp of 3 °C/min over the range -90 to 160 °C. Tensile data was collected on an Instron with crosshead speed of 50 mm/min.

Small-angle X-ray scattering data were collected with a customized, pinhole collimated 3 m camera. X-rays were generated with a Rigaku Ultrax18 rotating Cu anode generator operated at 45 kV and 100 mA and then filtered with Ni foil to select the Cu K α doublet ($\lambda = 1.542 \text{ \AA}$). Two-dimensional data sets were collected using a Molecular Metrology multiwire area detector at both 50 and 150 cm from the detector. Raw data were corrected for absorption and background noise and subsequently azimuthally averaged. The corrected data were placed on an absolute scale using a secondary standard, type 2 glassy carbon, and the data at both camera lengths were subsequently merged into one continuous data set for each sample. All data reduction and analysis were performed using Igor Pro v6.12A from Wavemetrics, Inc., using a suite of procedures developed at the Argonne National Laboratory.¹⁴

3.3.3 Synthesis of 1,4-bis(imidazol-1-yl)-butane

Imidazole (6.8 g, 0.1 mol) and KOH (8.0 g, 0.1 mol) were added to 120 mL acetonitrile in a 250 mL two-neck round bottomed flask equipped with an addition funnel and reflux condenser. 1,4-dibromobutane (6.8 g, 0.5 mol) was added and the reaction was heated to 85 °C for 4 h. Once cool, the mixture was filtered and acetonitrile was removed by rotoevaporation. The resulting liquid was poured into 150 mL of water. The final white solid product was collected and dried under vacuum at 30 °C for 48 h (95% yield). ¹H NMR (400 MHz, CDCl₃, 25 °C, δ): 1.55-1.95 (8H, m, alkyl protons), 3.75-4.05 (4H, m, imidazole protons).

3.3.4 Preparation of KP-SO₃[BisIm]⁺ Membrane:

A sulfonated pentablock copolymer solution in cyclohexane (10 wt%) was added to a two-necked, round bottomed flask equipped with a magnetic stir bar. A 0.5 molar equivalence of 1,4-bis(imidazol-1-yl)-butane was dissolved in methanol and added dropwise to the flask. The solution was stirred at 23 °C for 24 h and directly cast on a Mylar substrate using an adjustable film applicator. This method generated uniform membranes with controlled thickness at 40 mm.

3.4 Results and Discussion

1, 1'-(1, 4-Butanediyl)bis(imidazole) neutralized NexarTM sulfonated pentablock copolymers (KP-SO₃[BisIm]⁺) in a single quantitative neutralization step (Scheme 1). Variable temperature FTIR spectroscopy confirmed neutralization (Figures 1 and 2). The sulfonic acid NexarTM derivative (KP-SO₃H) exhibited H-bond dissociation as spectral shifts occurred in the sulfonic acid wavenumber region (1100 cm⁻¹ at 40 °C to 1160 cm⁻¹ at 195 °C) with increasing temperature.³⁵ Neutralizing the sulfonic acid units with bis-imidazolium converted H-bond interactions to electrostatic interactions. Consequently, the neutralized copolymer did not exhibit H-bond dissociation in the sulfonic acid wavenumber region.

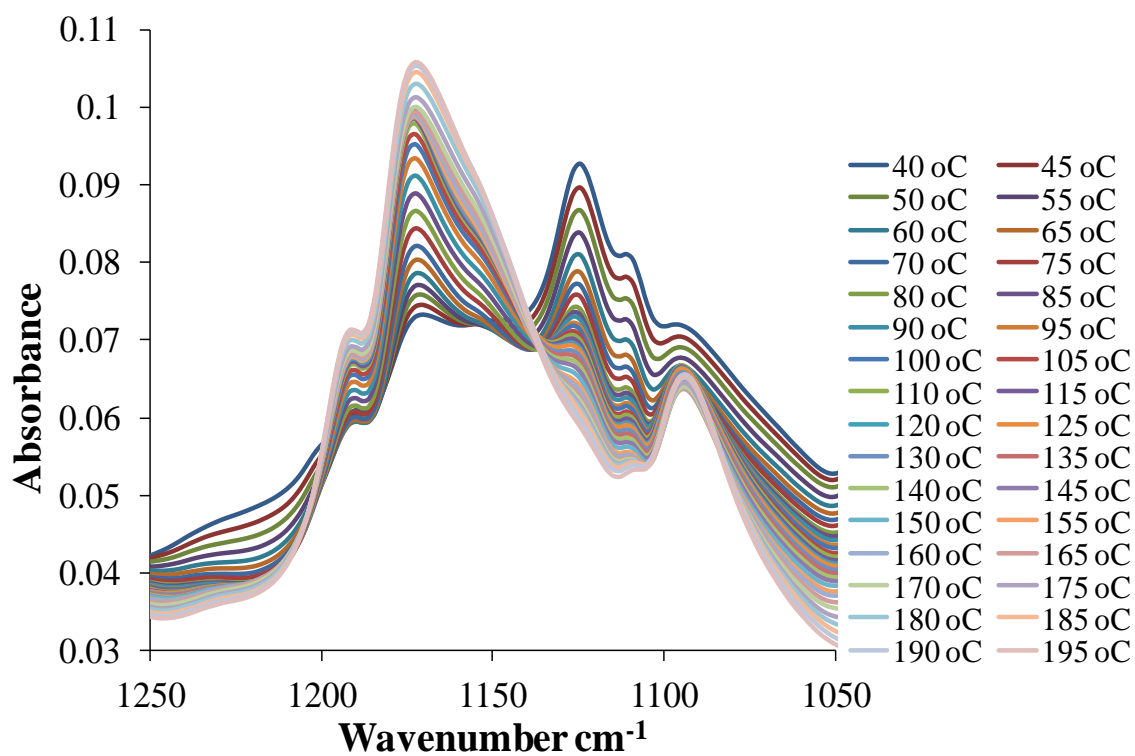


Figure 1. Variable temperature FTIR spectra for Nexar™ sulfonic acid membrane, KP-SO₃H

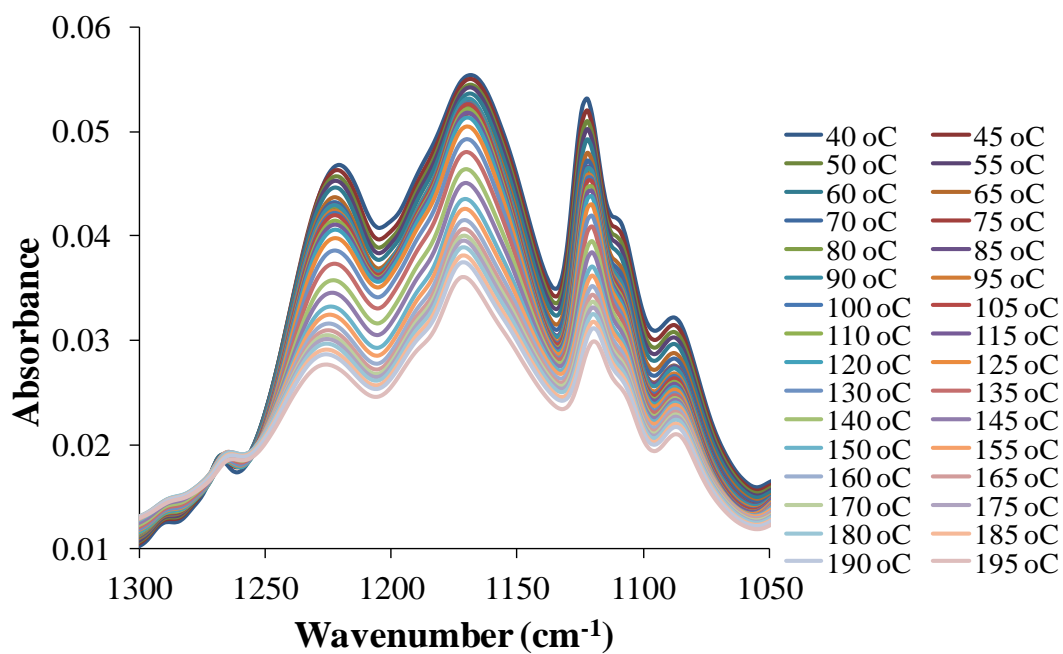


Figure 2. Variable temperature FTIR spectra for Nexar™ bis-imidazolium neutralized membrane, KP-SO₃[BisIm]⁺

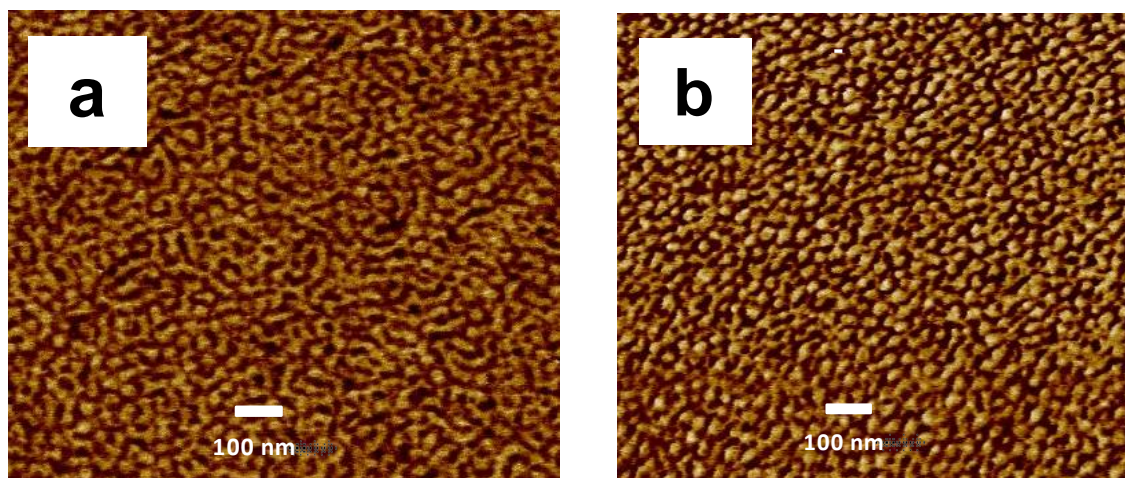


Figure 3. Surface morphology of (a) NexarTM polymer KP-SO₃H and (b) NexarTM polymer KP-SO₃[BisIm]⁺ solid membranes imaged with AFM.

AFM revealed well-defined microphase-separated morphology for the KP-SO₃[BisIm]⁺ solid membrane (Figure 2). The lighter regions in AFM represent hard phases, and darker regions represent soft regions. In comparison to the sulfonic acid containing NexarTM, KP-SO₃[BisIm]⁺ displayed more pronounced hard phases. Figure 3 highlights X-ray scattering results for both pentablock copolymer membranes. The limited number of scattering peaks prohibits exact morphological assignment for these copolymers. However, the bis-imidazolium neutralized copolymer exhibits scattering peaks shifted to a higher q value. This result suggests smaller microdomains. Winey *et. al.* observed similar SAXS patterns when comparing NexarTM sulfonated pentablock copolymers with various sulfonation levels.³⁶

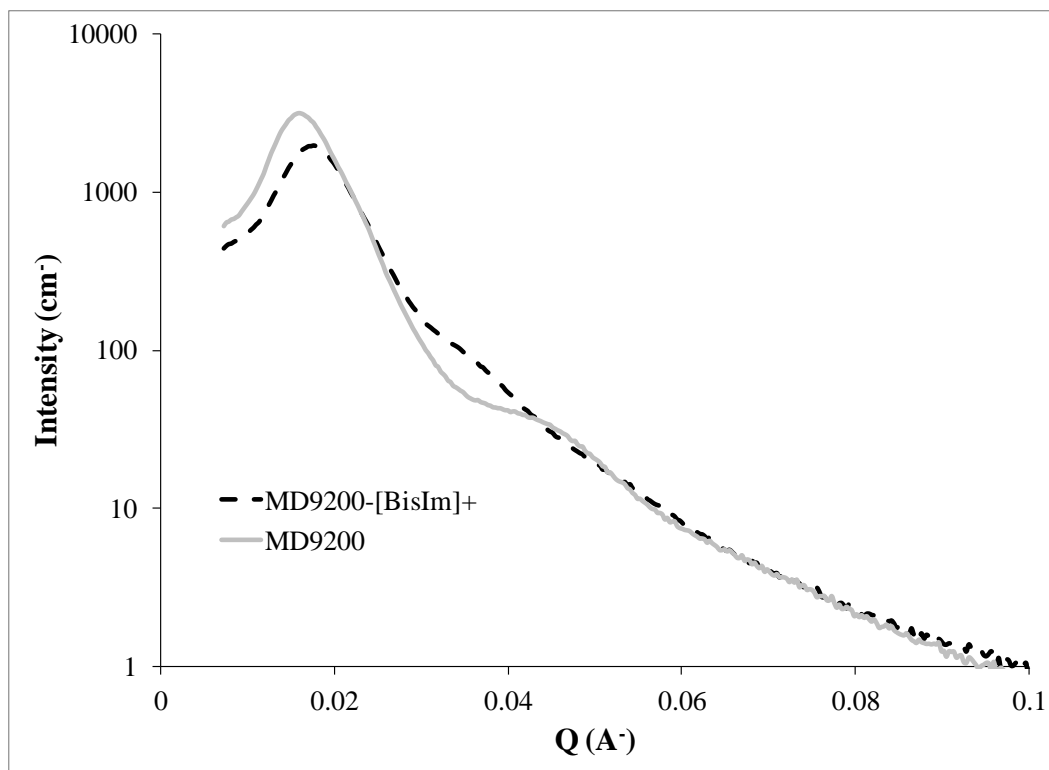


Figure 4. SAXS for non-neutralized and bis-imidazolium neutralized sulfonated pentablock copolymers

Figure 5 shows λ values (moles of water/ moles of sulfonation) vs. relative humidity. The obtained data agreed substantially with previous research.³⁷ Both samples demonstrated a linear increase in λ values from 0 °C to 60 °C. After reaching this point, the KP-SO₃H film revealed a strong change in slope and the membrane experienced high water sorption. The KP-SO₃[BisIm]⁺ neutralized membrane showed comparable trends, but showed less water sorption behavior. These two trends suggest that water molecules initially dissociate the sulfonic groups, forming hydronium ions.³⁷⁻³⁹ Water molecules cluster around these ions, thereby increasing water sorption.

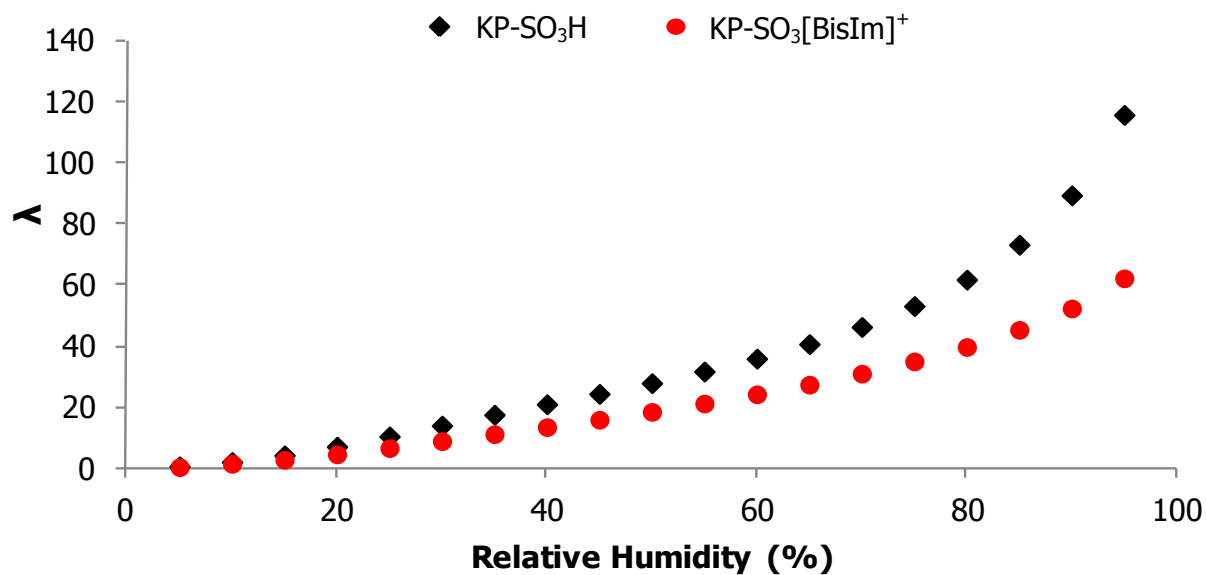


Figure 5. Degree of hydration of sulfonic groups λ (= moles of water/ moles of sulfonation) vs. relative humidity (%)

The stress–strain curves for the sulfonated pentablock copolymer and the bis-imidazolium neutralized copolymer are highlighted in figures 6 and 7. After experiencing a sharp post yield relaxation, both membranes strain hardened until failure. This enhanced toughness is attributed to hydrogenated isoprene blocks and to some degree of atmospheric water sorption.¹⁵ In comparison to the KP-SO₃H membrane, KP-SO₃[BisIm]⁺ revealed a slight decrease in strain % break. These results, highlighted in Table I, display the crosslinked behavior of the neutralized material.

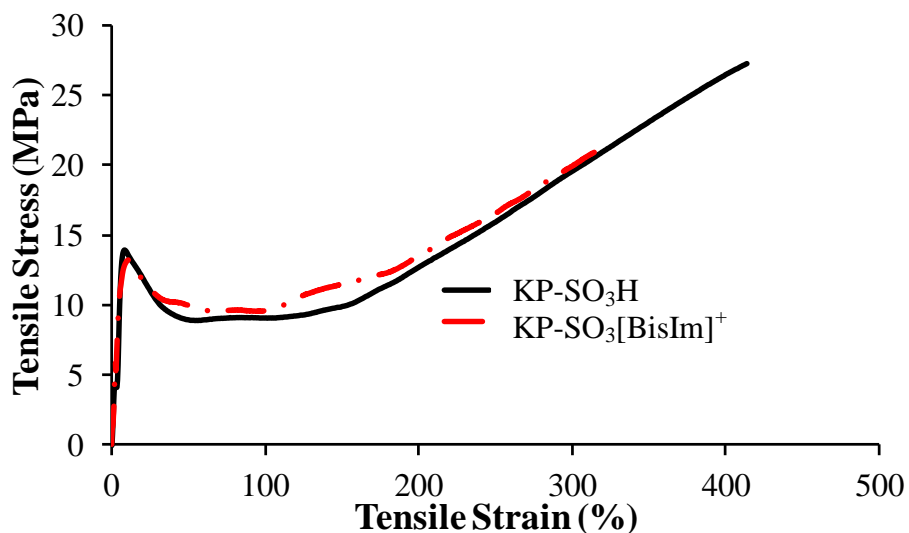


Figure 6. Tensile stress–strain curves for bis-imidazolium neutralized and non-neutralized sulfonated pentablock copolymers.

Table I Tensile stress–strain results for bis-imidazolium neutralized and non-neutralized sulfonated pentablock copolymers.

| Sample | Young's Modulus (MPa) | Yield Point (MPa) | Stress at Break (MPa) | Strain at Break (%) |
|---|-----------------------|-------------------|-----------------------|---------------------|
| KP-SO ₃ H | 276.91 ± 17 | 15.98 ± 2.4 | 26.14 ± 1.9 | 418.18 ± 33 |
| KP-SO ₃ [BisIm] ⁺ | 174.83 ± 21 | 16.53 ± 2.3 | 26.0 ± 4.6 | 304.14 ± 38 |

TGA and DMA provided the thermomechanical properties for the sulfonated pentablock copolymer and the bis-imidazolium neutralized polymer. An ethyl-imidazolium neutralized polymer sample (KP-SO₃[C₂Im]⁺) was also evaluated as a control. TGA data highlighted the neutralized samples for their enhanced thermal stability (Table II). These compositions withstood thermal degradation up to 400 °C. DMA revealed well-defined rubbery plateaus with high storage moduli for all samples (Figure 7). Additionally, all samples showed two distinct thermal transitions near -35 °C and 110 °C. These transitions corresponded the hydrogenated polyisoprene and poly(*tert*-butyl styrene) respective glass transition temperatures. These results

agreed with previous research.¹³ The bis-imidazolium neutralized samples revealed enhanced thermomechanical properties, with well-defined microphase separation and an increased flow temperature of 140 °C. These results indicated that the increased ionic content enhanced the storage modulus due to ionic aggregation. These findings agreed with previous mechanical relaxation studies regarding metal-salt neutralized ionomers.⁴⁰⁻⁴²

Table II. Thermal degradation temperatures for imadazolium neutralized and non-neutralized copolymers

| Sample | T _{d1} (°C) | T _{d2} (°C) |
|---|----------------------|----------------------|
| | 220 | 447 |
| KP-SO ₃ [C ₂ Im] ⁺ | 329 | 470 |
| KP-SO ₃ [BisIm] ⁺ | 397 | 480 |

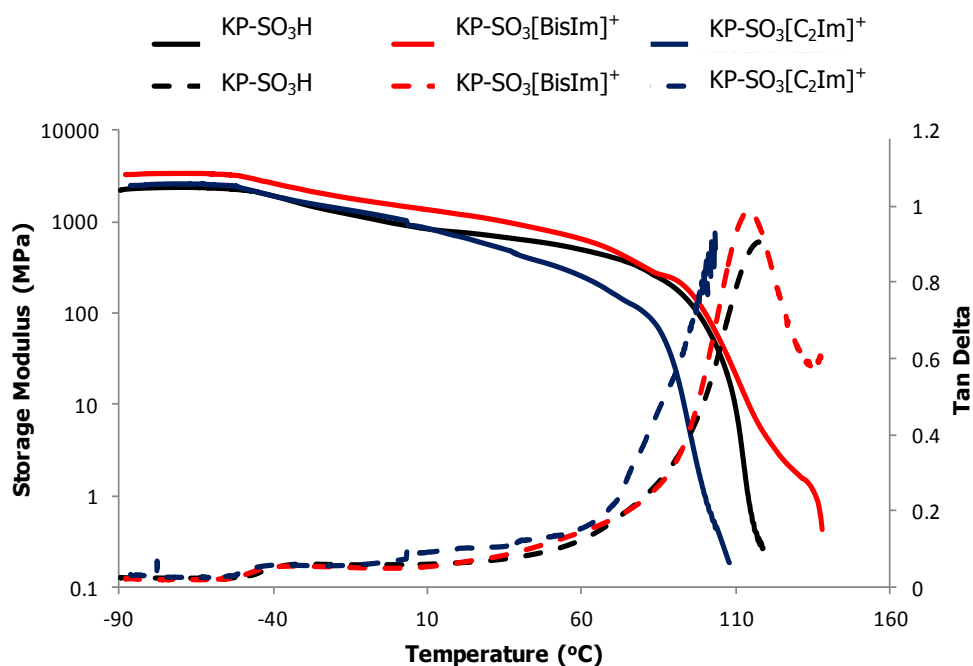


Figure 7. Dynamic mechanical temperature sweep for imadazolium neutralized and non-neutralized copolymers.

3.5 Conclusions:

In this study, the effects of bis-imidazolium neutralization on NexarTM morphology and membrane properties were probed. Variable temperature FTIR spectroscopy, AFM and SAXs studied the network system's morphology and suggested electrostatic crosslinked characteristics. Tensile analysis, dynamic mechanical analysis (DMA), thermogravimetric analysis (TGA), and vapor sorption thermogravimetric analysis (TGASA) investigated the polymer network's membrane performance. Neutralized systems demonstrated enhanced thermal stability, decreased water adsorption, and well-defined microphase separation. These findings highlight NexarTM sulfonated pentablock copolymers as reactive platforms for novel, bis-imidazolium crosslinked materials.

3.6 Acknowledgments

This work is partially supported by the U.S. Army Research Laboratory and the U.S. Army Research Office through the Ionic Liquids in Electro-Active Devices Multidisciplinary University Research Initiative (ILEAD MURI) program under contract/grant number W911NF-07-1-0452. The authors also thank Kraton Polymers LLC for their support. Additionally, many experiments were performed using instruments in the Nanoscale Characterization and Fabrication Laboratory (NCFL) operated at Virginia Tech.

3.7 References

- (1) Park, H. B.; Freeman, B. D.; Zhang, Z.-B.; Sankir, M.; McGrath, J. E. *Angewandte Chemie International Edition* **2008**, *47*, 6019.
- (2) Geise, G. M.; Lee, H.-S.; Miller, D. J.; Freeman, B. D.; McGrath, J. E.; Paul, D. R. *Journal of Polymer Science Part B: Polymer Physics* **2010**, *48*, 1685.
- (3) Willis, C. L.; Handlin, D. L., Jr.; Trenor, S. R.; Mather, B. D.; Kraton Polymers Research B.V., Neth. . 2007, p 98pp.
- (4) Decker, B.; Hartmann-Thompson, C.; Carver, P. I.; Keinath, S. E.; Santurri, P. R. *Chem. Mater.* **2010**, *22*, 942.
- (5) Tsang, E. M. W.; Zhang, Z.; Yang, A. C. C.; Shi, Z.; Peckham, T. J.; Narimani, R.; Frisken, B. J.; Holdcroft, S. *Macromolecules* **2009**, *42*, 9467.
- (6) Ghassemi, H.; Riley, D. J.; Curtis, M.; Bonaplata, E.; McGrath, J. E. *Appl. Organomet. Chem.* **1998**, *12*, 781.
- (7) Gu, S.; Cai, R.; Yan, Y. *Chem. Commun.* **2011**, *47*, 2856.
- (8) Elliott, J. A.; Wu, D.; Paddison, S. J.; Moore, R. B. *Soft Matter* **2011**, *7*, 6820.
- (9) Hickner, M. A.; Ghassemi, H.; Kim, Y. S.; Einsla, B. R.; McGrath, J. E. *Chem. Rev.* **2004**, *104*, 4587.
- (10) Harrison, W. L.; Hickner, M. A.; Kim, Y. S.; McGrath, J. E. *Fuel Cells* **2005**, *5*, 201.
- (11) Mauritz, K. A.; Moore, R. B. *Chem. Rev.* **2004**, *104*, 4535.
- (12) Green, M. D.; Choi, J.-H.; Winey, K. I.; Long, T. E. *Macromolecules* **2012**, *45*, 4749.
- (13) Gao, R.; Wang, D.; Heflin, J. R.; Long, T. E. *J. Mater. Chem.* **2012**, *22*, 13473.
- (14) Wu, T.; Wang, D.; Zhang, M.; Heflin, J. R.; Moore, R. B.; Long, T. E. *ACS Appl. Mater. Interfaces* **2012**, *4*, 6552.
- (15) Geise, G. M.; Willis, C. L.; Doherty, C. M.; Hill, A. J.; Bastow, T. J.; Ford, J.; Winey, K. I.; Freeman, B. D.; Paul, D. R. *Ind. Eng. Chem. Res.* **2013**, *52*, 1056.
- (16) Di, N. V.; Piga, M.; Giffin, G. A.; Lavina, S.; Smotkin, E. S.; Sanchez, J.-Y.; Iojoiu, C. *J. Phys. Chem. C* **2012**, *116*, 1370.
- (17) Tsuchida, E.; Nishide, H.; Ohyanagi, M.; Kawakami, H. *Macromolecules* **1987**, *20*, 1907.
- (18) Hsiue, G. H.; Yang, J. M. *J. Polym. Sci., Part A: Polym. Chem.* **1993**, *31*, 1457.
- (19) Nishide, H.; Kawakami, H.; Sasame, Y.; Ishiwata, K.; Tsuchida, E. *J. Polym. Sci., Part A: Polym. Chem.* **1992**, *30*, 77.
- (20) Basnayake, R.; Peterson, G. R.; Casadonte, D. J., Jr.; Korzeniewski, C. *J. Phys. Chem. B* **2006**, *110*, 23938.
- (21) Bath, B. D.; White, H. S.; Scott, E. R. *Anal. Chem.* **2000**, *72*, 433.
- (22) Yamaguchi, T.; Boetje, L. M.; Koval, C. A.; Noble, R. D.; Bowman, C. N. *Ind. Eng. Chem. Res.* **1995**, *34*, 4071.
- (23) Summers, B. L., Jr.; Gress, L. B.; Philipp, W. H.; Eastep, S. B.; Aero-Terra-Aqua Technologies Corporation, USA . 1997, p 11 pp.
- (24) Antonietti, M.; Conrad, J.; Thuenemann, A. *Macromolecules* **1994**, *27*, 6007.
- (25) Geise, G. M.; Willis, C. L.; Doherty, C. M.; Hill, A. J.; Bastow, T. J.; Ford, J.; Winey, K. I.; Freeman, B. D.; Paul, D. R. *Industrial & Engineering Chemistry Research* **2012**, *52*, 1056.

- (26) Brunsveld, L.; Folmer, B. J. B.; Meijer, E. W.; Sijbesma, R. P. *Chem. Rev.* **2001**, *101*, 4071.
- (27) Lin, X.; Navailles, L.; Nallet, F.; Grinstaff, M. W. *Macromolecules* **2012**, *45*, 9500.
- (28) Tin, P. S.; Chung, T. S.; Liu, Y.; Wang, R.; Liu, S. L.; Pramoda, K. P. *J. Membr. Sci.* **2003**, *225*, 77.
- (29) Taubert, A.; Wind, J. D.; Paul, D. R.; Koros, W. J.; Winey, K. I. *Polymer* **2003**, *44*, 1881.
- (30) Waldman, A. S.; Schechinger, L.; Govindarajoo, G.; Nowick, J. S.; Pignolet, L. H.; Labuza, T. *J. Chem. Educ.* **1998**, *75*, 1430.
- (31) Maiti, P. K.; Kremer, K.; Flimm, O.; Chowdhury, D.; Stauffer, D. *Langmuir* **2000**, *16*, 3784.
- (32) Pindzola, B. A.; Jin, J.; Gin, D. L. *J. Am. Chem. Soc.* **2003**, *125*, 2940.
- (33) Cashion, M. P.; Li, X.; Geng, Y.; Hunley, M. T.; Long, T. E. *Langmuir* **2010**, *26*, 678.
- (34) Choi, J.-H.; Kota, A.; Winey, K. I. *Industrial & Engineering Chemistry Research* **2010**, *49*, 12093.
- (35) Deimede, V.; Voyiatzis, G. A.; Kallitsis, J. K.; Qingfeng, L.; Bjerrum, N. J. *Macro molecules* **2000**, *33*, 7609.
- (36) Choi, J.-H.; Willis, C. L.; Winey, K. I. *J. Membr. Sci.* **2013**, *428*, 516.
- (37) Zawodzinski, T. A., Jr.; Derouin, C.; Radzinski, S.; Sherman, R. J.; Smith, V. T.; Springer, T. E.; Gottesfeld, S. *J. Electrochem. Soc.* **1993**, *140*, 1041.
- (38) Zawodzinski, T. A., Jr.; Springer, T. E.; Uribe, F.; Gottesfeld, S. *Solid State Ionics* **1993**, *60*, 199.
- (39) Zawodzinski, T. A., Jr.; Springer, T. E.; Davey, J.; Jestel, R.; Lopez, C.; Valerio, J.; Gottesfeld, S. *J. Electrochem. Soc.* **1993**, *140*, 1981.
- (40) Tachino, H.; Hara, H.; Hirasawa, E.; Kutsumizu, S.; Tadano, K.; Yano, S. *Macromolecules* **1993**, *26*, 752.
- (41) Capek, I. *Adv. Colloid Interface Sci.* **2005**, *118*, 73.
- (42) MacKnight, W. J.; Kajiyama, T.; McKenna, L. *Polym. Eng. Sci.* **1968**, *8*, 267.

Chapter 4: Investigating the Thermal Polymerization of 4-Vinylbenzyl piperidine

4.1 Abstract

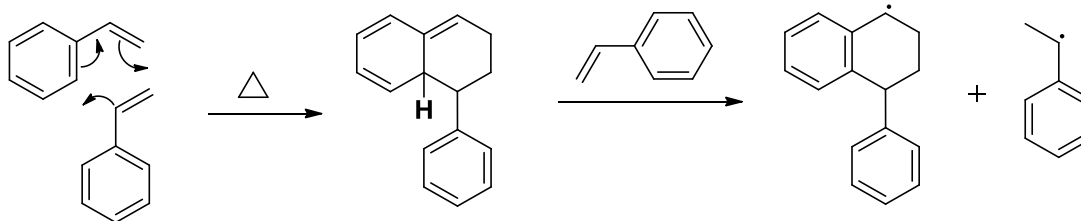
Living radical polymerizations typically require elevated temperatures, bulk concentrations, and extensive reaction times. These conditions also correspond to thermal autopolymerization requirements for styrenic monomers. In this study, *in situ* FTIR spectroscopy monitored styrene and 4-vinylbenzyl piperidine autopolymerizations. Pseudo-first-order thermal polymerization kinetics calculated observed rate constants for both monomers. An Arrhenius analysis derived thermal activation energy values for both monomers. 4-Vinylbenzyl piperidine exhibited activation energy 80 KJ/mol less than styrene. The monomer differs from styrene in its piperidinyl structure. Consequently, *in situ* FTIR spectroscopy also monitored styrene thermal polymerization with variable N-benzyl piperidine concentrations. Under these circumstances, styrene revealed an activation energy 60 KJ/mol less than its respective bulk value. The similarities in chemical structure between styrene and 4-vinylbenzyl piperidine suggested thermally initiated polymerization occurred by the Mayo mechanism. The unique substituent is proposed to offer additional polarity effects for enhancing polymerization rates.

Keywords: activation energy, FTIR, autopolymerization

4.2 Introduction:

Controlled living polymerization offers an efficient route for producing well-defined polymeric architectures with tunable molecular weights, molecular weight distributions, and stereochemistries.¹⁻¹³ Living strategies traditionally employ cationic and anionic initiators, promoting linear chain propagation in an electrostatic repulsive environment.¹⁴⁻¹⁹ Charged media sequesters undesirable chain transfer and termination reactions that commonly impede free radical polymerizations.^{20,21} However, these underlying harsh reaction conditions limit monomer tolerance and selection.^{22,23} Emerging controlled radical processes provide an alternative solution. Stable free radical (SFRP),^{22,24-27} atom transfer (ATRP),²⁸⁻³¹ and reversible addition-fragmentation transfer (RAFT)³²⁻³⁶ polymerizations are leading methods.

Living radical polymerizations typically require elevated temperatures, bulk concentrations, and extensive reaction times. These conditions also correspond to thermal autopolymerization requirements for styrenic monomers. Numerous studies disclose styrene autopolymerization and its posed challenge in living radical processes.^{25,37-39} The chemical process for this competing reaction is controversial and highly investigated. However, studies widely suggest that self-initiation follows the notable Mayo thermal mechanism (Scheme 1).^{39,40} Styrene monomer units initially react to form a [4+2] Diels-Alder adduct. The adduct reacts with available monomer and produces two free radicals for polymerization. Adjacent aromatic resonance stabilizes both radical structures.



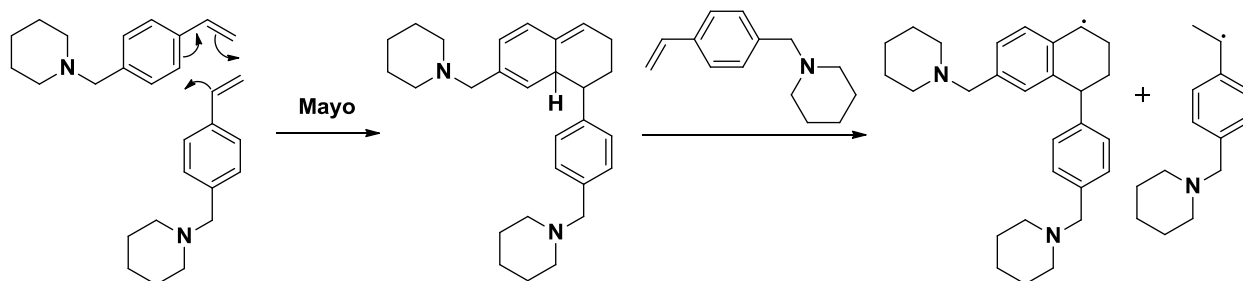
Scheme 1. Mayo thermal-initiation mechanism for styrene.

Investigations reveal that solvent, organic compounds and other additives exhibit strong effects on styrenic thermal polymerization. Mayo *et. al.* investigated chain transfer effects to over fifty organic compounds containing- aromatics, sulfides, halogens, nitrogen, and oxygen.⁴¹ These studies revealed that chain transfer offered radical stabilization in thermal polymerization when the transfer agents provided resonance and polar stabilization. Strong acids such as CSA and hydroiodic acid protonate the Dials-Alder adduct and inhibit thermal polymerization.^{26,41,42} Monteiro *et. al.* reported camphor sulfonic acid (CSA) effects to demonstrate controlled SFRP.³³

Research also highlights styrenic substituent effects on autopolymerization and SFRP.^{26,43,44} Styrenic monomers with additional polarity and resonance augment radical stabilization and thermal polymerization. These studies conventionally explore *para*-substituted styrenic monomers. Kazmaier *et. al.* noted increased SFRP rates for styrenic monomers containing electron-withdrawing groups.⁴⁴ Hawker *et. al.* maintained activated 2,2,6,6-tetramethylpiperidiny-1-oxy (TEMPO) concentrations and demonstrated controlled SFRP for styrene and styrenic derivatives.²⁴ Current studies also highlight fused ring effects on styrenic monomers. Long *et. al.* studied 2-vinylnaphthalene thermal polymerization and reported an observed rate constant one order of magnitude greater than styrene.^{25,37}

In situ Fourier transform infrared (FTIR) spectroscopy is an efficient analytical method for elucidating polymerization kinetic processes. Several studies emphasize its powerful experimental capability.^{45,46} In this study, *in situ* FTIR spectroscopy monitored styrene and 4-vinylbenzyl piperidine (VBP) autopolymerizations. Pseudo-first-order thermal polymerization kinetics calculated observed rate constants for both monomers. An Arrhenius analysis derived activation energy values for both monomers. VBP differs from styrene in its benzyl amine structure. Consequently, *in situ* FTIR spectroscopy was also employed to observe styrene

thermal polymerization with variable N-benzyl (BP) concentrations. The similarities in chemical structure between styrene and 4-vinylbenzyl piperidine suggested thermally initiated polymerization occurred by the Mayo mechanism (Scheme 2). The unique substituent is proposed to offer additional polarity effects for enhancing polymerization rates.



Scheme 2. Mayo thermal-initiation mechanism for 4-vinylbenzyl piperidine

4.3 Experimental

4.3.1 Materials.

Piperidine (99%), 4-vinylbenzyl chloride ($\geq 90\%$), and styrene (99%) were purchased from Sigma Aldrich and used as received unless otherwise noted. Styrene, inhibited by 10-15 ppm of *t*-butyl catechol, was distilled from calcium hydride and dibutyl magnesium. N-benzyl piperidine (99.9 %) was purchased from Acros and used as received.

4.3.2 Analytical Methods.

In situ FTIR analysis was conducted with a Mettler Toledo ReactIR 45M attenuated total reflectance reaction apparatus equipped with a light conduit and DiComp (diamond composite) insertion probe.

4.3.3 Synthesis of 4-Vinylbenzyl piperidine.

NaHCO_3 (5.02 g, 59.7 mmol) was added to 100 mL of a binary mixture of water/acetone (1:1 v:v) in a 250 mL two-neck round bottomed flask equipped with an addition funnel and reflux

condenser. To this mixture, piperidine (16.96 g, 199.2 mmol) was added and stirred until completely dissolved. At room temperature, 4-vinylbenzyl chloride (7.61 g, 49.8 mmol) was added drop-wise, after which the solution was heated to 50 °C and stirred for 20 h. Following the reaction, the solid salt remaining was filtered and discarded, and acetone was distilled under reduced pressure at 23 °C. The remaining solution was diluted with 500 mL of diethyl ether, and washed with 50 mL of ultrapure water six times. The organic phase was then washed with 100 mL of 2.0 M HCl three times, saving the aqueous washes. Then, 200 mL of 4.0 M NaOH was added to the acid washes, producing a cloudy heterogeneous solution. This mixture was extracted with 50 mL of diethyl ether three times, the organic phase was dried over anhydrous sodium sulfate, and the ether was removed under reduced pressure at 23 °C. VBP was isolated as a clear liquid upon distillation from calcium hydride and dibutyl magnesium (80%).

4.3.4 Thermal Polymerization of Styrene and 4-Vinylbenzyl piperidine

Thermal bulk polymerization of VBP and styrene monitored by *in situ* FTIR spectroscopy is described. The monomer (10.0 g) was added to a two neck 25- mL round-bottomed flask with a small magnetic stir bar. One neck was wire sealed with rubber septa. The DiComp probe was inserted into the second fitted neck and sealed tight. The probe tip was submerged below the monomer surface and the ReactIR analysis system was programmed to collect a spectrum every 1 min for 24 h. The flask was purged with nitrogen for 15 min and placed in an oil bath heated at 120 °C. FTIR analysis began. After 24 h, the thermally polymerized monomer was diluted with THF or chloroform and precipitated into methanol.

4.3.5 Thermal Polymerization of Styrene with N-benzyl piperidine

The following protocol describes a typical thermal solution polymerization of styrene. Monomer (3.5 g, 33.6 mmol, 3.85 mL) and BP (5.89 g, 33.6 mmol, 6.20 mL) were combined in a two neck

25-mL round-bottomed flask with a magnetic stir bar. One neck was wire sealed with a rubber septa and the other was tightly sealed with the DiComp probe. The probe tip was inserted below the surface of the reaction mixture and the ReactIR analysis system was programmed to collect a spectrum every 1 min for 24 h. The mixture was sparged with nitrogen for 15 min and set in a 120 °C oil bath. After the 24 h FTIR experiment, the reaction contents were diluted with chloroform and precipitated into methanol. The procedure was repeated, altering the monomer to BP molar equivalences from 1:1 to 1:0.1.

4.4 Results and Discussion

Literature precedence suggests that styrene readily undergoes thermal polymerization above 100 °C.^{37,38,41} Documentation highlighting additive effects on polymerization rates also exists.^{37,41} Consequently, this study employed *in situ* FTIR analysis to investigate both styrene and VBP thermal polymerization. The spectroscopic technique monitored monomer consumptions at 80 °C, 100 °C, and 120 °C (Figures 1 and 2). Pseudo-first-order kinetics analysis achieved thermal initiation rates for the various temperatures. The Arrhenius Equation accounted the observed rate constants and quantified thermal activation energy values for both monomers.

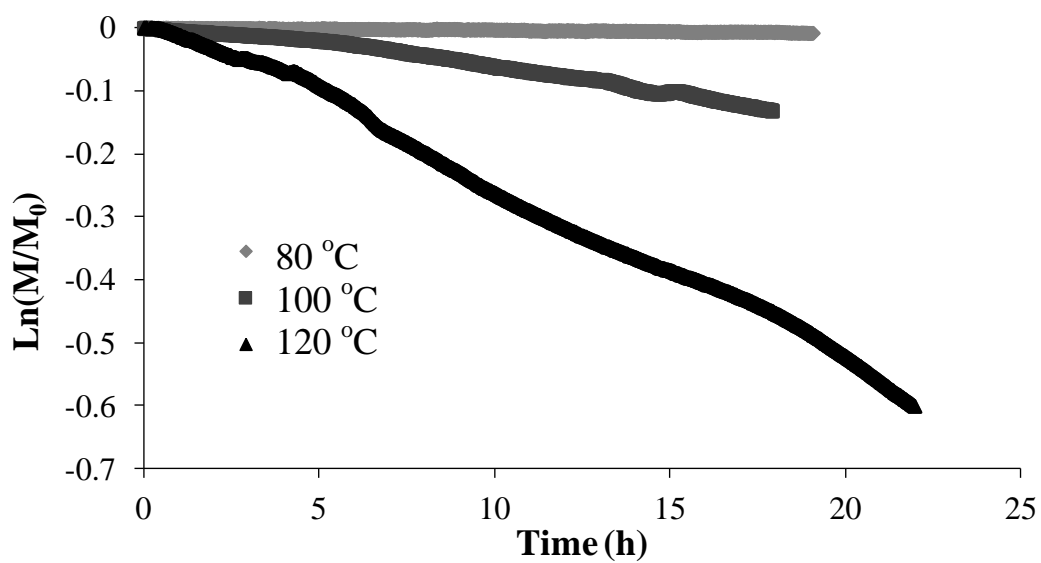


Figure 1. Pseudo-first-order kinetic plot for styrene thermal polymerization.

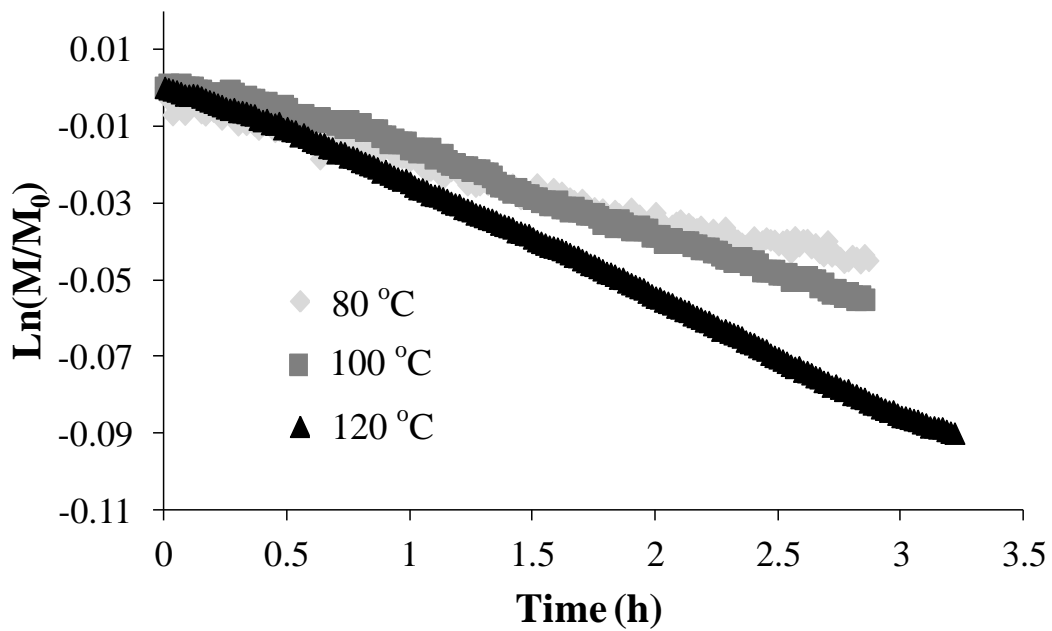


Figure 2. Pseudo-first-order kinetic plot for 4-vinylbenzyl piperidine thermal polymerization.

Styrene maintained steady polymerization rates over the temperature range, exhibiting minimal monomer consumption at 80 °C. An Arrhenius plot related these values as a function of $\ln k_{\text{obs}}$ vs. $1/T$ and derived the thermal activation energy value 113 kJ/mol (Figure 3). These results agreed with former research. Conversely, VBP exhibited notably increased polymerization rates. Observed rate constant values varied by ca. one order of magnitude in comparison to styrene. VBP also exhibited a markedly lower activation energy value. The monomer required 20.0 kJ/mol of activation energy, explaining its relative ease for thermal polymerization (Figure 4).

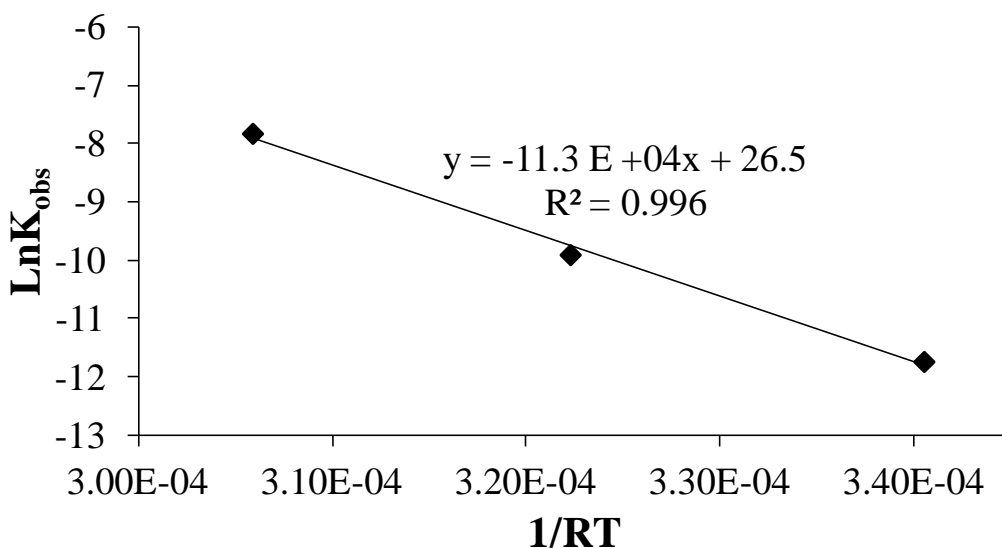


Figure 3. Arrhenius plot for the thermal polymerization of styrene at 80 °C, 100 °C, and 130 °C.

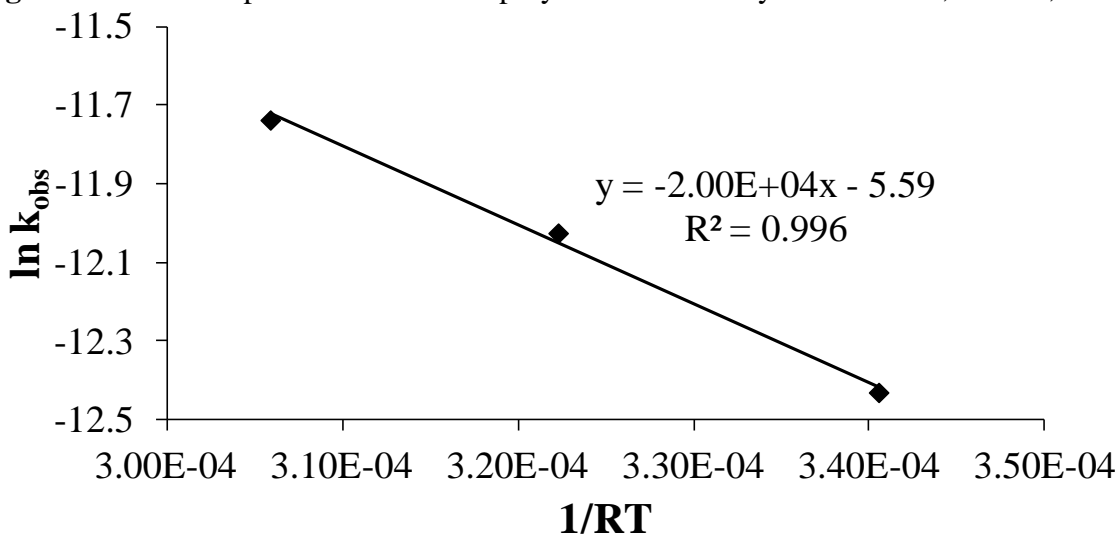
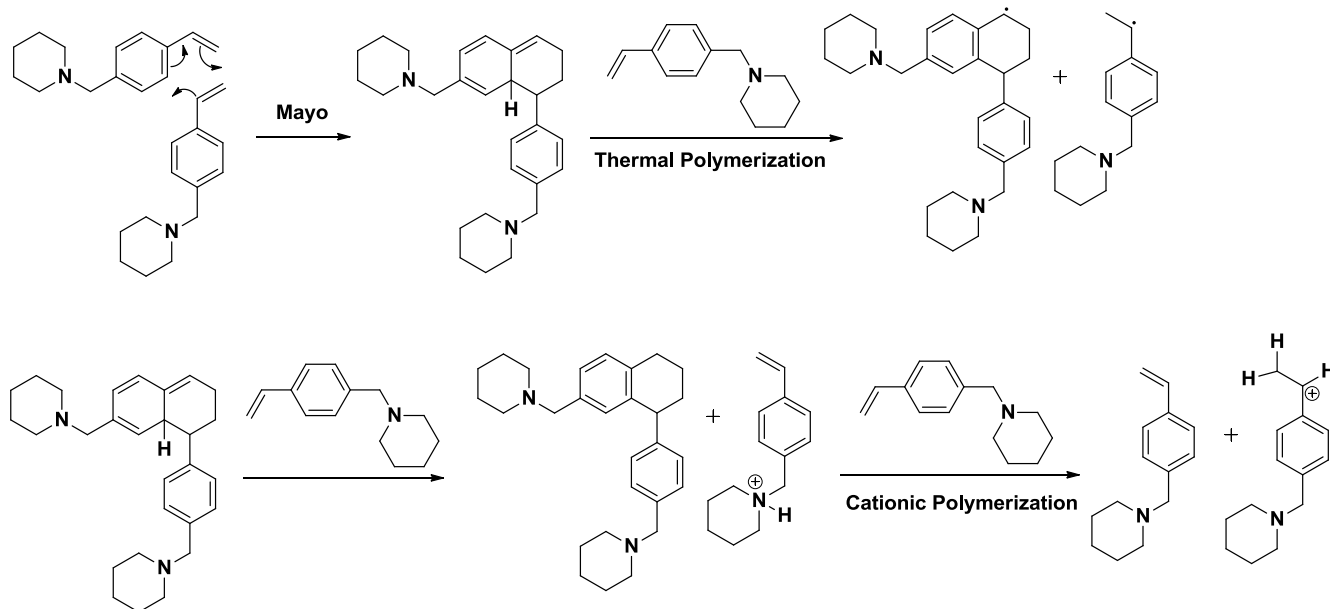


Figure 4. Arrhenius plot for the thermal polymerization of 4-vinylbenzyl piperidine at 80 °C, 100 °C, and 130 °C.

VBP is structurally comparable to styrene and assumed to undergo the proposed Mayo thermal polymerization mechanism. However, the cyclic amine provides additional basicity that allows VBP to deprotonate the Mayo adduct. The subsequent cationic piperidinium is proposed to induce a Friedel-Crafts polymerization (Scheme 3). This drastic acceleration in thermal polymerization rate is consistent with reported cationic polymerization effects.⁴³



Scheme 3. Proposed Mayo thermal polymerization mechanism of 4-vinylbenzyl piperidine with competing cationic polymerization mechanism

Numerous studies report additive effects on styrene thermal polymerization.^{38,41} This study employed *in situ* FTIR analysis to monitor a 1 to 1 molar equivalence, styrene to BP, reaction mixture at 80 °C, 100 °C, and 120 °C (Figure 5). Styrene thermal polymerization showed a significant increase compared to the corresponding bulk study. The investigation exploited pseudo-first-order kinetics to derive an activation energy value for styrene-BP thermal polymerization of 40.0 KJ/mol (Figure 6). The significant drop in activation energy suggested thermal interaction with BP. To confirm this hypothesis, a thermal study at 120 °C was performed for a 0.1 molar equivalence BP. The results showed the exact polymerization rate

constant, $8.0 \times 10^{-6} \text{ s}^{-1}$. A similar study with a 0.1 molar equivalence N-methyl piperidine resulted in a rate constant of $4.0 \times 10^{-6} \text{ s}$. These observations are consistent with the proposed mechanism involving an induced cationic polymerization.

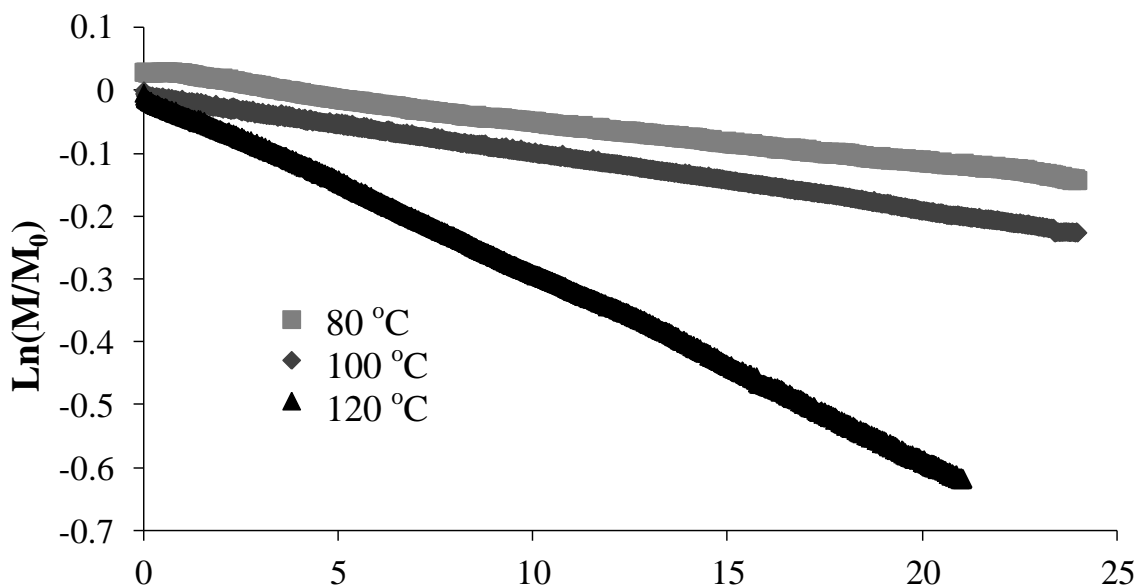


Figure 5. Pseudo-first-order kinetic plot for styrene thermal polymerization with N-benzyl piperidine

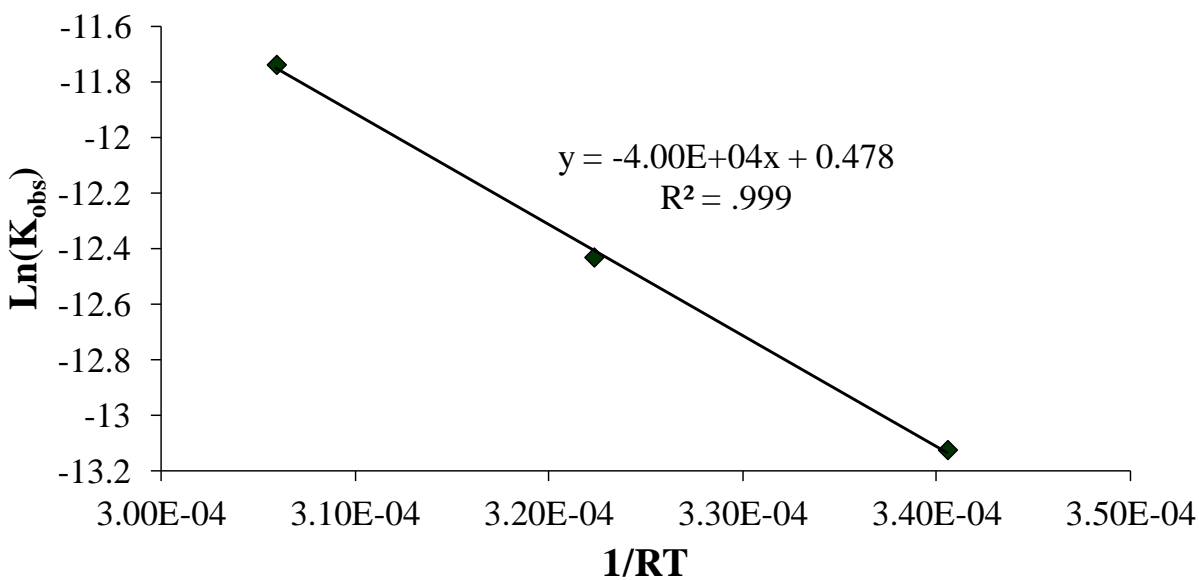


Figure 6. Arrhenius plot for the thermal polymerization of styrene thermal polymerization with N-benzyl piperidine at 80 °C, 100 °C, and 130 °C

4.5 Conclusions:

In situ FTIR spectroscopy monitored styrene and 4-vinylbenzyl piperidine VBP autopolymerizations. Pseudo-first-order thermal polymerization kinetics calculated observed rate constants for both monomers. The Arrhenius Equation accounted observed rate constants and calculated thermal activation energy values for both monomers. VBP exhibited activation energy 80 KJ/mol less than styrene. *In situ* FTIR spectroscopy monitored styrene thermal polymerization with variable BP concentrations. Under these circumstances, styrene revealed activation energy 60 KJ/mol less than its respective bulk value. These results suggested the effects of induced cationic polymerization on VBP autopolymerization. These effects are account for in the proposed mechanism for VBP thermal polymerization.

4.6 Acknowledgements.

This material is based on work supported by the U.S. Army Research Laboratory and the U.S. Army Research Office under contract/grant number W911NF-07-1-0452 Ionic Liquids in Electro-Active Devices Multidisciplinary University Research Initiative (ILEAD MURI).

4.7 References

- (1) Lacroix-Desmazes, P.; Delair, T.; Pichot, C.; Boutevin, B. *J. Polym. Sci., Part A: Polym. Chem.* **2000**, *38*, 3845.
- (2) Monteiro, M. J.; Sjoberg, M.; Van, d. V. J.; Gottgens, C. M. *J. Polym. Sci., Part A: Polym. Chem.* **2000**, *38*, 4206.
- (3) Listigovers, N. A.; Georges, M. K.; Odell, P. G.; Keoshkerian, B. *Macromolecules* **1996**, *29*, 8992.
- (4) Georges, M. K.; Hamer, G. K.; Listigovers, N. A. *Macromolecules* **1998**, *31*, 9087.
- (5) Wang, J.-S.; Matyjaszewski, K. *Macromolecules* **1995**, *28*, 7901.
- (6) Allen, R. D.; Yilgor, I.; McGrath, J. E. *ACS Symp. Ser.* **1986**, *302*, 79.
- (7) Deporter, C. D.; Long, T. E.; McGrath, J. E. *Polym. Int.* **1994**, *33*, 205.
- (8) Elkins, C. L.; Long, T. E. *Macromolecules* **2004**, *37*, 6657.
- (9) Williamson, D. T.; Elman, J. F.; Madison, P. H.; Pasquale, A. J.; Long, T. E. *Macromolecules* **2001**, *34*, 2108.
- (10) Yamauchi, K.; Lizotte, J. R.; Hercules, D. M.; Vergne, M. J.; Long, T. E. *J. Am. Chem. Soc.* **2002**, *124*, 8599.
- (11) Yilgor, I.; McGrath, J. E. *Polym. Prepr. (Am. Chem. Soc., Div. Polym. Chem.)* **1985**, *26*, 57.
- (12) Rodlert, M.; Harth, E.; Rees, I.; Hawker, C. J. *J. Polym. Sci., Part A: Polym. Chem.* **2000**, *38*, 4749.
- (13) Thurn-Albrecht, T.; Steiner, R.; DeRouchey, J.; Stafford, C. M.; Huang, E.; Bal, M.; Tuominen, M.; Hawker, C. J.; Russell, T. P. *Adv. Mater. (Weinheim, Ger.)* **2000**, *12*, 787.
- (14) Sogah, D. Y.; Hertler, W. R.; Webster, O. W.; Cohen, G. M. *Macromolecules* **1987**, *20*, 1473.
- (15) Teyssie, P.; Fayt, R.; Hautekeer, J. P.; Jacobs, C.; Jerome, R.; Leemans, L.; Varshney, S. K. *Makromol. Chem., Macromol. Symp.* **1990**, *32*, 61.
- (16) Kunkel, D.; Mueller, A. H. E.; Janata, M.; Lochmann, L. *Makromol. Chem., Macromol. Symp.* **1992**, *60*, 315.
- (17) Webster, O. W. *Science (Washington, D. C., 1883-)* **1991**, *251*, 887.
- (18) Faust, R.; Kennedy, J. P. *Polym. Bull. (Berlin)* **1986**, *15*, 317.
- (19) Sawamoto, M. *Prog. Polym. Sci.* **1991**, *16*, 111.
- (20) Szwarc, M. *Nature (London, U. K.)* **1956**, *178*, 1168.
- (21) Szwarc, M.; Levy, M.; Milkovich, R. *J. Am. Chem. Soc.* **1956**, *78*, 2656.
- (22) Hawker, C. J.; Bosman, A. W.; Harth, E. *Chem. Rev. (Washington, D. C.)* **2001**, *101*, 3661.
- (23) Greszta, D.; Mardare, D.; Matyjaszewski, K. *Macromolecules* **1994**, *27*, 638.
- (24) Devonport, W.; Michalak, L.; Malmstroem, E.; Mate, M.; Kurdi, B.; Hawker, C. J.; Barclay, G. G.; Sinta, R. *Macromolecules* **1997**, *30*, 1929.
- (25) Lizotte, J. R.; Long, T. E. *Macromol. Chem. Phys.* **2003**, *204*, 570.
- (26) Georges, M. K.; Kee, R. A.; Veregin, R. P. N.; Hamer, G. K.; Kazmaier, P. M. *J. Phys. Org. Chem.* **1995**, *8*, 301.
- (27) Benoit, D.; Harth, E.; Fox, P.; Waymouth, R. M.; Hawker, C. J. *Macromolecules* **2000**, *33*, 363.

- (28) Borguet, Y. P.; Tsarevsky, N. V. *Polym. Chem.* **2012**, *3*, 2487.
- (29) Lu, J.; Yan, F.; Texter, J. *Prog. Polym. Sci.* **2009**, *34*, 431.
- (30) Qiu, J.; Matyjaszewski, K. *Macromolecules* **1997**, *30*, 5643.
- (31) Tsang, E. M. W.; Zhang, Z.; Yang, A. C. C.; Shi, Z.; Peckham, T. J.; Narimani, R.; Frisken, B. J.; Holdcroft, S. *Macromolecules (Washington, DC, U. S.)* **2009**, *42*, 9467.
- (32) Allen, M. H.; Hemp, S. T.; Zhang, M.; Zhang, M.; Smith, A. E.; Moore, R. B.; Long, T. E. *Polym. Chem.* **2013**, *4*, 2333.
- (33) Monteiro, M. J.; Hodgson, M.; De, B. H. *J. Polym. Sci., Part A: Polym. Chem.* **2000**, *38*, 3864.
- (34) Stokes, K. K.; Orlicki, J. A.; Beyer, F. L. *Polym. Chem.* **2011**, *2*, 80.
- (35) Wang, R.; Lowe, A. B. *J. Polym. Sci., Part A: Polym. Chem.* **2007**, *45*, 2468.
- (36) Wu, T.; Wang, D.; Zhang, M.; Heflin, J. R.; Moore, R. B.; Long, T. E. *ACS Appl. Mater. Interfaces* **2012**, *4*, 6552.
- (37) Lizotte, J. R.; Erwin, B. M.; Colby, R. H.; Long, T. E. *J. Polym. Sci., Part A: Polym. Chem.* **2002**, *40*, 583.
- (38) Katzer, J.; Pauer, W.; Moritz, H.-U. *Macromol. React. Eng.* **2012**, *6*, 213.
- (39) Mayo, F. R. *J. Amer. Chem. Soc.* **1968**, *90*, 1289.
- (40) Chong, Y. K.; Rizzardo, E.; Solomon, D. H. *J. Am. Chem. Soc.* **1983**, *105*, 7761.
- (41) Gregg, R. A.; Mayo, F. R. *J. Am. Chem. Soc.* **1953**, *75*, 3530.
- (42) Keoshkerian, B.; Georges, M. K.; Boils-Boissier, D. *Macromolecules* **1995**, *28*, 6381.
- (43) Ma, J. W.; Cunningham, M. F.; McAuley, K. B.; Keoshkerian, B.; Georges, M. K. *J. Polym. Sci., Part A: Polym. Chem.* **2001**, *39*, 1081.
- (44) Kazmaier, P. M.; Daimon, K.; Georges, M. K.; Hamer, G. K.; Veregin, R. P. N. *Macromolecules* **1997**, *30*, 2228.
- (45) Storey, R. F.; Donnalley, A. B.; Maggio, T. L. *Macromolecules* **1998**, *31*, 1523.
- (46) Pasquale, A. J.; Long, T. E. *Macromolecules* **1999**, *32*, 7954.

Chapter 5: Anionic Polymerization of 4-Vinylbenzyl piperidine: Developing a New Class of Ammonium Based Ionic Polymers

5.1 Abstract

Living anionic polymerization offers an efficient route for producing well-defined polymeric structures with controlled molecular weights, molecular weight distributions, stereochemistries, and functional termination capabilities. We disclose the following research focused on the living anionic polymerization of 4-vinylbenzyl piperidine for achieving novel piperidinyl-containing polymers. Homopolymer and copolymer architectures of this design offer structural integrity, and emphasize base stability along the cyclic amino sites. These investigations introduce piperidinyl macromolecules as paradigms for a new class of ammonium based ionic materials. Their design broadens the potential avenues for block copolymer synthesis through the facile synthetic strategy of living anionic polymerization. Available co-monomers for the synthesis of a wide variety of piperidinyl-containing copolymers encompass styrenics, methacrylates, isoprenes, butadienes, etc. We emphasize this synthetic strategy for the production of a variety of piperidinyl-containing block copolymer types consisting in di-, tri-, tetra-, and pentablock structures.

Keywords: anionic polymerization, poly(ionic liquids), alkylation, glass transition

5.2 Introduction

Polymeric ionic liquids (PILs) are unique macromolecules that incorporate cationic or anionic pendant sites along a polymer backbone. PILs offer beneficial IL properties such as ionic conductivity, thermal and chemical stability, and anion exchange capability. These features blend with enhanced performing polymers to provide novel conductive materials with robust mechanical stability, efficient processability, and tunable macromolecular design. PILs are versatile systems that continuously emerge in growing technologies such as water purification^{1,2}, gas separation^{3,4}, gene delivery^{5,6}, biosensors⁷, fuel cells^{8,9}, and actuators.¹⁰⁻¹²

Charge stability represents a constant concern in all these studies, as well as the demand for structural compatibility for various commercial applications. Numerous studies heavily address PILs containing imidazole^{4,12-17}, triazole¹⁸, and pyridine^{19,20} rings. These cationic structures exhibit alkylation efficiency, thermal stability, and base stability. Current sources suggest that styrenic monomers functionalized with cyclic amines, such as pyrrolidine and piperidine, offer comparable material performance.^{21,22} However, few studies exist related to this concept and these monomers remain novel to the polymer chemistry field. In this study, we introduce the controlled anionic polymerization of novel piperidinyl-containing polymers.

The Goodyear Tire and Rubber Company demonstrated precedence for this strategy through the controlled anionic polymerization of cyclic amines such as 1-(4-vinylphenethyl)pyrrolidine with styrene butadiene rubber.²¹ Ethylene spacers limit these derivatives, however, which increases the susceptibility for Hoffman elimination degradation.^{23,24} Altering the spacer to a single methylene unit sterically hinders the amine and drives degradation toward more favorable substitution mechanisms.

We describe herein for the first time the controlled living anionic polymerization and characterization of 4-vinylbenzyl piperidine (VBP). This synthetic strategy offers an efficient route for producing novel piperidinyl- based macromolecules with well-defined structures and low degrees of compositional heterogeneity (homopolymers and block copolymers).²⁵ Available co-monomers for the synthesis of a wide variety of piperidinyl-containing copolymers include styrenics, methacrylates, isoprenes, butadienes, etc. We also report alkylation studies with bromoalkanes, revealing the production of a new class of ammonium containing ionic polymers. All polymers investigated were characterized using ¹H NMR and THF SEC.

5.3 Experimental

5.3.1 Materials.

Piperidine (99%), 4-vinylbenzyl chloride ($\geq 90\%$), *tert*-butylstyrene (99.9%), iodomethane (99.5%) and 1.4 M *sec*-butyllithium solution in hexanes (*sec*BuLi, Aldrich), were purchased from Sigma Aldrich and used as received. 4-vinylbenzyl piperidine was synthesized according to a modified procedure previously reported in the literature.²⁶ Cyclohexane (Burdick & Jackson, HPLC) was passed through an activated molecular sieve column (Aldrich, 60 Å mesh) and activated alumina column immediately prior to use.

5.3.2 Analytical Methods.

¹H NMR spectroscopy was performed on a Varian Unity 400 at 400 MHz in deuterated chloroform. Size-exclusion chromatography (SEC) was used to determine the molecular weights of piperinyl-containing polymers at 40 °C in THF at 1 mL/min. THF SEC was performed on a Waters SEC equipped with two Waters Styragel HR5E (THF) columns, a Waters 717plus autosampler, and a Waters 2414 differential refractive index detector. Reported molecular weights are relative to polystyrene.

5.3.3 Monomer Synthesis: 4-vinylbenzyl piperidine.

NaHCO₃ (5.02 g, 59.7 mmol) and 2,6-Di-tert-butyl-4-methylphenol (0.152g) was added to 100 mL of a binary mixture of water/acetone (1:1 v:v) in a 250 mL two-neck round bottomed flask equipped with an addition funnel and reflux condenser. To this mixture, piperidine (16.96 g, 199.2 mmol) was added and stirred until completely dissolved. At room temperature, 4-vinylbenzyl chloride (7.61 g, 49.8 mmol) was added drop-wise, after which the solution was heated to 50 °C and stirred for 20 h. Following the reaction, the solid salt remaining was filtered and discarded, and acetone was distilled under reduced pressure at 23 °C. The remaining solution was diluted with 500 mL of diethyl ether, and washed with 50 mL of ultrapure water six times. The organic phase was then washed with 100 mL of 2.0 M HCl three times, saving the aqueous washes. Then, 200 mL of 4.0 M NaOH was added to the acid washes, producing a cloudy heterogeneous solution. This mixture was extracted with 50 mL of diethyl ether three times, the organic phase was dried over anhydrous sodium sulfate, and the ether was removed under reduced pressure at 23 °C. VBP was isolated as a yellow liquid (90%).

5.3.4 Poly(vinylbenzyl piperidine) Synthesis.

To a 100-mL flame dried, nitrogen purged, and sealed round bottom flask with stir bar, (5 mL, 4.95 g) VBP and 25 mL of cyclohexane were added. The reaction flask was heated to 50 °C for 10 min. *Sec*-butyl lithium (0.35 mL, 0.5 mmol) was injected to the reaction solution via a syringe. The reaction mixture was stirred for 5 h at 50 °C. The reaction was terminated with nitrogen-degassed methanol. The polymer solution was precipitated into methanol and dried at reduced pressure and room temperature for 48 h.

5.3.5 *In situ* FTIR Monitoring and Anionic Polymerization 4-Vinylbenzyl piperidine

The anionic polymerization of VBP monitored by *in situ* FTIR spectroscopy is described. The monomer (2.0 g) and 8 mL of dry cyclohexane were added to a two neck 25- mL flame dried round-bottomed flask with a small magnetic stir bar. One neck was wire sealed with rubber septa. The DiComp probe was inserted into the second fitted neck and sealed tight. The probe tip was submerged below the monomer surface and the ReactIR analysis system was programmed to collect a spectrum every 1 min for 5 h. The flask was purged with nitrogen for 15 min and placed in an oil bath heated at 50 °C. *Sec*-butyl lithium (0.02 mL) initiated growth of a 10 K polymer. FTIR analysis began. After 5 h, the thermally polymerized monomer was diluted with THF or chloroform and precipitated into methanol.

5.3.6 Poly(*tert*-butyl styrene-co-vinylbenzyl piperidine) Synthesis.

To a 100-mL flame dried, nitrogen purged, and sealed round bottom flask with stir bar, (3 mL, 3.30 g) tBS and 25 mL of cyclohexane were added. The reaction flask was heated to 50 °C for 10 min. *Sec*-butyl lithium (0.35 mL, 0.5 mmol) was injected to the reaction solution via a syringe. The reaction mixture stirred for 1 h at 50 °C. VBP (3 mL, 2.97 g) was sequentially added to the reaction mixture. The reaction stirred for 25 min at 50 °C. The reaction was terminated with nitrogen-degassed methanol. The polymer solution was precipitated into methanol and dried at reduced pressure and room temperature for 48 h.

5.3.7 Poly(*tert*-butyl styrene-co-isoprene-co-vinylbenzyl piperidine) Synthesis.

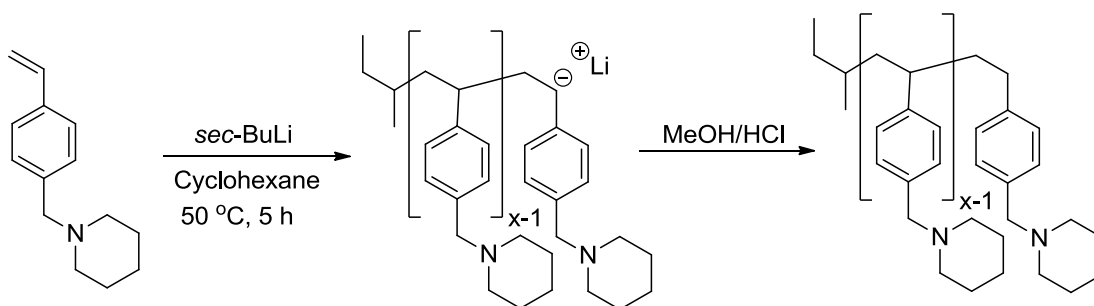
To a 100-mL flame dried, nitrogen purged, and sealed round bottom flask with stir bar, (3 mL, 3.30 g) tBS and 50 mL of cyclohexane were added. The reaction flask was heated to 50 °C for 10 min. *Sec*-butyl lithium (0.35 mL, 0.5 mmol) was injected to the reaction solution via a syringe. The reaction mixture stirred for 1 h at 50 °C. Isoprene (2.6 mL, 2.2 g) was sequentially

added to the reaction mixture and allowed to stir for 1h at 50 °C. VBP (5.25 mL, 5.19 g) was sequentially added to the reaction mixture. The reaction stirred for 25 min at 50 °C. The reaction was terminated with nitrogen-degassed methanol. The polymer solution was precipitated into methanol and dried at reduced pressure and room temperature for 48 h.

5.3.8 Alkylation Reaction on Piperidinyl Containing Copolymers

The following protocol describes a typical alkylation on VBP-containing polymers. 2.00 g PolyVBP and 2.00 molar equivalence of 4-(bromomethyl)-benzyltriphenylphosphonium bromide was dissolved in 25 mL of chloroform. The reaction components were allowed to mix and reflux at 50 °C for 24 h. The resulting piperidinium polymer precipitated from the reaction solution. The final product was isolated and re-precipitated into di-ethyl ether. The final polymer was allowed to dry under vacuum at 30 °C for 48 h.

5.4 Results and Discussion



Scheme 1. General reaction scheme for the anionic polymerization of 4-vinylbenzyl piperidine

VBP was successfully synthesized in a single step substitution reaction (Scheme 1). Scheme 2 depicts the anionic polymerization strategy for synthesizing polyVBP. *In situ* fourier transform infrared spectroscopy (FTIR) monitored the polymerization. Pseudo-first-order kinetics analysis was applied to calculate VBP propagation rate k_p of 2.7 L mol⁻¹ s⁻¹ (Figure 1).

Long *et. al.* reported propagation rates constants for styrene ($2.0 \text{ L mol}^{-1} \text{ s}^{-1}$) and isoprene ($1.5 \text{ L mol}^{-1} \text{ s}^{-1}$).²⁷ As expected, VBP exhibited a propagation rate comparable to styrene. The final product was precipitated in methanol. $^1\text{H-NMR}$ confirmed the polymer structure (Figure 2). SEC verified that the target molecular weight was achieved (Figure 3). The final polymer exhibited a molecular weight of 9.7 K/mol with a PDI of 1.27.

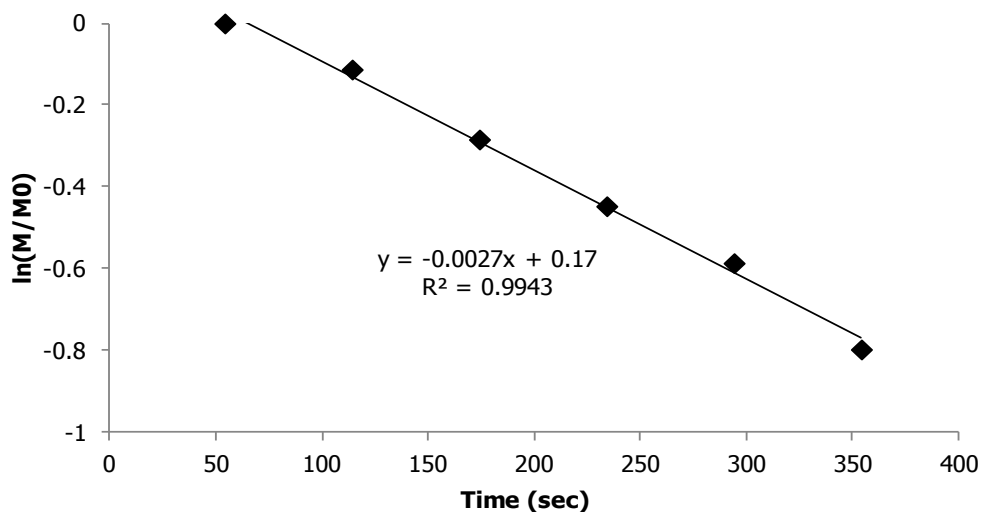


Figure 1. Pseudo-first-order kinetic plot for VBP anionic polymerization.

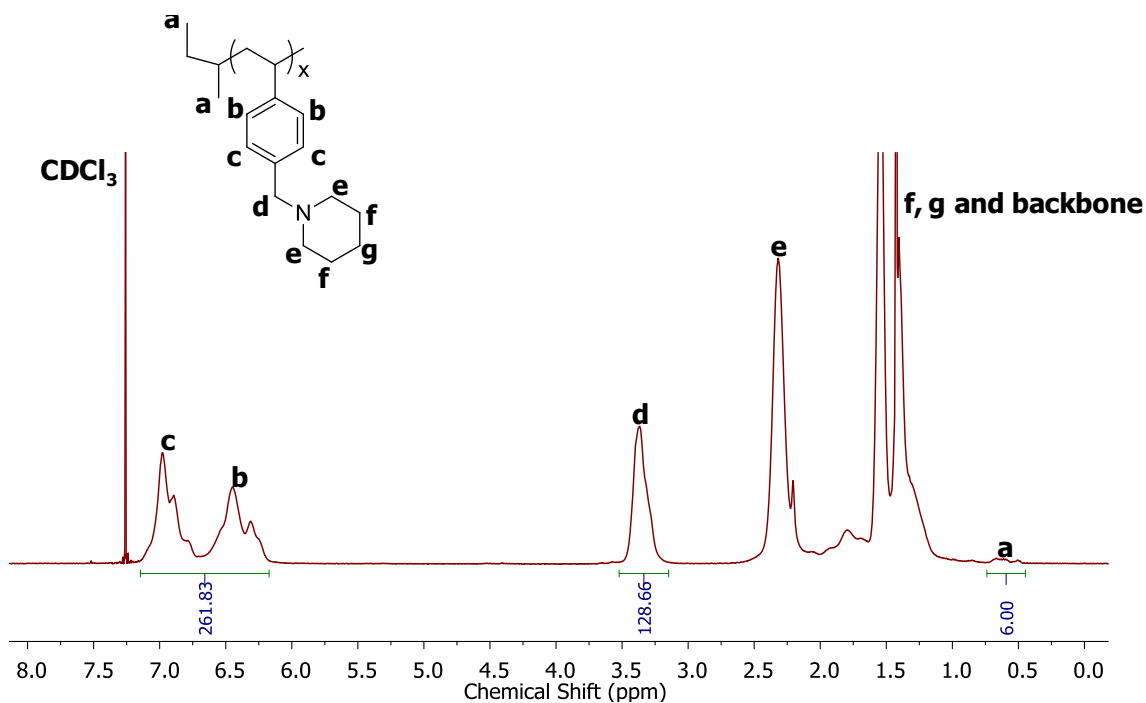


Figure 2. $^1\text{H-NMR}$ characterization of poly(VBP). 400 MHz, CDCl_3 , 22 $^\circ\text{C}$

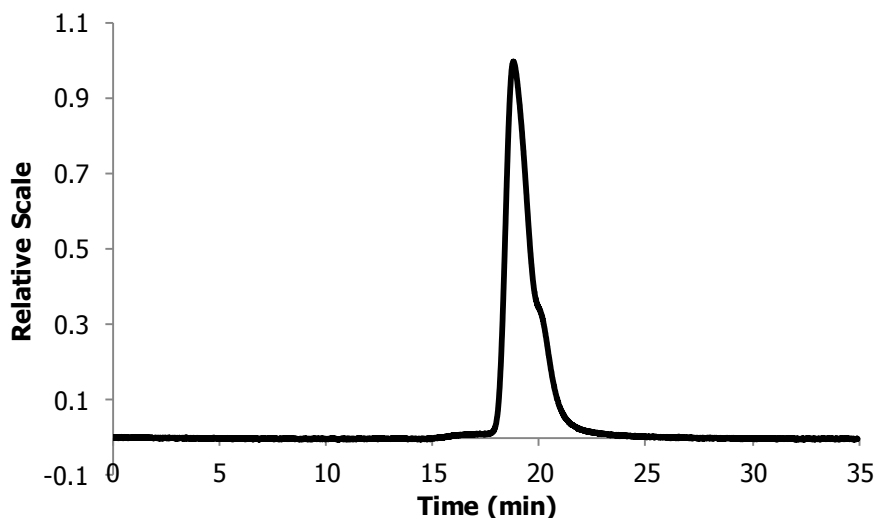
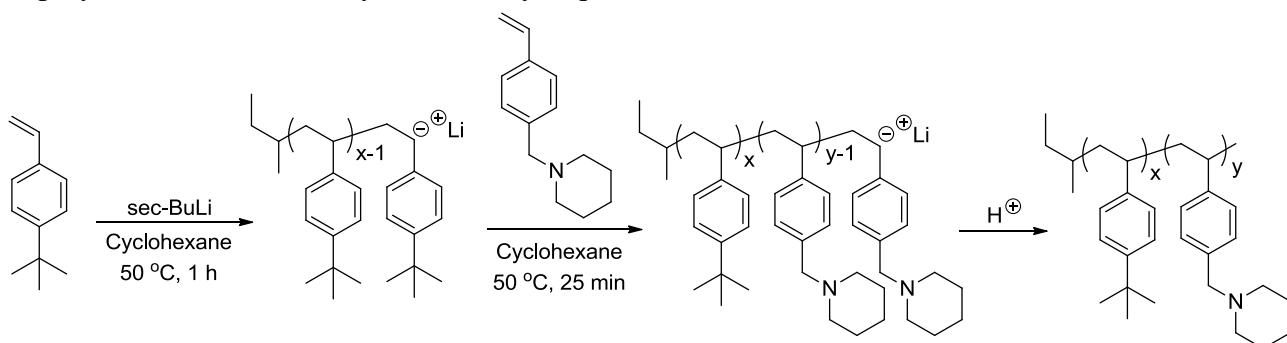
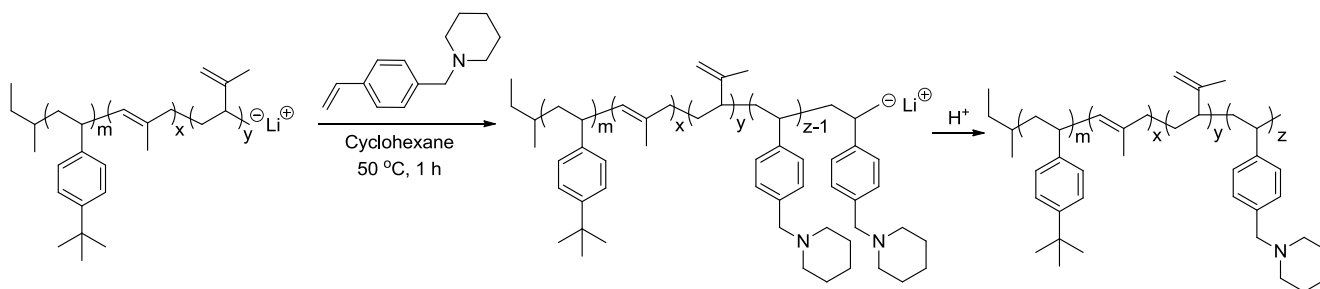


Figure 3. THF SEC trace for poly(VBP). THF SEC, 1 mL/min, 40 °C, absolute molecular weight, light scattering detector

This study emphasized anionic polymerization as an efficient synthetic strategy for the production of a variety of piperidinyI-containing block copolymer types. Previous studies highlight anionic polymerization for the production of well-defined block copolymers containing 2-vinylpyridine²⁸⁻³⁴, 4-vinylpyridine^{35,36}, and 4-vinylbenzyl dimethylamine.^{37,38} We copolymerized VBP with *tert*-butyl styrene and isoprene to demonstrate the novel production of piperidinyI based AB and ABC polymers. Poly(*tert*-butylstyrene-co-vinylbenzyl piperidine) [poly(tBS-coVBP)] and poly(*tert*-butylstyrene-co-isoprene-co-vinylbenzyl piperidine) [poly(tBS-I-VBP)] were synthesized by sequential monomer addition (Scheme 2 and 3).



Scheme 2. Anionic copolymerization of poly(tBS-co-VBP) from sequential monomer addition.

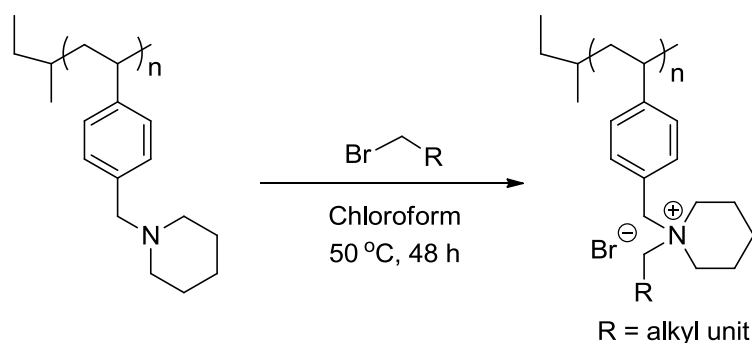


Scheme 3. Anionic copolymerization of poly(tBS-I-VBP) from sequential monomer addition

$^1\text{H-NMR}$ confirmed the structural compositions for all the piperidinyll- containing polymers. THF SEC determined the corresponding number average molecular weights. Table I summarizes these molecular weight values. All of the polymers examined reached the target number-average molecular weights with narrow molecular weight distributions. This confirmed successful piperidinyll- based polymer assembly through controlled anionic polymerization. These results broaden the potential avenues for piperidinyll- based polymers as a new class of ammonium based ionic materials.

Table I. Number-average molecular weights and narrow molecular weight distributions of piperidinyll composites.

| Sample | Target \overline{M}_n | SEC \overline{M}_n | $\overline{M}_w/\overline{M}_n$ |
|---------------|-------------------------|----------------------|---------------------------------|
| PVBP | 10 K | 9.7 K | 1.27 |
| P(tBS-co-VBP) | 5K-5K | 9.3 K | 1.22 |
| P(tBS-I-VBP) | 15K-10K-25K | 49.4 K | 1.28 |



Scheme 4. Alkylating Poly(VBP) with bromoalkanes to develop a new class of ammonium containing charged polymers

PILs are often achieved by postpolymerization modification methods, including alkylation.^{39,40} Scheme 4 depicts the general alkylation reaction on poly(VBP) for achieving unique poly(piperidinium) PILs. This method is applicable for any bromoalkane. Recently, we demonstrated a post modification with 4-(bromomethyl)-benzyltriphenylphosphonium bromide (TPhPBr). Ammonium and phosphonium containing polymers are highly noted for their antibacterial properties.⁴¹⁻⁴⁸ Recent studies now show structures containing both salts exhibit even better bacterial resistance.^{49,50} This feature is ideal for applications in water purification^{51,52} and gene delivery.^{5,49}

¹H NMR revealed quantitative alkylation with TPhPBr. Thermogravimetric analysis (TGA) and differential scanning calorimetry (DSC) probed the thermomechanical properties of both polymers (Table II). TGA revealed thermal stability for both polymers, but indicated a slight decrease in stability for Poly(VBP-TPhPBr)⁺. DSC analysis showed an increase in glass transition (T_g) temperature values. The increase in T_g is rationalized by the incorporation of charged species and bulky phenyl substituents.

Table II. Thermomechanical properties for polyVBP and poly(VBP-TPhPBr)+

| Sample | T_{d1} | T_{d2} | T_g |
|------------------|-----------------------|-----------------------|----------------------|
| polyVBP | 373 | ----- | 82 |
| Poly(VBP-TPhPBr) | 311 | 447 | 176 |

5.5 Conclusions

Living anionic polymerization offers an efficient route for producing well-defined polymeric structures with controlled molecular weights, molecular weight distributions, stereochemistries, and functional termination capabilities. In this study, we demonstrated living anionic polymerization of VBP for achieving novel piperidinyl-containing polymers. We copolymerized VBP with tert-butyl styrene and isoprene to demonstrate its potential research avenues in AB and ABC type copolymers. Finally, we highlighted the versatility of post alkylation for producing novel piperidinium based PILs.

5.6 Acknowledgements

This material is based on work supported by the U.S. Army Research Laboratory and the U.S. Army Research Office under contract/grant number W911NF-07-1-0452 Ionic Liquids in Electro-Active Devices Multidisciplinary University Research Initiative (ILEAD MURI).

5. 7 References

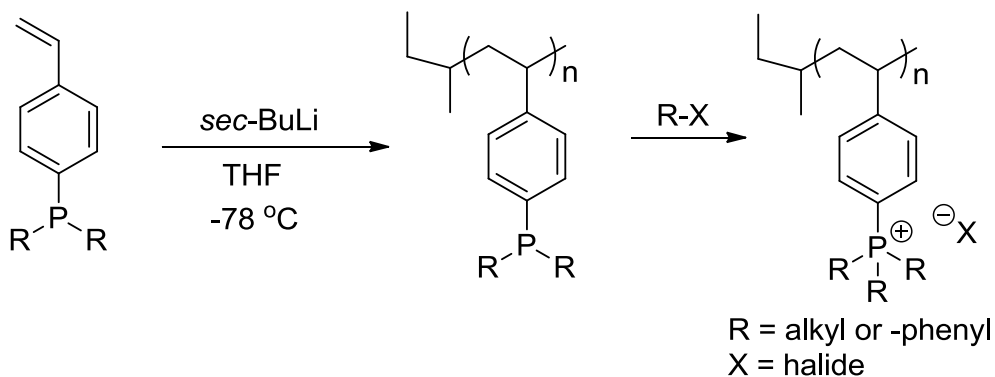
- (1) Hatakeyama, E. S.; Ju, H.; Gabriel, C. J.; Lohr, J. L.; Bara, J. E.; Noble, R. D.; Freeman, B. D.; Gin, D. L. *J. Membr. Sci.* **2009**, *330*, 104.
- (2) Wang, K.; Zeng, Y.; He, L.; Yao, J.; Suresh, A. K.; Bellare, J.; Sridhar, T.; Wang, H. *Desalination* **2012**, *292*, 119.
- (3) Zhang, Y.; Zhang, S.; Lu, X.; Zhou, Q.; Fan, W.; Zhang, X. P. *Chem.--Eur. J.* **2009**, *15*, 3003.
- (4) Shannon, M. S.; Hindman, M. S.; Danielsen, S. P. O.; Tedstone, J. M.; Gilmore, R. D.; Bara, J. E. *Sci. China: Chem.* **2012**, *55*, 1638.
- (5) Hemp, S. T.; Smith, A. E.; Bryson, J. M.; Allen, M. H.; Long, T. E. *Biomacromolecules* **2012**, *13*, 2439.
- (6) Monge, S.; Canniccioni, B.; Graillot, A.; Robin, J.-J. *Biomacromolecules* **2011**, *12*, 1973.
- (7) Anderson, E. B.; Long, T. E. *Polymer* **2010**, *51*, 2447.
- (8) Ghassemi, H.; Riley, D. J.; Curtis, M.; Bonaplata, E.; McGrath, J. E. *Appl. Organomet. Chem.* **1998**, *12*, 781.
- (9) Gu, S.; Cai, R.; Yan, Y. *Chem. Commun.* **2011**, *47*, 2856.
- (10) Gao, R.; Wang, D.; Heflin, J. R.; Long, T. E. *J. Mater. Chem.* **2012**, *22*, 13473.
- (11) Wu, T.; Wang, D.; Zhang, M.; Heflin, J. R.; Moore, R. B.; Long, T. E. *ACS Appl. Mater. Interfaces* **2012**, *4*, 6552.
- (12) Green, M. D.; Choi, J.-H.; Winey, K. I.; Long, T. E. *Macromolecules* **2012**, *45*, 4749.
- (13) Allen, M. H.; Hemp, S. T.; Zhang, M.; Zhang, M.; Smith, A. E.; Moore, R. B.; Long, T. E. *Polym. Chem.* **2013**, *4*, 2333.
- (14) Deimede, V.; Voyiatzis, G. A.; Kallitsis, J. K.; Qingfeng, L.; Bjerrum, N. J. *Macromolecules* **2000**, *33*, 7609.
- (15) Gieselman, M. B.; Reynolds, J. R. *Macromolecules* **1992**, *25*, 4832.
- (16) Green, M. D.; Long, T. E. *Polym. Prepr.* **2009**, *50*, 434.
- (17) Green, M. D.; Long, T. E. *Polym. Rev.* **2009**, *49*, 291.
- (18) Dimitrov-Raytchev, P.; Beghdadi, S.; Serghei, A.; Drockenmuller, E. *J. Polym. Sci., Part A: Polym. Chem.* **2013**, *51*, 34.
- (19) Lee, B. S.; Mahajan, S.; Janda, K. D. *Tetrahedron Lett.* **2005**, *46*, 807.
- (20) Sambhy, V.; Peterson, B. R.; Sen, A. *Angew. Chem., Int. Ed.* **2008**, *47*, 1250.
- (21) Adel Farhan Halasa, W.-L. H., Jin-Ping Zhou, Chad Aaron Jasiunas, Corey Stanton Yon; The Goodyear Tire & Rubber Company: 2005.
- (22) Couture, G.; Alaaeddine, A.; Boschet, F.; Ameduri, B. *Progress in Polymer Science* **2011**, *36*, 1521.
- (23) Fraser, K. J.; MacFarlane, D. R. *Australian Journal of Chemistry* **2009**, *62*, 309.
- (24) Kang, B.-G.; Kang, N.-G.; Lee, J.-S. *Macromolecules* **2010**, *43*, 8400.
- (25) Morton, M.; Fetters, L. J. *Rubber Chemistry and Technology* **1975**, *48*, 359.
- (26) Miyake, T.; Takeda, K.; Tada, K.; Asahi Chemical Industry Co., Ltd., Japan . 1984, p 31 pp. Cont.
- (27) Long, T. E.; Liu, H. Y.; Schell, B. A.; Teegarden, D. M.; Uerz, D. S. *Macromolecules* **1993**, *26*, 6237.

- (28) Gido, S. P.; Schwark, D. W.; Thomas, E. L.; do, C. G. M. *Macromolecules* **1993**, *26*, 2636.
- (29) Katsampas, I.; Roiter, Y.; Minko, S.; Tsitsilianis, C. *Macromol. Rapid Commun.* **2005**, *26*, 1371.
- (30) Mogi, Y.; Kotsuji, H.; Kaneko, Y.; Mori, K.; Matsushita, Y.; Noda, I. *Macromolecules* **1992**, *25*, 5408.
- (31) Mogi, Y.; Mori, K.; Matsushita, Y.; Noda, I. *Macromolecules* **1992**, *25*, 5412.
- (32) Price, C.; Lally, T. P.; Stubbersfield, R. *Polymer* **1974**, *15*, 541.
- (33) Suzuki, J.; Seki, M.; Matsushita, Y. *J. Chem. Phys.* **2000**, *112*, 4862.
- (34) Tsitsilianis, C.; Katsampas, I.; Roiter, Y.; Minko, S.; Stavrouli, N.; Gotsopoulos, M. *Polym. Prepr.* **2006**, *47*, 798.
- (35) Arai, K.; Kotaka, T.; Kitano, Y.; Yoshimura, K. *Macromolecules* **1980**, *13*, 1670.
- (36) Kudose, I.; Kotaka, T. *Macromolecules* **1984**, *17*, 2325.
- (37) Funabashi, H.; Miyamoto, Y.; Isono, Y.; Fujimoto, T.; Matsushita, Y.; Nagasawa, M. *Macromolecules* **1983**, *16*, 1.
- (38) Shibayama, M.; Hasegawa, H.; Hashimoto, T.; Kawai, H. *Macromolecules* **1982**, *15*, 274.
- (39) Tomoi, M.; Hosokawa, Y.; Kakiuchi, H. *J. Polym. Sci., Polym. Chem. Ed.* **1984**, *22*, 1243.
- (40) Parent, J. S.; Penciu, A.; Guillen-Castellanos, S. A.; Liskova, A.; Whitney, R. A. *Macromolecules* **2004**, *37*, 7477.
- (41) Popa, A.; Iliu, G.; Iliescu, S.; Dehelean, G.; Pascariu, A.; Bora, A.; Davidescu, C. M. *Mol. Cryst. Liq. Cryst.* **2004**, *418*, 195.
- (42) Beyth, N.; Yudovin-Farber, I.; Bahir, R.; Domb, A. J.; Weiss, E. I. *Biomaterials* **2006**, *27*, 3995.
- (43) Harney, M. B.; Pant, R. R.; Fulmer, P. A.; Wynne, J. H. *ACS Appl. Mater. Interfaces* **2009**, *1*, 39.
- (44) Kim, Y. H.; Sun, G. *Text. Res. J.* **2000**, *70*, 728.
- (45) Sheldon, B. G.; Wingard, R. E., Jr.; Weinshenker, N. M.; Dawson, D. J.; Dynapol, USA . 1983, p 30 pp.
- (46) Takai, K.; Ohtsuka, T.; Senda, Y.; Nakao, M.; Yamamoto, K.; Matsuoka, J.; Hirai, Y. *Microbiol. Immunol.* **2002**, *46*, 75.
- (47) Kanazawa, A.; Ikeda, T.; Endo, T. *J. Polym. Sci., Part A: Polym. Chem.* **1993**, *31*, 1467.
- (48) Tashiro, T. *Macromol. Mater. Eng.* **2001**, *286*, 63.
- (49) Kenawy, E.-R.; Abdel-Hay, F. I.; El-Shanshoury, A. E.-R. R.; El-Newehy, M. H. *J. Polym. Sci., Part A: Polym. Chem.* **2002**, *40*, 2384.
- (50) Kenawy, E.-R.; Abdel-Hay, F. I.; El-Shanshoury, A. E.-R. R.; El-Newehy, M. H. *J. Controlled Release* **1998**, *50*, 145.
- (51) Sagle, A. C. *Journal of membrane science* **2009**, *340*, 92.
- (52) Hatakeyama, E. S.; Ju, H.; Gabriel, C. J.; Lohr, J. L.; Bara, J. E.; Noble, R. D.; Freeman, B. D.; Gin, D. L. *Journal of membrane science* **2009**, *330*, 104.

Chapter 6: Future Directions

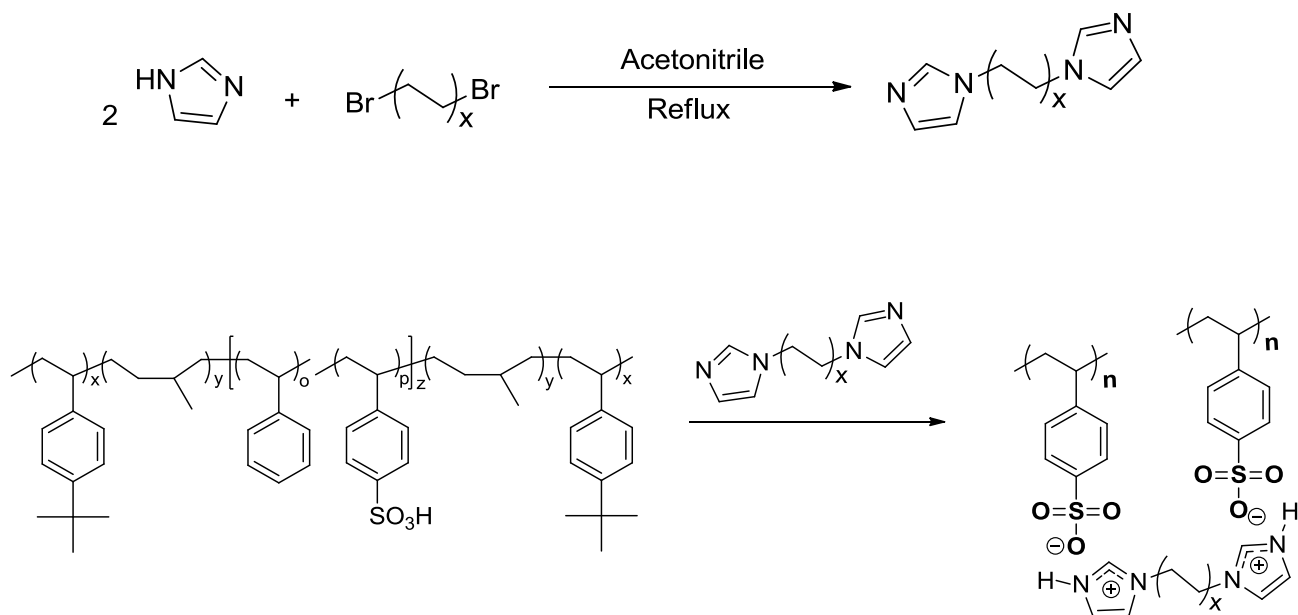
6.1 Controlled polymerization of 4-(diphenylphosphino) styrene

Research is progressively demonstrating the enhanced cationic nature for phosphonium containing polymers. Phosphorus is more electropositive than nitrogen, which attributes to its increased cationic behavior. Few studies exist related to the controlled polymerization of phosphonium monomers. Current research highlights controlled free radical methods including ATRP and RAFT. Future synthesis can involve controlled anionic polymerization strategies. This route will allow controlled polymerization of phosphines followed by subsequent alkylation. Pursuing this method will enable the production of well-defined phosphonium containing block copolymers with various substituents.



6.2 Bis-imidazolium Neutralized Nexar™ Pentablock Copolymers

Recent studies revealed that imidazolium-containing polymers showed promise as electromechanical transducers due to their reasonably high ionic conductivity, acceptable affinity to ionic liquids, and tailored structures and morphologies. Recently, in our research group, ABA copolymers were synthesized containing a poly(1-(4-vinylbenzyl)imidazole-co-Butyl acrylate) random copolymer middle block. Imidazolium sulfonate-containing Nexar™ pentablock copolymer–ionic liquid membranes were also developed for electroactive actuators. These polymers exhibited tailored ionic conductivity and thermal properties. Extending Nexar™ modification with bis-imidazole compounds can expand the library of electroactive devices. These physically crosslinked compositions will improve ion transport by restricting cation mobility. Additionally, varying the alkyl spacer will provide an opportunity to tune mechanical properties.



6.3 Synthesis ABC Piperidinyl Containing Copolymers

Living anionic polymerization of 4-vinylbenzyl piperidine offers potential avenues for block copolymer synthesis through the facile synthetic strategy of living anionic polymerization achieved novel piperidinyl-containing polymers. Future work will emphasize AB, BC, ABC copolymers. Previous literature reports AB, BC, ABC polymers with styrene, isoprene, and 4-vinylbenzyl dimethylamine. This work highlighted the unique morphology complimenting a PS(60K)-(PA64K)-PI(40K) ABC polymer. Future research will expand on this topic, emphasizing morphological studies on ABC piperidinyl containing polymers.

